University doctoral (Ph.D.) thesis

Katalin Erdélyi

Role of poly(ADP-ribose) polymerase-1 (PARP-1) and poly(ADP-ribose) glycohydrolase (PARG) in the regulation of cell death and in the expression of inflammatory mediators

UNIVERSITY OF DEBRECEN
DOCTORAL SCHOOL OF MOLECULAR MEDICINE

DEBRECEN, 2009

University doctoral (Ph.D.) thesis

Role of poly(ADP-ribose) polymerase-1 (PARP-1) and poly(ADP-ribose) glycohydrolase (PARG) in the regulation of cell death and in the expression of inflammatory mediators

Katalin Erdélyi

Supervisor:

Dr. László Virág

University of Debrecen, Medical and Health Science Center
Department of Medical Chemistry

2009

1. TABLE OF CONTENT

2. ABBREVIATIONS

ABTS	2,2'-Azino-bis-(3-ethylbenzothiazoline-6-sulfonic acid
AIF	apoptosis-inducing factor
AP-1	activator protein-1
ATF	activating transcription factor-2
ATP5B	ATP synthase, H^+ transporting, mitochondrial F1 complex, beta polypeptide
BRCT	breast cancer associated protein C-terminus
BSA	bovine serum albumine
CHAPS	3-[(3-Cholamidopropyl)dimethylammonio]-1-propanesulfonate hydrate
CREB	cAMP response element binding
DAPI	4',6-diamidino-2-phenylindole
DEVD-AMC	tetrapeptide-amino-4-methylcoumarine conjugate
DHR	dihydrorhodamine
DMSO	dimethyl sulfoxide
DTT	dithiotreitol
ECL	enhanced chemiluminescence reagents
EDTA	ethylene-diamine tetraacetic acid
EGTA	ethylene-glycol tetraacetic acid
ELISA	enzyme linked immunosorbent assay
EMSA	electrophoretic mobility shift assay
ERK	extracellular signal-regulated kinase
GT	gallotannin
HEPES	4-(2-hydroxyethyl)-1-piperazineethanesulfonic acid
HSSB	human single-stranded DNA binding protein
IFN-γ	interferon-gamma
IL-1β	interleukin 1 beta
JNK	c-Jun NH_2-terminal kinase
LPS	lipopolysaccharide
MAPK	Mitogen-activated protein kinase
MNNG	N-methyl-N-nitro-N-nitrosoguanidine
NAD^+	nicotinamide adenine dinucleotide
NF-κB	nuclear factor-κB

NLS	nuclear localization signal
PARG	Poly(ADP-ribose) glycohydrolase
PARP	Poly(ADP-ribose) polymerase
PBS	phosphate buffered saline
PEI	polyethylenimine
PEI	polyethylenimine
PI	propidium-iodid
PMSF	phenyl-methyl-sulphonyl fluoride
PP1c	protein phosphatase 1
PP2A	protein phosphatase 2Ac
SAPK	stress-activated protein kinase
SDS	sodium dodecyl sulfate
SSB	single-strand breaks
TBE	tris-borate-EDTA
TBS	tris-buffered saline
TCA	trichloroacetic acid
TNFα	tumor necrosis factor alpha
XRCC1	x-ray reapir cross-complementing protein

3. INTRODUCTION

Poly(ADP-ribosyl)ation was discovered almost 50 years ago when Chambon and his coworkers first described the homopolymer of ADP-ribose units derived from nicotionamide adenine dinucleotide (NAD^+) hydrolysis with the simultaneous release of nicotinamid (Chambon et al., 1963). It is a reversible post-translational protein modification implicated in the regulation of a number of biological functions such as maintenance of genomic stability, transcriptional regulation, energy metabolism, centromere function, telomere dynamics, mitotic spindle formation during cell division and cell death. It occurs in almost all nucleated cells of mammals, plants and lower eukaryotes, but is absent in yeast.

3.1. Poly(ADP-ribosyl)ation cycle

Poly(ADP-ribose) is a linear or branched homopolymer of repeating ADP-ribose units linked by glycosidic ribose-ribose 1" 2' bonds synthesized by members of the poly(ADP-ribose) polymerase (PARP) family. The synthesis of poly(ADP-ribose) polymers requires distinct enzymatic activities:

PARPs catalyse the formation of ADP-ribose from the oxidized form of NAD^+ by cleavage of the glycosidic bond between nicotinamide and ribose. Subsequently PARPs mono(ADP-ribosyl)ate the substrate protein (initiation): glutamate, aspartate and carboxyterminal lysine residues of acceptor proteins are covalently modified by the addition of ADP-ribose unit, via formation of an ester bond between the protein and the ADP-ribose residue. (Burzio et al., 1979; Ogata et al., 1980; Suzuki et al., 1986). Subsequently the enzymes catalyse an elongation and branching reaction using additional ADP-ribose units from NAD^+. This generates novel ribosyl-ribosyl linkages and eventually results in the formation of polymers with chain lengths of approximately 200 ADP-ribose units. The average branching frequency of the polymer is approximately one branch per linear section of 20-50 units of ADP-ribose (Hayashi et al., 1983). The half-life of the polymer is estimated to be less than 1 min, it is rapidly degraded by poly(ADP-ribose) glycohydrolase (PARG) and ADP-ribosyl protein lyase (**Figure 1.**).

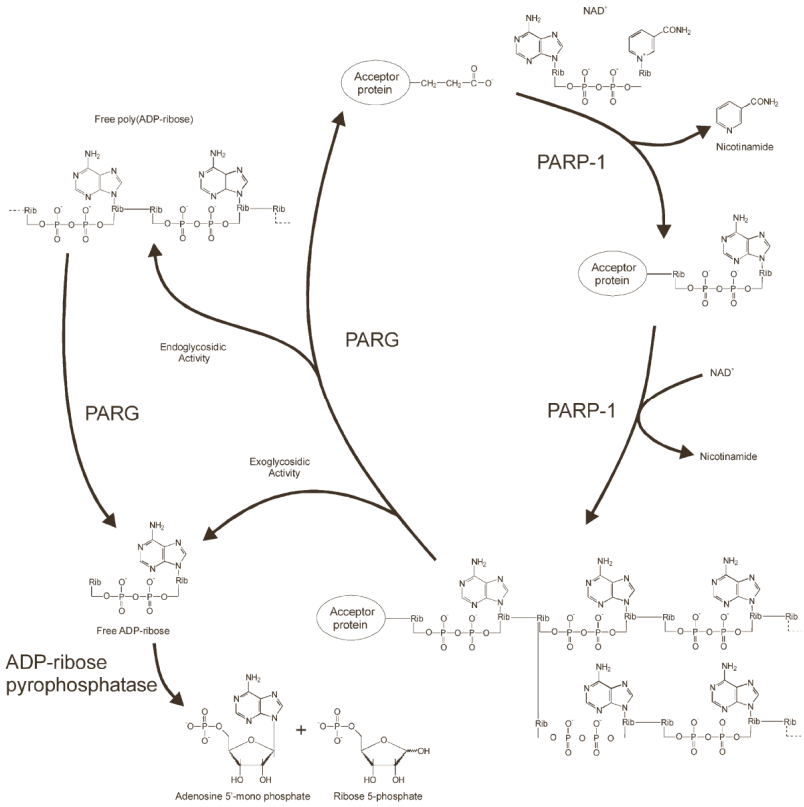

Figure 1. Poly(ADP-ribose) metabolism. *Poly(ADP-ribose) is a branched polymer synthesized on acceptor proteins by PARPs using NAD$^+$ as a donor of ADP-ribose units. The ADP-ribose units in the linear chains are linked by 1" 2' ribose-ribose glycosidic bonds. Poly(ADP-ribosyl)ation is transient and reversible. The degradation of poly(ADP-ribose) is catalyzed by PARG which has both exoglycosidase and endoglycosidase activities that hydrolyze the glycosidic linkage between the ADP-ribose units of poly(ADP-ribose) producing free ADP-ribose. Remaining protein-proximal ADP-ribose monomers are removed by ADP-ribosyl protein lyase (Diefenbach and Bürkle, 2005)*

3.1.1. The physiological consequences of poly(ADP-ribosyl)ation

The constitutive level of poly(ADP-ribose) are usually very low in unstimulated cells (D'Amours et al., 1999), however, in response to mitogenic stimuli or genotoxic stress (i.e. in the presence of DNA strand breaks) the PARP activity and the level of poly(ADP-ribose) may increase 10- to 500-fold.

The consequences of linking a long, negatively charged polymer to a protein are potentially profound. Each residue in poly(ADP-ribose) contains an adenine moiety capable of base stacking and hydrogen bonding as well as two phosphate groups that carry negative charges. Thus, poly(ADP-ribose) may alter protein activity by functioning as a site-specific covalent modification, a protein-binding matrix, or a steric block.

Accumulation of poly(ADP-ribose) polymers causes electrostatic repulsion of proteins so that prevent any interaction with other protein or other anionic molecules such as DNA. Also, the addition of ADP-ribose residues near catalytic or regulatory sites on enzymes may modify enzymatic properties as has been frequently established for the phosphorylation of proteins (Amé et al., 2000).

3.2. Poly(ADP-ribose) synthesis by PARP

PARPs are an ancient family of enzymes. Amé et al., have been identified 18 different PARP proteins. However, Otto et al. characterized only 17 different PARPs by in silico studies (Amé et al., 2004; Otto et al., 2005).

PARP-1, the founding family member, has been studied most extensively. It accounts for more than 90% of the poly(ADP-ribosyl)ating capacity of the cells. PARP-1 protein occurs in high copy number in most cells of multicellular eukaryotes with the notable exception of terminally differentiated granulocytes (Bhatia et al., 1995). The structure-function relationship of PARP-1 is well understood. The 116-kDa PARP-1 is a highly conserved enzyme and displays a characteristic three domain structure (1-3) (which can be further broken down into 6 motifs (A-F), with 4 of them having been assigned a particular function) (Amé et al., 2004) (**Figure 2.**).

(1) At the amino terminal end one can find the **DNA binding domain**, containing three zinc finger motifs (A). The first two are responsible for interaction with DNA breaks, while the third zinc finger may have function in the enzyme dimerisation (Langelier et al., 2007). Motif B containing a bipartite nuclear localization signal (NLS) is responsible for the nuclear homing of PARP-1 and also a caspase-3 cleavage site.

(2) The **automodification domain** contains a BRCT (breast cancer associated protein C-terminus) motif (D). Automodification can inhibit PARP-1 DNA binding, protein-protein interaction, and ADP-ribosyl transferase activity, ultimately inactivating the protein.

(3) The **catalytic domain** with motif F is the smallest PARP-1 fragment retaining catalytic activity. An evolutionally well-conserved sequence of approximately 50 amino acids is known as the "PARP signature". This site contains the NAD^+ acceptor sites and critical residues involved in the initiation, elongation and branching of poly(ADP-ribose) polymers.

Nothing is known so far concerning the function of motifs C and E.

PARP-1 is a molecular sensor of DNA breaks and it has a key role in the spatial and temporal organization of their repair. Its enzymatic activity is dependent on the binding of the enzyme to damaged DNA, an effect mediated by allosteric alteration in the structure of the enzyme (D'Amours et al., 1999). A closer inspection of the literature, however, reveals that PARP-1 can also bind with high affinity and in a cooperative manner to other DNA structures (e.g. cruciform, curved, supercoiled, and crossover as well as specific double-stranded sequences) (Kraus and Lis, 2003). Moreover, a DNA damage independent PARP activation pathway has also been described (Homburg et al., 2000).

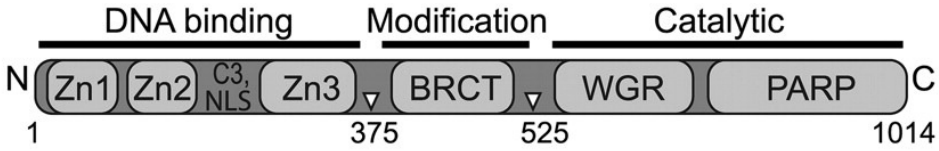

Figure 2. Schematic structure of PARP-1. *PARP-1 has a highly conserved structural and functional organization including N-terminal DNA binding domain with 3 Zn-finger motifs and a nuclear localization signal; its central automodification domain contains a BRCT protein-protein interaction motif; and the C-terminal catalytic domain with a WGR (the name denotes the sequence in a highly conserved region) and a contiguous 50 amino-acid sequence, the "PARP signature" motif that forms the active site. (Langelier et al., 2007)*

More then 30 nuclear substrates of PARPs have been identified in vivo and in vitro. (Althaus and Richter 1987). Among these substrates, one finds almost exclusively proteins involved in the metabolism of nucleic acids and in the maintenance of chromatin architecture. The most prominent target protein (acceptor) of poly(ADP-ribosyl)ation is PARP-1 itself. Poly(ADP-ribose) polymers are covalently attached to the automodification domain which leads to the enzymatic inactivation of PARP and also the release from the DNA (Alvarez and Gonzalez 1993).

Many other acceptor proteins have been described: histones (Tanuma et al., 1985, Rouleau et al., 2004) p53 (Alvarez and Gonzalez 2001), DNA ligases (Ohashi et al., 1983), DNA polymerases (Yoshihara et al., 1985), DNA topoisomerases (Scovassi et al., 1993), DNA dependent protein kinases (Ruscetti et al., 1998) human single-stranded DNA binding protein HSSB (Eki and Hurwitz 1991) DNA repair proteins and transcription factors (see page 21 and 26-27 for more details).

3.3. Poly(ADP-ribose) catabolism by poly(ADP-ribose) glycohydrolase

Poly(ADP-ribosylation) is a dynamic process because poly(ADP-ribose) polymer is rapidly degraded by **poly(ADP-ribose) glycohydrolase (PARG**) and **ADP-ribosyl protein lyase**. The half-life of the polymer is estimated to be less than 1 min, indicating a concerted activation of poly(ADP-ribose) synthesizing and degrading enzymes. With both endo- and exoglycosidase activities PARG catalyses the hydrolysis of glycosidic bonds between ADP-ribose units and thereby generates free ADP-ribose (Bonicalzi et al., 2005). Because the K_m value of PARG is much lower for larger $(ADP\text{-}ribose)_n$ polymers than for smaller ones, the enzyme probably removes and catabolizes bigger fragments first. PARG then stwiches to exoglycosidase mode and removes ADP-ribose units one by one. (Hatakeyama et al., 1986). The release of the ADP-ribose unit most proximal to the protein is catalyzed by PARG and/or by ADP-ribosyl protein lyase (Oka et al., 1984).

In mammals, PARG is encoded by a single gene which localizes to human chromosome 10q11.23 (Amé et al., 1999). In the full length (111-kDa) enzyme the regulatory domain is located at the amino-terminal site while the catalytic domain can be found at the carboxy-terminal. Until recently, five different splice variants have been described (Figure 3.): the low abundance and full lenght isoform PARG-111, the two cytoplasmic isoforms PARG-102 that lacks exon 1 and PARG-99 that lacks exon 1 and 2 (Meyer-Ficca et al., 2004); the cytoplasmic and nuclear isoform PARG-60 and the PARG-55 localized strictly to the mitochondria (Meyer et al., 2007). Whether all isoforms exist simultaneously in all mammalian species remains to be investigated.

Recently, a 39-kD mitochondrial protein termed **ADP-ribose-protein-hydrolase-3** (ARH3) has been isolated which possesses a glycohydrolase activity although it is structurally unrelated to the PARG (Oka et al., 2006).

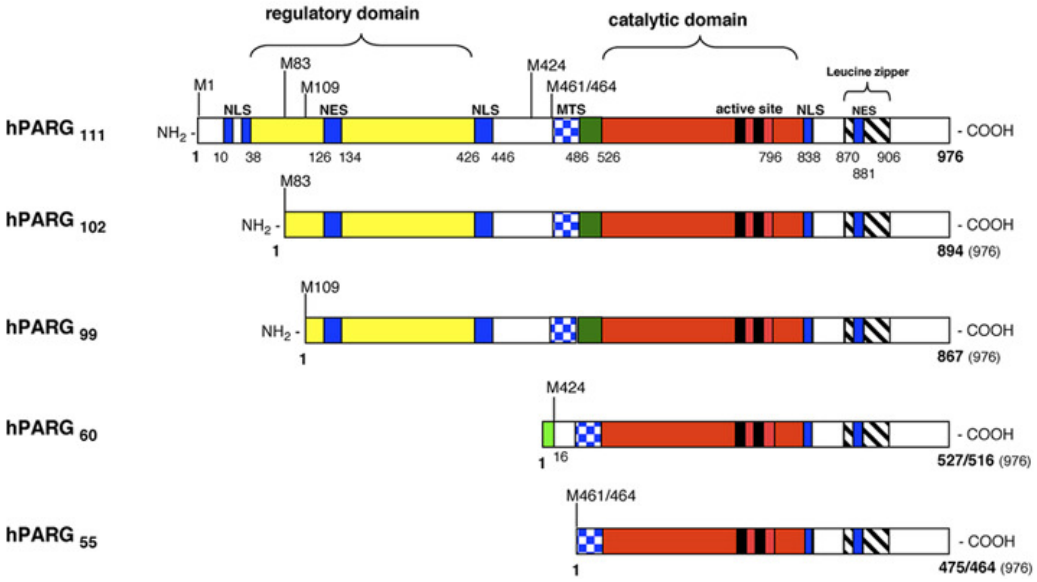

Figure 3. The domain architecture of the five human PARG isoforms. *Full length PARG protein has 18 exon and localizes to the nucleus. PARG-102 lacks exon1 while PARG-99 lacks both exon1 and 2. Since the NLS is in the exon1, PARG-102 and PARG-99 exhibit perinuclear localization. hPARG-60 contains sequences of 16 amino acids which is not found in the other isoforms. The two shortest PARG isoforms localize to the cytoplasm. NLS: nuclear localization signals; NES: nuclear export signals; MTS: mitochondrial targeting sequence. Active sites: E728, E738, E756, E757 and T995 (Hassa and Hottiger 2008).*

3.3.1. Cellular function of PARG

To elucidate the cellular function of PARG, pharmacological inhibition of the enzyme appeared to be a viable approach. In the 90th and the early 2000 years, several in vitro studies suggested that tannins (gallotannin, ellagitannin or tannic acid), could be potent inhibitors of PARG (Tanuma et al., 1989 a,b; Tsai et al., 1991).

Tannic acids are naturally occuring (oaks, fir, certain willows, chestnut, birch, alder, tea) water-soluble polyphenol compounds which primarily consist of a glucose core esterified with gallic acid or its derivatives (**Figure 4.**).

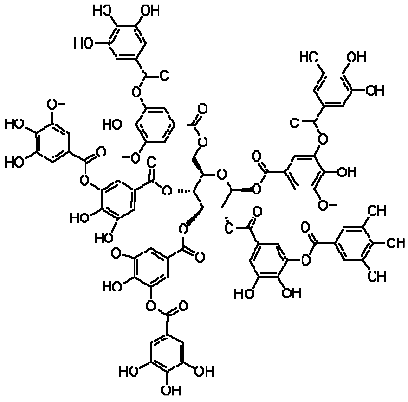

Figure 4. Molecular structure of gallotannin. *Hydrolysable tannins or tannic acid are composed of gallic acid or its condensation product ellagic acid esterified to the hydroxyl groups of glucose. Each hydrolysable tannin molecule is usually composed of a core D-glucose and 6 to 9 galloyl groups.*

Ying et al. (2000) have shown that the PARG inhibitor gallotannin can markedly reduce death of astrocytes after oxidative stress. Interestingly, it was observed that gallotannin slows down the turnover of the ADP-ribose polymer and thus limits NAD^+ depletion that would otherwise lead to cell death. These naturally occurring PARG inhibitory compounds provided cytoprotection in two PARP-mediated cytotoxicity systems: N-methyl-D-aspartate (NMDA)-stimulated neurons (Ying at al 2001) and oxidatively stressed HaCaT cells (Bakondi et al., 2004). Moreover, it has been shown that these tannins lead to accumulation of poly(ADP-ribose).

Gallotannin and other tannins also have been shown to exert various biological effects ranging from anti-inflammatory to anticancer and antiviral effects (Uchiumi et al., 1996; Van Molle et al., 2000; Feldman et al., 2001). The mechanism underlying the anti-inflammatory effect of tannins include the scavenging of radicals (antioxidant effect) (Hagerman et al., 1999) and inhibition of the expression of inflammatory mediators, such as cytokines, inducible nitric-oxide synthase and cyclooxygenase-2 (Lee et al., 2003). Most of these studies focused on the effects of tannins on immune cells with special regard to mononuclear cells and macrophages. Despite of all of these beneficial effects of tannins, the lack of specificity limits their use in cell-based studies.

However, the ADP-ribose analogue adenosine diphosphate-(hydroxymethyl)-pyrrolidinediol (ADP-HPD) was identified as a partial, noncompetitive PARG inhibitor with an IC_{50} of approximately 0,33 μM (Slama et al., 1995). Although it seems to be a specific PARG inhibitor, ADP-HPD is not cell permeable, which is critical for cell culture-based experiments.

Since potent, cell-permeable, specific PARG inhibitory componds are still not commercially available, other molecular appoaches are needed for understanding the physiological role of poly(ADP-ribose) catabolism.

In *Drosophila melanogaster* a loss-of-function mutant that lacks the conserved catalytic domain of PARG was described. This mutant exhibits lethality in the larval stages at the normal developmental temperature of 25°C. However, about 25% of the mutants progressed to the adult stage at 29°C but showed progressive neurodegeneration with reduced locomotor activity and a shortened lifespan. In association with this, extensive accumulation of poly-ADP-ribose could be detected in the central nervous system. These results suggest that poly-ADP-ribose metabolism is required for maintenance of the normal function of neuronal cells (Hanai et al., 2004).

Depletion of the full length (but not the 60kDa) PARG protein by deletion of exon 2 and 3 of the murine parg gene produces viable and fertile mice expressing hypersensitivity to genotoxic alkylating agents and ionizing radiation. These data indicate that the full length PARG plays an important role in DNA damage responses (Cortes et al., 2004). Immortalized fibroblast cells derived from these hypomorphic mutant mouse model exhibited reduced formation of XRCC1 foci, delayed H2AX phosphorylation, decreased DNA break intermediates during repair and increased cell death following N-methyl-N-nitro-N-nitrosoguanidine (MNNG) treatment (Gao H et al., 2007).

However, disruption of parg gene by targeting exon 4 in the germline of mice, leading to complete suppression of functional PARG, causes early lethality due to poly(ADP-ribose) accumulation. In fact, trophoblast stem cell lines derived from these parg-null early embryos are viable, but only in the presence of PARP inhibitors. In addition, these cells are hypersensitive to the cytotoxic effects of a DNA alkylating agent. These results provide evidence that the failure to degrade poly(ADP-ribose) has deleterious consequences. Further, they define a role for PARG in embryonic development and a protective role in response to genotoxic stress (Koh et al., 2004).

Although the gene knockout approach has offered some important insights into PARG function, the embryonic lethality has precluded further functional studies.

In recent studies, RNA interference was used to selectively down-regulate PARG in murine and human cells. Blenn et al. (2006) showed that PARG-silenced murine fibroblast cells are more resistant to oxidant-induced apoptosis while exhibiting delayed poly(ADP-ribose) degradation. No difference was observed in their response to the DNA alkylating agent MNNG.

3.4. The diverse biological functions of poly(ADP-ribosyl)ation

3.4.1. PARP-1 in the maintenance of genomic integrity

Although PARP-1 knock out mice are viable and fertile, they exhibit hypersensitivity to ionizing radiation and are more sensitive to the lethal effects of alkylating agents. Primary fibroblasts and splenocytes derived from these animals exhibited an elevated frequency of recombination, gene amplification, sister chromatide exchange and micronuclei formation after treatment with genotoxic agents. Increased genomic instability, namely spontaneous frequency of sister chromatide exchange has been

observed even in the absence of DNA damage, implicating an important role for PARP-1 in the maintenance of genomic integrity (Shall and Murcia 2000).

3.4.2. PARP-1 in DNA repair

A plethora of studies has firmly established that poly(ADP-ribosyl)ation significantly contributes to cellular recovery from cytotoxicity in proliferating cells inflicted with low or moderate levels of DNA damage by alkylation, oxidation or ionizing radiation, thus establishing PARP-1 as a survival factor.

Single-strand breaks (SSB) are one of the most frequent DNA lesions produced by endogen reactive oxygen species or generated by oxidative agents or ionizing radiation. SSB are also intermediate products in various aspects of DNA metabolism, including DNA repair, replication and recombination. During base excision repair (BER), SSB are produced by DNA glycosylases and apuronic/apyrimidinic (AP) endonucleases at the site of base damage.

Trucco et al (1998) observed that PARP-1 null cells repair DNA breaks induced by methyl-methanesulfonate (MMS) much more slowly than do the wild type cells, although the deficient cells do eventually repair all the breaks. It suggests that PARP-1 is not absolutely needed for BER, but it does increase the efficiency and speed of repair process very significantly. PARP-1 efficiently detects the presence of SSB by its N-terminal zinc finger motives; the occurrence of a break is immediately translated into a posttranslational modification of histon H1 and H2B leading to relaxation of the chromation structure and therefore to increased DNA accessibility (Dantzer et al., 2006). Auto-poly(ADP-ribosyl)ation of PARP-1 triggers the recruitment of XRCC1 (X-ray repair cross-complementing) which coordinates and stimulates the repair process to the damaged DNA site (Masson et al., 1998; Okano et al., 2003). Although no enzymatic activity has been attributed to XRCC1, it has been proposed to serve as a molecular scaffold or docking platform for other repair proteins (DNA ligase III, PARP-1 and DNA polymerase-β) (Thomson and West 2000). The native chromatin structure is finally restored after degradation of poly(ADP-ribose) by PARG (**Figure 5.**).

Pharmacological inhibition of PARP-1 has been established as an effective means of sensitizing malignant cells to DNA damaging γ-irradiation. The PARP inhibitor ABT-888 reduced clonogenic survival in lung cancer cells and inhibited DNA repair after irradiation and also increased tumor growth delay in murine models (Albert et al., 2007).

The importance of PARG for SSB-repair and cell survival remains to be elucidated. It has been reported that PARG interacts with XRCC1 (Keil et al., 2006) and that mice lacking PARG exhibit sensitivity to alkylating agents and γ-irradiation (Cortes et al., 2004; Koh et al., 2004). However, it has been also reported that depletion of PARG protects MEF from hydrogen peroxide-induced cell death and that PARG is dispensable for SSB-repair after oxidative stress (Blenn et al., 2006). In an other report, Caldecott's group identified PARG as a novel and critical component of SSB-repair that accelerates this process in concert with PARP-1 (Fisher et al., 2007).

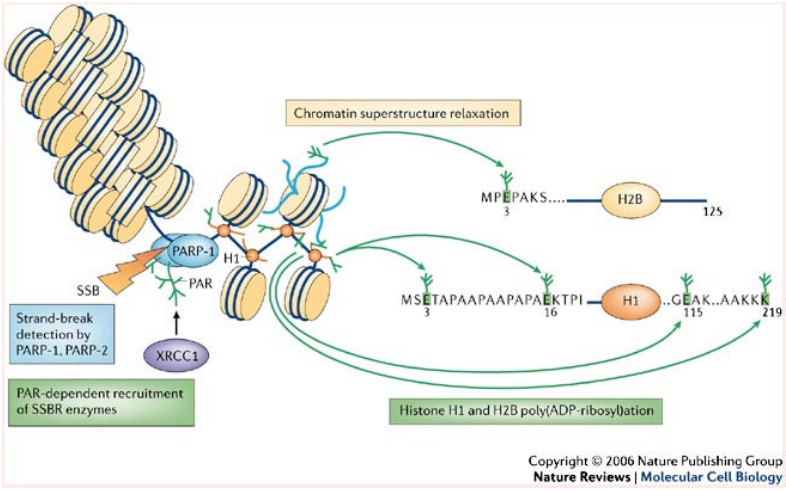

Figure 5. *Following the detection of single-strand-DNA breaks (SSBs) by PARP-1 and PARP-2, poly(ADP-ribose) synthesis at the DNA damage site triggers both the recruitment of the SSB-repair scaffold protein XRCC1 and the relaxation of the chromatin superstructure as mediated by the poly(ADP-ribosyl)ation of histone H1 and histone H2B tails. Together this facilitates access to the DNA lesion of repair enzymes that interact with XRCC1. (Schreiber et al., 2006)*

In the case of double strand breaks (DSB), PARP-1 and other PARP proteins are thought to promote homologous recombination-mediated repair through the recruitment and poly(ADP-ribosyl)ation of factors involved in non-homologous end joining (NHEJ) including Ku70 and DNA-PKcs, resulting in the inhibition of their ability to bind free ends (Shrivastav et al., 2008).

PARP-1 seemed to contribute to BRCA1- and BRCA2-dependent double stand break (DSB) repair. BRCA1 and BRCA2 are tumor-suppressor proteins important for DSB repair by homologous recombination. Mutation of these genes cause predisposition to breast and ovarian cancer. BRCA deficient cells treated with PARP-1 inhibitor show major mitotic chromosome aberration and a loss of formation of RAD51 foci, suggesting defects

in DSB repair involving RAD51-dependent homologous recombination. (Farmer et al., 2005)

3.4.3. PARP-1 and cell death

Cell death by necrosis occurs as a consequence of acute, excessive exposure to a pathological insult. It is characterized by cell swelling followed by disruption of the cell membrane leading to the release of the cellular content in the environment, triggering inflammation of surrounding tissues. Apoptosis, also called programmed cell death, is a mechanism by which a cell commits suicide in response to different stimuli like DNA damage, signals from neighboring cells, or extracellular chemical signals. In apoptotic cell death, cellular content is separated into vesicles that are engulfed by macrophages with little or no detrimental consequences for neighboring cells. In contrast to necrosis, apoptosis is an energy-dependent process that is generally executed by caspases (**c**ystein, **asp**artic acid prote**ase**), proteases activated to cleave specific substrates in order to inactivate cellular processes.

Interestingly, PARP-1 is inactivated during the execution phase of apoptosis. PARP-1 is cleaved by caspase-3 and -7 into an 24-kDa N-terminal fragment (p24) containing the DBD and an 89-kDa C-terminal fragment (p89) that retains basal, but not DNA-damage activated, enzymatic activity (Kaufmann et al., 1993). This cleavage eliminates PARP-1 activation in response to DNA fragmentation during apoptosis, protecting the cells from ATP depletion and subsequent necrotic death. In addition, by preventing futile attempts of DNA repair, PARP-1 cleavage may help commit cells to the apoptotic pathway (Soldani and Scovassi, 2002). Cleavage of PARG during apoptosis by caspase-3 was also reported (Affar et al., 2001).

Mitochondria play an amplification role in many apoptotic models and can also release factors involved in caspase-independent cell death including apoptosis-inducing factor (AIF). Nascent AIF has a mitochondrial localization sequence that is cleaved upon entry into the intermembrane space (Susin et al., 1999). In healthy cells, AIF is retained in the mitochondria where it is believed to perform an oxidoreductase function based on the presence of a FAD binding domain in the N-terminus and its redox activity (Miramar 2001). However, upon certain stimuli, AIF translocates to the nucleus and initiates large scale (50kb) DNA fragmentation and chromatin condensation by recruiting or activating endonucleases (Ye H 2002). The translocation of AIF into the nucleus is impaired in

PARP-1$^{-/-}$ fibroblasts after treatment with the DNA-alkylating agent MNNG that potently activates PARP-1. Exactly how PARP-1 activation triggers the release of AIF from mitochondria is not clear, however a product of poly(ADP-ribose) metabolism could serve as a potential signal (Yu et al., 2000).

Over 20 years ago, Berger suggested that massive DNA damage causes an excessive activation of PARP-1 which, in turn, depletes NAD^+ pools within only a few minutes. Consequently, the main NAD^+-dependent metabolic pathways such as glycolysis and mitochondrial respiration are impaired, leading to reduced ATP production and cellular dysfunction. Moreover, under these precarious conditions phosphoribosyl pyrophosphate synthetase (PPS) and nicotinamide mononucleotide adenylyl transferase (NMNAT) consume ATP in an effort to resynthesize NAD^+, worsening the energetic shortage and contributing to the generation of a lethal, futile cycle (**Figure 6**.) (Berger 1986).

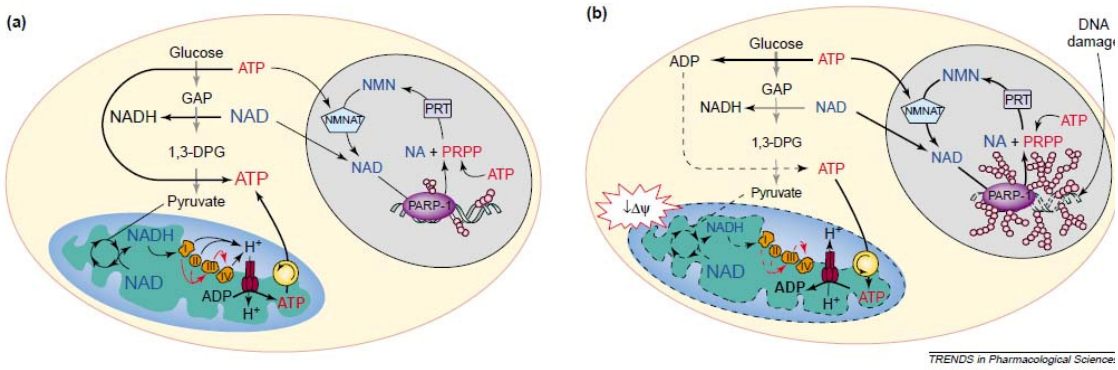

Figure 6. *Normally, in the presence of NAD^+ and pyruvate, the Krebs cycle supplies NADH to the respiratory chain, triggering the electron flux. Mitochondrial respiration generates ATP (**A**.). Overactivation of PARP-1 causes drastic depletion of the pyridine nucleotide pool, consequently the NAD^+-dependent pathways such as glycolysis and mitochondrial respiration are impaired (**B**) (Chiarugi 2002).*

This cellular suicide mechanism has been implicated in the pathomechanisms of neurodegenerative disorders, cardiovascular dysfunction and various other forms of inflammation. Pharmacological inhibition or genetic ablation of PARP-1 significantly improved cellular energetic status and cell viability after exposure to necrosis-inducing agents (**Figure 7.**).

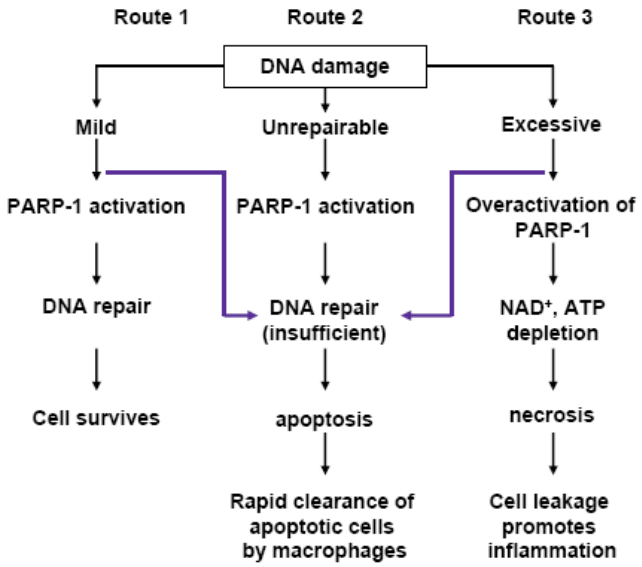

Figure 7. **The intensity of DNA damaging stimuli determines the fate of cells: survival, apoptosis, or necrosis.** *In the case of mild DNA damage, poly(ADP-ribosyl)ation facilitates DNA repair and thus cell survival (route 1). More severe genotoxic stimuli activate the p53 dependent (or independent) apoptotic pathway (route 2). The most severe DNA damage may cause excessive PARP activation, depleting cellular NAD^+/ATP stores leading to necrosis (route 3). Pharmacological inhibition of PARP-1 in cells entering route 1 inhibits repair and thus diverts cells to route 2 (blue arrow). The inhibition of PARP in cells entering route 3 preserves cellular energy stores and thus enables apoptotic machinery to operate (blue arrow) (Virag and Szabo, 2002).*

Important to notice that the mechanism underlying the choice of PARP-1 dependent cell death pathways (i.e. necrosis vs apoptosis) in response to genotoxic stimuli may be influenced by the type, strength and duration of the stimuli, as well as cell type. Actively proliferating cells, such as cancer cells, are dependent on glucose catabolism through anaerobic glycolysis for ATP production. Nonproliferating cells, in contrast, can catabolize a variety of metabolic substrates, including amino acids and lipids, and maintain ATP levels through oxidative phosphorylation in the mitochondria. PARP-1 activation in the nucleus preferentially depletes the nuclear and cytosolic pools of NAD^+, but not the mitochondrial pools, thereby inhibiting glycolysis, but not oxidative phosphorylation. Consequently, proliferating cells are most sensitive to PARP-1 activation, becoming depleted of ATP and dying by necrosis. In contrast, nonproliferating cells are resistant to ATP depletion and cell death under the same condition (Zong 2004). Similarly, in MNNG-treated astrocytes, the decision between cell death or survival is regulated by the availability of metabolic substrates. Supplying substrates that bypass cytosolic glycolysis

for ATP production enhances cell survival (Ying et al., 2005). Thus, PARP-1 activity plays a central role in this form of “programmed necrosis”.

3.4.4. PARP-1 in transcriptional regulation

It is widely accepted that PARP-1 functions as an architectural nucleosome binding factor/chromatine chaperone and as chromatin modifying enzyme. The formation of the negatively charged poly(ADP-ribose) polymers and the transfer of these polymers to acceptor proteins such as histones initiate electrostatic repulsion between histones and DNA. The subsequent remodeling of the chromatin architecture enhances the accessibility of genes for the transcriptional machinery and thus enhances transcription (**Figure 8.**) (D'Amours et al 1999, Chiarugi 2002). The other possibility for PARP-1 to regulate transcription is to function as part of enhancer/promoter binding complexes in conjunction with other DNA binding factors and coactivators.

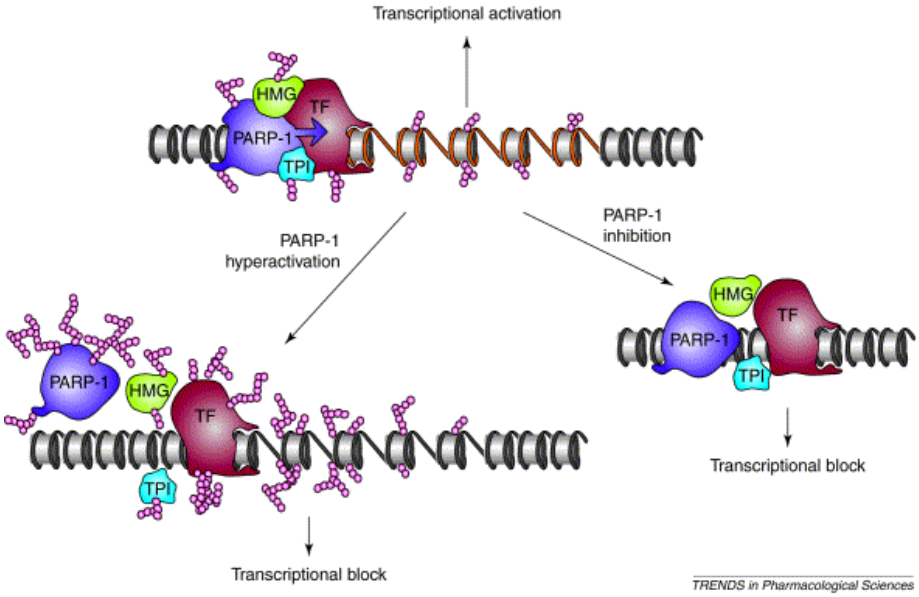

Figure 8. **A proposed model for the control of transcription by PARP-1.** Under basal conditions, the poly(ADP-ribosyl)ating activity of PARP-1 is targeted to histones, causing DNA bending and converting chromatin into a transcriptionally active structure. ADP-ribose chains are also transferred to components of the transcriptional apparatus including transcription factors (TF), proteins of the high mobility group (HMG), topoisomerases (TPI) and PARP-1 itself. This way, poly(ADP-ribosyl)ation participates with acetylation, methylation and phosphorylation in the architectural remodeling of chromatin that assists transcription. Poly(ADP-ribose) also regulates the promoter activity by allowing the proper arrangement of the enhanceosome. In conditions of massive PARP-1 activation, however, the electrostatic repulsion among the negatively charged polymers impairs transcription by

inhibiting enhanceosome assembly and separating PARP-1 from DNA. The same repression of transcription occurs when PARP-1 inhibition blocks poly(ADP-ribose)-induced DNA bending and enhanceosome complex formation (Chiarugi 2002).

PARP-1 has been shown to associate with and regulate the function of several transcription factors: Activating protein-2, AP-2 (Kannan et al., 1999); factor Yin Yang-1, YY1 (Oei et al., 1997); Oct-1 (Nie et al 1998); transcription enhancer factor 1, TEF-1 (Butler and Ordahl, 1999); B-MYB (Cervellera and Sala, 2000; Santilli et at., 2001) and nuclear factor-κB (NF-κB).

Of special interest is the regulation of NF-κB-mediated transcription by PARP-1 bacause NF-κB and PARP-1 have both been demonstrated to play a pathophysiological role in a number of inflammatory disorders. The strongest indication for a direct role or PARP-1 and NF-κB dependent transcription was the impaired expression of NF-κB dependent pro-inflammatory mediators in PARP-$1^{-/-}$ mice.

3.4.4.1.Inflammation

Inflammation is a complex biological response of vascular tissues to harmful stimuli such as pathogens, damaged cells, or irritants. Acute inflammation is the initial response of the body to harmful stimuli and it is achieved by the increased movement of leukocytes from the blood into the injured tissues. It is initiated by cells already present in all tissues, mainly resident macrophages, dendritic cells. At the onset of an infection, these cells undergo activation and release inflammatory mediators (cytokines and chemokines) responsible for the clinical signs of inflammation. The mediator molecules also alter the blood vessels to permit the migration of leukocytes, mainly neutrophils, outside of the blood vessels into the tissue.

Cytokines

Cytokines are substances that are secreted mainly by endothelial, epithelial cells and resident macrophages and which carry signals locally between cells, and thus have an effect on other cells. The current terminology refers to cytokines as immunomodulating agents since they are critical to the development and functioning of both the innate and adaptive immune response. Cytokines act through cell surface receptor on the target cell subsequently initiating cascades of intracellular signaling that alter cell function. This may

include the upregulation and/or downregulation of several genes and their transcription factors, resulting in the production of chemokines and other cytokines, an increase in the number of surface receptors for other molecules, or the suppression of their own effect by feedback inhibition (Carpenter et al., 2002). The cytokines tumor necrosis factor alpha (TNF-α) and interleukin-1beta (IL-1β) are key proinflammatory mediators. Both of them are potent inducers of chemokine production by many cell types including pulmonary epithelial cells. These chemokines produced by airway epithelial cells play a critical role in regulating local inflammatory processes in the lung.

Chemokines

Chemokines are 8-12 kDa, basic proteins that are the major mediators of leukocyte migration. Their name is derived from their ability to induce directed ***chemotaxis*** in nearby responsive cells; they are chemotactic cytokines. There are nearly 50 distinct chemokines and 19 chemokine receptors. Their classification based on 3D structure containing conserved cysteine motifs forming essential disulfide bonds between the first and third and the second and fourth cysteines (Christopherson and Hromas, 2001) (**Figure 9.**) (**Table 1.**).

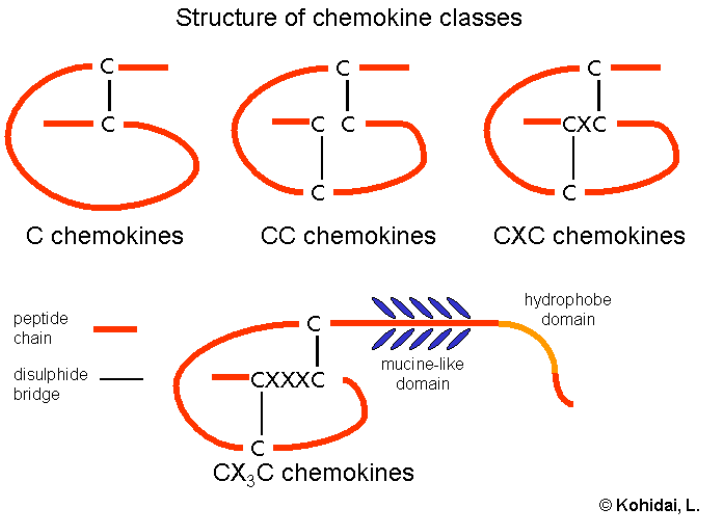

Figure 9. The number and spacing of the first cysteines in the amino acid sequence are used to classify chemokines into four subfamilies: C, CC, CXC, CX3C

family	gene name	gene product name	common name	chemotactic activity
CC	SCYA2	CCL2	MCP-1 monocyte chemotactic protein	monocytes,T cells, basophils, NK cells, progenitors
	SCYA4	CCL4	MIP-1β macrophage inflammatory protein-1β	Monocytes, T cells, dendritic cells, NK cells, progentitors
	SCYA5	CCL5	RANTES Regulated upon Activation, Normal T-cell Expressed, and Secreted	T cells, eosinophils, basophils, NK cells, dendritic cells
	SCYA8	CCL8	MCP-2 monocyte chemotactic protein-2	monocytes, T cells, eosinophils, basophils, NK cells
	SCYA20	CCL20	MIP-3α macrophage inflammatory protein-3	T cells, B cells
CXC	SCYB5	CXCL5	ENA-78 epithelial-derived neutrophil-activating peptide 78	neutrofils
	SCYB6	CXCL6	GCP-2 granulocyte chemotactic protein 2	neutrofils
CX3C	SCYD1	CX3CL1	fractalkine	effector T cells

Table 1. Incomplete list of chemokines, and their target cell types for chemotaxis

The major role of chemokines is to act as chemoattractants to guide the migration of cells. Cells that are attracted by chemokines follow a signal of increasing chemokine concentration towards the source of the chemokine. Some chemokines control cells of the immune system during processes of immune surveillance, such as directing lymphocytes to the lymph nodes so they can screen for invasion of pathogens by interacting with antigen-presenting cells residing in these tissues. These are known as **homeostatic chemokines** and are produced and secreted without any need to stimulate their source cell(s). Some chemokines have roles in **development**; they promote angiogenesis, or guide cells to tissues that provide specific signals critical for cellular maturation**. Inflammatory chemokines** function mainly as chemoattractants for leukocytes, recruiting monocytes, neutrophils and other effector cells from the blood to sites of infection or tissue damage (**Figure 10.**). Certain inflammatory chemokines activate cells to initiate an immune response or promote wound healing. They are released by many different cell types and serve to guide cells of both the innate and the adaptive immune system.

These proteins exert their biological effects by interacting with G protein-linked transmembrane receptors called chemokine receptors that are selectively found on the

surfaces of their target cells. Chemokines can be both beneficial and harmful by either stimulating an appropriate immune response to microbial invasion, or by mediating pathologic tissue destruction in autoimmune diseases, atherosclerosis, allograft rejection, and neoplasia (Laing and Secombes, 2004).

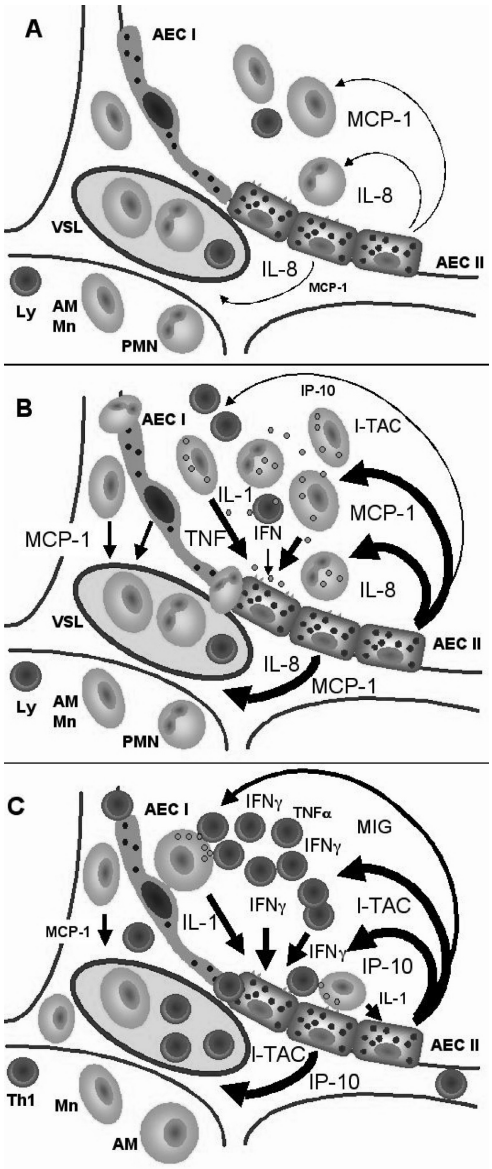

Figure 10. *The attraction of leukocytes from the circulation to inflamed lungs depends on the activation of both the leukocytes and the resident cells within the lung. Alveolar epithelial cells type II (AECII) drive leukocyte trafficking in host defense and specific immune response. The schematic drawing shows spatial distribution of chemokine expression and leukocyte recruitment: in healthy condition (A) two chemokines, MCP-1 and IL-8 are expressed constitutively by AECII and provide the physiological influx of monocytes (Mn), neutrophils (PMN) and lymphocytes (Ly) into alveolar space from pulmonary vasculature (VSL). In the initial phase of alveolar inflammation caused by inflammatory agents (**B**), increasing alveolar macrophage (AM) and particularly epithelial expression of chemokines is paralleled by pronounced recruitment of Mn, PMN, and Ly to the alveolar compartment. Further development of the immune response (**C**) leads to the expression of high levels of CXCL9, CXCL10, and CXCL11 in AEC-II induced by IFN-γ and/or TNF-α, and IL-1β and associated with recruitment of activated T cells (Th1) to the interstitium and alveolar space (Pechkovsky DV 2005).*

Among the transcription factors that are involved in the signalling pathways during the inflammatory processes we have focused on the NF-κB and AP-1 in this study.

NF-κB

NF-κB encompasses a family of inducible transcription factors, which has traditionally been linked to cellular immune and inflammatory response. These proteins

share a conserved 300-amino acid region within their amino termini, termed the Rel homology domain, which is responsible for DNA binding, dimerization, nuclear translocation, and interaction with heterologous transcription factors. All vertebrate Rel proteins can form homodimers (e.g. p50-p50, p65-p65, cRel-cRel) or heterodimer (p50-p65) except for RelB, which can only form heterodimers (e.g. p50-RelB, p65-RelB). The classical heterodimer NF-κB consists of the two subunits p50 and p65. In most cells, NF-κB is present as a latent, inactive, IκB (inhibitor κB)-bound complex in the cytoplasm. Treatment of cells with cytokines such as **IL-1 or TNF-α**, viral proteins, LPS, phorbol esters, UV or γ-irradiation leads to the rapid phosphorylation of IκB that leads to the ubiquitination and subsequently to the proteasomal degradation of the inhibitory protein. In turn, NF-κB rapidly enters the nucleus and activates gene expression by binding to 9-10 bp DNA sites as dimers. NF-κB plays a central role in the regulation of gene expression of many genes involved in mammalian immune and inflammatory responses, including cytokines, cell adhesion molecules, complement factors, and a variety of immune receptors (Gilmore 1999, Hassa and Hottiger 2002), (**Figure 11.**).

AP-1

The redox sensitive transcription factor AP-1 is composed of a mixture of heterodimeric protein complexes derived from the Fos and Jun families, including c-Fos, FosB, Fra-1, Fra-2, c-Jun, JunB and JunD (Wisdom R 1999). AP-1 activity was found to be induced by many stimuli including serum, growth factors, cytokines, T cell activators, UV irradiation, phorbol esters and oncogenes. Depending on the composition of the dimers they recognize either 12-O-tetradecannoylphorbol-13-acetate response elements (TRE, 5'-TGA(G/C)TCA)-3') or cAMP-resonse element (5'-TGACGTCA-3') which are located in the promoter region of genes encoding cytokines, chemokines, adhesion molecules and transcription factors. Whereas Jun/Fos heterodimers preferentially bind to the TRE elements, dimers containing ATF2 (e.g. ATF2/ATF2 or c-Jun/ATF2 dimers) bind to cAMP-response element). Phosphorylation of AP-1 family members by mitogen-activated protein kinases JNK, p38MAPK, and ERK1/2 is required for transactivation activity (**Figure 11.**).

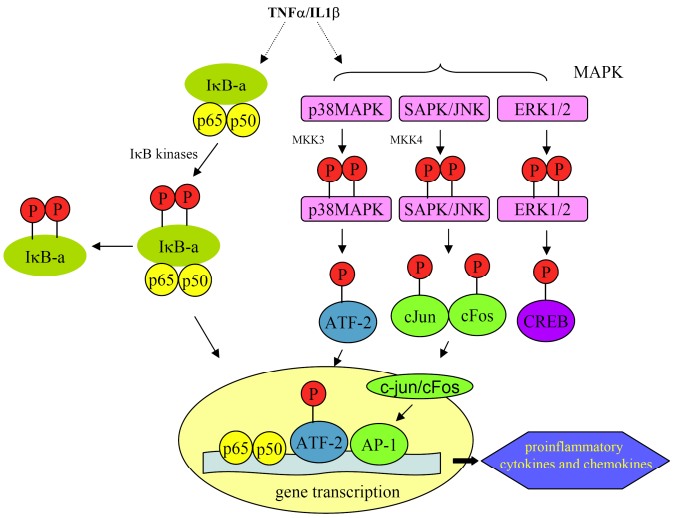

Figure 11. Schematic illustration of key molecular events and signaling pathways induced by inflammatory cytokines. *Activation of NF-κB has been shown to occur through the activation of upstream protein kinases, phosphorylating the IκB kinase complex. Activation of this complex serves to mediate phosphorylation, ubiquitination, and degradation of IκB followed by nuclear translocation of NF-κB. Phosphorylation of AP-1 family members (c-Jun, cFos, ATF2) by mitogen activated protein kinases lead to their dimerization and subsequently DNA binding.*

3.4.4.2. Role of PARP-1 in inflammation

De Murcia's group identified deficient NF-κB activation as the underlying mechanism of the endotoxin resistance of PARP-$1^{-/-}$ mice. In TNFα treated fibroblasts, IκB degradation and nuclear translocation of p65 was found unaltered in PARP-$1^{-/-}$ cells whereas DNA binding of p65 was markedly reduced. Thus, it was proposed that PARP-1 is required for NF-κB-mediated transactivation (Oliver et al., 1999). Chang and Alvarez-Gonzales (2001) found that non-poly(ADP-ribosyl)ated PARP-1 can bind to NF-κB-p50 + consensus oligonucleotide complex. Upon modification of PARP-1, the complex dissociated suggesting that PARP-1 enzyme activity regulated the interaction between the enzyme and the transcription factor. However, Hassa and Hottiger have demonstrated that DNA binding and catalytic activity of PARP-1 is not required for the NF-κB coactivator function. They proposed that PARP-1 physically interacts with the Mediator complex, p300/CBP and with both subunits of NF-κB (p50 and p65), resulting in enhanced transactivation (Hassa et al., 2003).

However, the requirement for PARP-1 enzymatic activity for the NF-κB coactivator function is in line with the anti-inflammatory effect of PARP inhibitors, as reflected by suppressed production in inflammatory mediators in animals treated with PARP inhibitors. Many studies have demonstrated that PARP inhibitors selectively regulated the expression of cytokines and chemokines in inflammatory disease models. Defective iNOS expression both at the level of protein and mRNA in LPS- and IFN-γ stimulated PARP-$1^{-/-}$ fibroblast cells was observed by Szabo (1998). Furthermore, PARP-1 inhibition reduced the expression of ICAM-1, P-selectin, E-selectin and mucosal addressin cell adhesion molecule-1 in cytokine-stimulated human umbilical vein endothelial cells. Moreover, decreased expression of these adhesion molecules has also been found after reperfusion injury in the hearts of PARP-1 deficient mice compared with their wild-type counterparts (Virag and Szabo, 2002). Reduced expression of chemokines and adhesion molecules may be responsible for the reduced migration of inflammatory cells, the most common anti inflammatory effect of PARP inhibition as observed in animal studies (Zingarelli et al.1998; Hasko et al., 2002). However, it is not known whether macrophages or parenchymal cells are the main targets of PARP inhibitors in these diseases.

PARP-1 has also been implicated in the regulation of AP-1-driven transcriptional activity. Zingarelli's group reported alterations in AP-1 activation in oxidatively stressed or IL-1-treated murine PARP-1 knockout fibroblast. They found decreased AP-1 DNA binding in PARP-$1^{-/-}$ cells after peroxynitrite, hydrogen peroxide or IL-1 stimuli. Furthermore, increased basal JNK activity and c-Jun phosphorylation were found to accompany these changes (Andreone et al., 2003). In a myocardial reperfusion injury model, the same group reported that cardioprotection observed in PARP-$1^{-/-}$ mice was associated with a reduction of AP-1 DNA binding. Microarray analyses revealed that expression of several AP-1-dependent genes of proinflammatory mediators and heat shock proteins was altered in knockout animals (Zingarelli et al., 2003).

We can conclude that the function of PARP-1 and poly(ADP-ribosyl)ation as a regulator of inflammatory signal transduction and transactivation shows marked cell-type and stimulus dependency.

4. AIMS OF THE STUDY

Three different studies (Boulares et al., 2003; Virág et al., 2004; Suzuki et al., 2004) have provided evidence for the involvement of PARP activation in rodent models of asthma. PARP inhibitors and PARP-1 knockout phenotype provided protection against the allergic inflammation. Moreover, a common finding in all three studies was the reduction of inflammatory cell migration by PARP inhibition or the PARP-1 knock out phenotype. Virag et al. (2004) have indicated that this effect may be selective as the PARP inhibitor suppressed mainly the migration of neutrofil cells but not of eosinophils. All three studies have also indicated that PARP-1 is involved in the regulation of the production of certain proinflammatory cytokines and chemokines and other inflammatory mediators. However, the exact molecular mechanism for that and the possible role of PARG in these processes is fairly unknown.

On the other hand, many of pharmacological studies as well as numerous reports based on the use of PARP-1 knock out mice have demonstrated that inhibition or genetic ablation of PARP-1 provides remarkable protection from oxidative stress-related conditions (Virag and Szabo 2002). Little is known, however, about the role of poly(ADP-ribose) polymers and PARG protein in these cellular events.

For these reasons we would like

1. to investigate the effect of PARP-1 inhibitor PJ34 and a potent PARG inhibitor gallotannin in the TNFα/IL-1β induced chemokine and cytokine gene-expression in A549 human lung epithelial cells, and

2. the role of PARP-1 and PARG proteins in hydrogen peroxide induced cell death in A549 cells.

5. MATERIALS AND METHODS

5.1. Cell culture and treatments

All experiments involved A549, a human lung adenocarcinoma cell line representative of distal respiratory epithelium. The cell line was grown and maintained in a 5% CO_2 incubator at 37°C using RPMI-1640 containing 10% fetal bovine serum (FBS) and 100 U/mL penicillin, and 100 µg/mL streptomycin (Sigma-Aldrich Co., St. Loius MO). Before the cytokine treatment, cells were grown to confluency and incubated in serum-free medium for 12 hours. Where used, 10 µM PARP inhibitor PJ34 (Inotek Corporation, Beverly, MA.) (for detailed information on PJ34, see Jagtap and Szabo (2005)) and the PARG inhibitory 30 µM gallotannin (GT) (Fluka, Sigma-Aldrich Co., St. Loius MO) were added 30 min prior to stimulation by recombinant human TNFα (20 ng/mL) and recombinant human IL-1β (5 ng/mL), both purchased from R&D Systems (Minneapolis, MN). Transformed human kidney cell line, HEK 293T, was maintained in Dulbecco's modified Eagle's medium (DMEM) supplemented with 10% FBS, 2 mM glutamine, 100 U/mL penicillin, and 100 µg/mL streptomycin at 37°C, 5% CO_2.

Mesenhymal stem cells were isolated from umbilical cords according to Jo et al (2008) and maintained in DMEM containing 10% fetal bovine serum (FBS) and 100 U/mL penicillin, and 100 µg/mL streptomycin (Sigma-Aldrich Co., St. Loius MO) at 37°C, 5% CO_2 after obtaining informed consent from donors. The protocol was approved by the Ethical Board of the Medical and Health Science Center of the University of Debrecen under permission no. 2754-2008.

Unless specified otherwise, all reagents were purchased from Sigma-Aldrich Co. (St. Loius MO.)

5.2. Production of lentiviruses and infection of A549 cells

For shRNA-mediated stable knockdown, we employed a Mission Lentiviral-mediated gene specific shRNA system (Sigma-Aldrich Co., St. Loius MO). Short-hairpin RNAs (shRNAs) cloned into the lentivirus vector pLKO.1-puro were chosen from the human libary (MISSION TRC-Hs 1.0) and purchased in bacterial glycerol stock form. pLKO.1-puro empty vector was used as a negative control. Lentiviral vectors were produced and used according to the manufacturer's protocol. In brief, bacterial glycerol stocks were propagated in LB Broth Base medium overnight and purified using Wizard Plus Midipreps

DNA Purification System (Promega Co., Madison WI). Five different shRNAs to hPARP-1 and PARG were transiently transfected into HEK 293T cells using polyethylenimine (PEI) as a transfection reagent and subsequently tested for silencing efficiency by RT-PCR and Western blot; the shRNA CCG-GGC-AGC-TTC-ATA-ACC-GAA-GAT-TCT-CGA-GAA-TCT-TCG-GTT-ATG-AAG-CTG-CTT-TTT (sense-linker-antisense) for PARP-1 and CCG-GGC-CTA-GGA-AAT-TCT-CCT-CCA-TCT-CGA-GAT-GGA-GGA-GAA-TTT-CCT-AGG-CTT-TTT-G (sense-linker-antisense) for PARG were chosen for stable transduction, since they were most efficient in knockdown of both mRNA and protein. The control shRNA and the shRNAs to PARP-1 and PARG were cotransfected with the packaging plasmids (Sigma-Aldrich Co., St. Loius MO) into HEK 293T cells to generate lentivirus particles using PEI as a transfection reagent. Infectious lentiviruses were harvested at 48 hours posttransfection and filtered through 0,45 μm nitrocellulose filters. Virus titers were determined by cell culture titration; 10-fold serial dilutions of the concentrated viruses were used to infect 10^5 A549 cells in a six-well plate. After 24 hours, transduced cells were selected and expanded in the presence of puromycin at final concentration of 5 μg/mL. Seven days later cells were fixed with 4% formaldehyde and subsequently stained with hematoxyline for 20 min at room temperature. Cells were then washed with tapwater and air dried, colonies were counted and virus titers were calculated. The infection of A549 cells with control, shPARP-1 and shPARG lentivirus particles was carried out by addition of lentivirus into the cell culture with a multiplicity of infection of 10. Following transduction, virus-containing supernatant was removed after 24 hours and cells were selected with 5 μg/mL puromycin.

5.3. Macroarray

Profiles of TNFα/IL-1β-induced gene expression from A549 cells were determined by using the protocol of GEArray pathway-specific expression arrays from SuperArray (Superarray Bioscience Co., Frederick, MD). After treatment with TNFα and IL1-β for 4 hours, total RNA (2 μg) was isolated using SV Total RNA Isolation System (Promega Co., Madison WI) according to the manufacturer's instruction. Concentration and purity of the isolated RNA was measured spectrophotometrically at 260 nm and 280 nm. For the synthesis of cDNA probe, GEAprimer mix and reverse transcriptase primers were used. The resulting cDNA probes were hybridized to gene-specific cDNA fragments on the membranes. The relative expression level of each gene was determined by comparing the

signal intensity of each gene in the array to the signal of housekeeping genes (β-actin and GAPDH).

5.4. RNA isolation and RT-PCR

Total RNA was isolated using TRIZOL (Applied Biosystems, Foster City, CA) according to the manufacturer's instruction. Concentration and purity of the isolated RNA was measured spectrophotometrically at 260 nm and 280 nm. Reverse transcription was performed using MMLV-Reverse Transcriptase (Promega Co., Madison WI). A mix of 2 μg total RNA and 1 μL of Random Primers (Promega Co., Madison WI) in a total volume of 15 μL was incubated for 5 min at 70°C and cooled on ice. After adding 5 μL of M-MLV 5x Reaction Buffer (Promega Co., Madison WI), 10 mM dNTPs, 1 μL Ribonuclease Inhibitor (Promega Co., Madison WI) and finally 2 μL of MMLV Reverse Transcriptase (Promega Co., Madison WI) in a total volume of 25 μL, the reaction mix was incubated for 1 hour at 37°C.

PCR reactions for **chemokine and cytokine** mRNA-s were performed using RedTaq Polymerase (Sigma-Aldrich Co., St. Loius MO) in a reaction mixture containing 2.5 U polymerase, 10 nmol of each primer, 4-8 μL cDNA and PCR buffers as supplied by the manufacturer in a total volume of 50 μL. PCR conditions were as follows: 1 cycle of denaturation at 94°C for 2 min; 30 cycles of denaturation at 92°C for 30 sec, annealing at the calculated Tm °C (see in Table 2.) for 30 sec and extension at 72°C for 30 sec (IL-1β, MIP-1β, IL-1α, MCP-2, RANTES, IL-8, MCP-1) or 1 min (β-actin); 1 cyle of final extension at 72°C for 10 min.

PCR reactions for **PARP-1 and PARG** genes were performed using GoTaq Polymerase (Promega Co, Madison WI) in a reaction mixture containing 5 U polymerase, 10 nmol of each primer, 2-4 μL cDNA and PCR buffers as supplied by the manufacturer in a total volume of 25 μL. PCR conditions were as follows: 1 cycle of denaturation at 94°C for 2 min; 30 cycles of denaturation at 92°C for 30 sec, annealing at the calculated 63°C for 30 sec and extension at 72°C for 1 min; 1 cyle of final extension at 72°C for 10 min. Products were run on 1-2% agarose gel and visualized by ethidium bromide staining. PCR primers used for the analysis were designed based on sequences deposited in the UniGene database. Their sequence, calculated Tm and expected lenghts of PCP products are listed in **Table 2**.

Primer	Accession number	Sequence (5' to 3')	Tm (°C)	Expected product size (bp)
IL-1β	AY137079		59	363
forward		GAA GTA CCT GAG CTC GCC AG		
reverse		GTT CAG TGA TCG TAC AGG TGC		
MIP-1β	NM_002984		62	279
forward		GAA GCT CTG CGT GAC TGT CCT		
reverse		CAT ACA CGT ACT CCT GGA CCC		
IL-1α	X03833		62	350
forward		GCT ATG GCC CAC TCC ATG AAG		
reverse		AGC AGC CGT GAG GTA CTG ATC		
MCP-2	X99886		59	259
forward		GGT TTC TGC AGC GCT TCT GT		
reverse		CTT CAT GGA ATC CCT GAC CC		
RANTES	NM_002985		72	162
forward		ACC ACA CCC TGC TGC TTT GCC TAC ATTGCC		
reverse		CTC CCG AAC CCA TTT CTT CTC TGG GTT GGC		
IL-8	NM_000584		67	272
forward		GAC TTC CAA GCT GGC CGT GGC T		
reverse		ACT TCT CCA CAA CCC TCT GCA CC		
β-actin	NM_001101		61	712
forward		CGG GAA ATC GTG CGT GAC AT		
reverse		GAA CTT TGG GGG ATG CTC GC		
MCP-1	NG_012123		56	150
forward		GAT CTC AGT GCA GAG GCT CG		
reverse		TGC TTG TCC AGG TGG TCC AT		
hPARP-1	NM_001618		63	740
forward		CGT CAC TGC CTG GAC CAA GTG		
reverse		GCC CAA AGC AGA GGA CAG AAG A		
hPARG	NM_003631		63	769
forward		GCC CAA AGC AGA GGA CAG AAG A		
reverse		CGG TTT CCT TGAT GAA CGT CCC		

Table 2. Primers used in the PCR reactions

5.5. Real Time mRNA analysis

Two microgram of RNA was reverse transcribed as described above. Quantitative real-time PCR analysis was performed using an ABI PRISM 7500 sequence detector system (Applied Biosystems, Foster City, CA). Power SYBR Green PCR Master Mix reagents were purchased from Applied Biosystems and reactions were carried out according to the manufacturer's protocol in 25 μL total volume. For real-time monitoring, 40 cycles of 94°C for 30 sec and 63°C for 1 min were performed. The relative abundance of mRNAs was calculated by the comparative cycle of threshold (C_T) method with β-actin mRNA as the invariant control. The primers used for PCR were are listed in **Table 3.**

Primer	Sequence (5' to 3')
hACTIN	
forward	GAA GTA CCT GAG CTC GCC AG
reverse	TGA TCC ACA TCT GCT GGA AGG T
hPARP-1	
forward	CAG CTT CAT AAC CGA AGA TTG CT
reverse	CGA AAT AGA TCC CTT TAC CAA ACA TG
hPARG	
forward	CTG TTG GAG ATG TGT ATA AGC TGT TG
reverse	GGA CTC GAC AGC ATG GTA TAT GAA

Table 3. Primers used in the Real Time quantitative PCR reactions

5.6. Nuclear extract preparation for EMSA analysis

Nuclear protein extracts were prepared from treated cells grown to 90% confluence in T25 culture flasks. All nuclear extraction procedures were performed on ice with ice-cold reagents. Cells were washed with PBS and harvested by scraping into 1 mL of PBS and pelleted at 5,000 rpm for 5 min. The pellet was resuspended in 400 μL of buffer „A" (10 mM HEPES pH 7.9, 10 mM KCl, 0.1 mM EDTA, 0.1 mM EGTA, 1 mM DTT, 0.5 mM PMSF, protease inhibitors) and allowed to swell on ice for 15 min. After adding Nonidet P-40 to a final concentration of 0.5%, the cells were vortexed for 10 sec. After centrifugation at 10,000 rpm for 2 min the pellet was isolated and resuspended in 50 μL of buffer „B" (20 mM HEPES pH 7.9, 420 mM NaCl, 0.5 mM EDTA, 0.5 mM EGTA, 1 mM DTT, 0.5 mM PMSF, protease inhibitors) and incubated on ice for 20 min with occasional vortexing. Nuclear extracts were recovered after centrifugation for 10 min at 10,000 rpm. Protein

concentrations were determined with Coomassie Plus Protein Assay reagent (Pierce Biotechnologie Inc., Rockford, IL) and samples were stored at -70^{o}C until use for EMSA.

5.7. Electrophoretic mobility shift assay (EMSA)

The consensus NF-κB (5'-AGTTGAGGGGACTTTCCCAGG-3') and AP-1 (5'-CGCTTGATGACTCAGCCGGAA-3') probes were obtained from Sigma-Aldrich (St. Loius MO). The probes were labeled with 1-3 biotinylated ribonucleotides using Biotin 3'End DNA labeling kit (Pierce Biotechnologie Inc., Rockford Illinois) following the manufacturer's instruction. Gel shift assay was performed using a LightShift Chemiluminescent EMSA kit (Pierce Biotechnologie Inc., Rockford, IL). Briefly, binding reactions containing 10 μg of nuclear extracts and 1 nmol oligonucleotide were performed for 30 min in binding buffer (2.5% glycerol, 0.05% Nonidet P-40, 50 mM KCl, 5 mM $MgCl_2$, 1 mM EDTA, 10 mM Tris pH 7.6, 50 ng poly(dI·dC)). Protein-nucleic acid complexes were resolved using a non-denaturating polyacrylamide gel consisting of 5% acrylamide (29:1 ratio of acrylamide/bisacrylamide) and run in 0.5x TBE (45 mM Tris-HCl, 45 mM boric acid, 1 mM EDTA) for 1 hour at constant voltage (100 V). Gels were transferred to Bio Bond-Plus nylon membrane (Sigma-Aldrich Co., St. Loius MO) (80 mA, 45 min). DNA was cross-linked to the membrane by UV-cross-linker. DNA was incubated in blocking solution (supplied by the LightShift kit) followed by the incubation of the membrane with streptavidin-peroxidase. After extensive washing, signal was detected with chemiluminescence solution (supplied with the kit).

5.8. Western blot analysis

Cells were maintained in 6 well plates or T25 flask. Following treatment, cells were washed once in PBS and collected by scraping into 200 μL ice-cold lysis buffer containing 62.5 mM Tris-HCl pH 6.8, 2% SDS, 10% glycerol, 50 mM DTT, 1 mM PMSF, 1 mM NaF, 1 mM Na_3VO_4, protease inhibitors. The extracts were further lysed with sonication and supernatant was collected after centrifugation. Protein concentrations were determinated using the Coomassie assay and 20 μg protein was loaded per lane on an 10% SDS-polyacrylamide gel. For poly(ADP-ribose)polymer analysis, proteins were loaded on 8% SDS-polyacrilamide gel, then separated electrophoretically and transferred to nitrocellulose membranes. For immunoblotting, membranes were blocked with 5% non-fat dry milk in Tris-buffered saline containing 0.05% Tween20 (TBSTw) for 90 min. Primary

antibodies against phospho-IκB-α (Ser32/36); JNK/SAPK, phospho-JNK/SAPK (Thr183/Tyr185); p38MAPK, phospho-p38MAPK (Thr180/Tyr182), phospho-ATF2 (Thr71), phospho-ERK (Thr202/Tyr204), phospho CREB (Ser133) were purchased from Cell Signaling Technology (Beverly, MA); phospho-cJun (Ser63/73) from Santa Cruz Biotechnology (Santa Cruz, CA.); hPARP-1 from AbCam (Cambridge, MA), ATP5B from Sigma-Aldrich (St. Loius, MO.). For poly(ADP-ribose) polymer detection 10H (Biomol GmbH, Hamburg, Germany) were applied. Primary antibodies were diluted 1:1000 in 1% non-fat dry milk/PBSTw overnight at 4°C. After washing three times in TBSTw, secondary antibodies (peroxidase-conjugated goat anti-mouse IgG or anti-rabbit IgG, (Sigma-Aldrich Co., St. Loius MO) were applied at 5000 fold of dilutions in 1% non-fat dry milk/PBSTw for 1 hour. Blots were washed in TBSTw three times, once in TBS, incubated in ECL, Supersignal WestPico Chemiluminescent substrate (Pierce Biotechnologie Inc., Rockford IL) and exposed to photographic film.

5.9. Immunofluorescent staining

NF-κB p65 polyclonal antibody (Santa Cruz Biotechnology, Santa Cruz, CA.) was used to monitor NF-κB nuclear translocation. Poly(ADP-ribose) was detected using 10H monoclonal anti-poly(ADP-ribose) antibody (Biomol GmbH, Hamburg, Germany). Immunocytochemistry was performed as described earlier (Bürkle et al, 1993) with slight modifications as follows. Cells were treated in ice-cold 10% trichloroacetic acid (TCA) for 10 min, fixed by successive 5 min washes in 70%, 90%, and 100% ethanol at -20°C. In case of and NF-κB nuclear translocation, TCA treatment was omitted. Following rehydration with PBS, coverslips were blocked in 5% horse serum diluted in PBS-Triton X-100 (PBS-Tx) for 1 hour and were then incubated with the first antibody diluted in the blocking buffer (1:200) overnight at 4°C. After 5x5 min washes in PBSTx, coverslips were incubated with biotinylated horse anti-mouse or anti-rabbit IgG diluted in blocking buffer (1:300) for 1 hour at room temperature. Excess antibody was removed by 5x5 min washes in PBSTx. Incorporated biotin was detected by streptavidin-AlexaFluor-488 (Molecular Probes, Eugene, OR) diluted in PBS (1:100) for 30 min at room temperature. Coverslips were washed (4x5 min) with PBS, mounted in Antifade medium and viewed with a Zeiss Axiolab microscope. Pictures were taken with a Zeiss Axiocam digital camera.

5.10. Immunofluorescent staining of AIF and confocal microscopy

For monitoring the AIF translocation we used AIF antibody (Santa Cruz Biotechnology, Santa Cruz, CA.). Following hydrogen peroxide treatment cells were washed with PBS than fixed by 10% paraformaldehyde, diluted in PBS, for 10 min. Cells were than washed with PBS and blocked in 1% BSA diluted in PBS-Tx for 1 hour. Coverslips were then incubated with the first antibody diluted in the blocking buffer (1:200) overnight at 4°C. After 5x5 min washes in PBSTx, coverslips were incubated with biotinylated horse anti-rabbit IgG diluted in blocking buffer (1:300) for 1 hour at room temperature. Excess antibody was removed by 5x5 min washes in PBSTx. Incorporated biotin was detected by streptavidin-AlexaFluor-488 (Molecular Probes, Eugene, OR) diluted in PBS (1:100) for 30 min at room temperature. For nuclear staining 1 µg/mL propidium iodide, diluted in PBS, was used for 5 min. Coverslips were then washed with PBS, mounted in Antifade medium. Images were taken with Olympus FV1000 confocal laser scanning microscope. For visualizing the distribution of AIF three-dimensional stacks were acquired at 1-µm optical thickness. Three-dimensional reconstructions and x-y-z projections were created with the FV10-ASW 1.7 software.

5.11. Immunocytochemical detection of poly(ADP-ribose)

Monitoring the effect of shRNAs, cells were treated with hydrogen peroxide for different periods of time. Cells were then fixed in ice cold methanol for 10 min and hydrated by successive 5 min washes in PBS. Endogen peroxidase activity was eliminated by hydrogen peroxide treatment (0.5% hydrogen peroxide diluted in methanol) for 10 min at room temperature followed by washing with PBS. Coverslips were blocked in 1% BSA diluted in PBS-Tx for 1 hour and were then incubated with 10H monoclonal anti-poly(ADP-ribose) antibody (Biomol GmbH, Hamburg, Germany) diluted in blocking buffer (1:100) for 2 hours at room temperature. After 4x5-min washes in PBSTx, coverslips were incubated with biotinylated horse anti-mouse IgG, diluted in blocking buffer (1:300) for 1 hour at room temperature. Excess antibody was removed by 4x5-min washes in PBSTx, and the bound antibody was visualised with the ABC detection system (Vector Laboratories, Burlingame, CA) and 3,3'-diaminobenzidene substrate. Coverslips were viewed with a Zeiss Axiolab microscope (Carl Zeiss, Oberkochen, Germany). Pictures were taken with a Zeiss Axiocam digital camera.

5.12. Phosphatase activity assay

The catalytic subunits of protein phosphatase 1 (PP1c) and 2A (PP2A) were prepared from rabbit skeletal muscle and the two types of phosphatase were separated by heparin-Sepharose chromatography (Gergely et al., 1984). PP1c was purified from the heparin-Sepharose-bound fraction to homogenity on an affinity coloumn prepared by coupling the N-terminal PP1c-binding fragment of the myosin phosphatase target subunit to Sepharose matrix (Toth et al., 2000). PP2A was further purified from the heparin-Sepharose flow through fractions on a fast protein liquid chromatography Mono Q Column (Amersham Biosciences, Uppsala, Sweden). Phoshatases were incubated for 5 minutes with GT at final concentrations of 0.5, 2, 10, 50 μM. The activity of PP1c and PP2A was determined with ^{32}P-labeled 20-kDa gizzard myosin light chain as substrate. Assays were performed at 30°C for 10 min, then the released $^{32}P_i$ was determined (after precipitation of proteins with 10% TCA and centrifugation at 10,000 rpm for 1 min) from the supernatant in a liquid scintillation analyzer (Tricarb 2800TR, Perkin-Elmer, Waltham, MA).

5.13. ABTS-assay

The antioxidant capacity was determined using the $ABTS^+$ decolorisation assay (Re et al., 1998). 2,2'-Azino-bis-(3-ethylbenzothiazoline-6-sulfonic acid) (ABTS) (Sigma-Aldrich Co., St. Loius MO) was used as a free radical provider and was generated by reacting this compound (7.4 mM) with potassium persulphate (2.45 mM) overnight. The solution was diluted with Glycine-HCl (50 mM, pH 4.5) to obtain an absorbance of 1.5 at 414 nm. An aliquot (140 μL) of the solution was added to 10 μL of sample into 96 well plate and the standard curve was prepared using similar volume of L-ascorbic acid. All readings were taken with Multiskan MS plate reader (Labsystem, Vantaa, Finland) after 30 min of reaction time when the absorbance appeared to reach a plateau.

5.14. DHR-assay

Peroxynitrite scavenging effect was measured by monotoring the oxidation of dihydrorhodamine DHR123 (Molecular Probes, Eugene, OR) according to a modification of the method of Kooy et al. (1994). The working solution of DHR123 was 5 μM diluted in (90 mM NaCl, 50 mM Na_2PO_4 pH 7.4, 5 mM KCl). Peroxynitrite scavenging by the

oxidation of DHR123 was measured with a Fluoreskan Ascent FL plate reader (Thermo Labsystem, Vantaa, Finland) with exitation and emission wavelength of 485 and 527 nm, respectively, at room temperature in the presence or absence of the test-compound. Final concentration of peroxynitrite was 50 μM.

5.15. Measurement of PARP activity

PARP activity of cell lysates was determined with the classical PARP activity assay based on the incorporation of isotope from ^{3}H-NAD^{+} into TCA precipitable proteins, as described (Virag et al., 1998). Briefly, cells were seeded into 6 well plates overnight, medium was removed from the cells 20 min after hydrogen-peroxide treatment and cells were incubated at 37°C in 0.5 mL assay buffer [56 mM HEPES pH 7.5, 28 mM KCl, 28 mM NaCl, 2 mM $MgCl_2$, 0.01% digitonin, and 0.125 μM ^{3}H-NAD^{+} (0.5 μCi per mL)]. Cells were then scraped and transferred into eppendorf tubes. Next, 200 μL ice-cold 50% TCA was added to the samples and tubes were incubated for 4 hours at 4°C. Samples were then spin down (10,000 rpm, 10 min) and the pellets were washed twice in ice-cold 5% TCA and solubilized overnight in 250 μL 2% SDS/0.1 N NaOH at 37°C. The contents of the tubes were added to scintillation liquid and radioactivity was determined in a liquid scintillation analyzer (Tricarb 2800TR, Perkin-Elmer, Waltham, MA).

5.16. Cell viability assay (MTT)

Cell viability was assessed by the colorimetric MTT assay, as described previously (Virag et al., 1998). Briefly, cells were treated with hydrogen peroxide in a 96 well plate. 24 hours later MTT was added to the cells in a final concentration of 0.5 mg/mL and incubated for an additional hour. The medium was then aspirated and the formazan crystals were dissolved by the addition of 100 μL dimethylsulphoxide. Optical density was determined in a Multiskan MS plate reader (Labsystem, Vantaa, Finland) at 550 nm test wavelength with 690 nm as a reference wavelength.

5.17. Intracellular NAD^{+} measurement

The recycling assay was used with minor modifications, as described (Ying et al., 2001). Cells were seeded into six well plates a day before the experiment. 24 hours after hydrogen peroxide treatment, cells were extracted in 0.5 N $HClO_4$, neutralized with 3 M

KOH/125 mM Gly-Gly buffer (pH 7.4), and centrifuged at 10,000 rpm for 5 min. Supernatants were mixed with a reaction medium containing 0.1 mM 3-[4,5-dimethylthiazol-2-yl]-2,5-diphenyl-tetrazolium bromide, 0.9 mM phenazine methosulfate, 13 U/ml alcohol dehydrogenase, 100 mM nicotinamide, and 5.7% ethanol in 61 mM Gly-Gly buffer (pH 7.4). Absorbance was determined in a Multiskan MS plate reader (Labsystem, Vantaa, Finland) at 560 nm immediately and after 10 min. NAD^+ levels were calculated from a standard curve generated with known concentration of NAD^+.

5.18. Assessment of intracellular ATP levels

To measure intracellular ATP levels, we used the luminometric ApoSENSOR Cell Viability Assay Kit (BioVision, Mountain View, CA) according to the manufacturer's protocol. Following 24 hours of hydrogen peroxide treatment ATP concentration was calculated as a percentage of untreated cell control. Assays were performed in three independent experiments.

5.19. Clonogenic assay

A single cell suspension was prepared at a density of $5x10^5$ cells/mL by treatment with 0.05% trypsin + 0.02% EDTA. After treatment with hydrogen peroxide for 1 hour at 37°C, cells were washed in order to remove hydrogen peroxide. Cells were further diluted in culture medium to get 10^2 up to 10^4 cells/mL and plated onto 6 well plates followed by culture at 37°C for 10 days. Cells were fixed with 4% formaldehyde, then stained with hematoxilin for 10 min. After intensive washing with tap water, plates were air dried and colonies were counted.

5.20. Propidium-iodide uptake

Hydrogen peroxide-induced cytotoxicity was measured by propidium iodide uptake as described previously (Bai et al., 2001). Cells were seeded into six well plates the day before the experiment. After 24 hours of hydrogen peroxide treatment, cells were stained with 5 μg/mL propidium iodide (PI) solution for 15 min. Floating and adherent cells were then collected and centrifuged for 5 minutes at 2000 rpm, washed with PBS and analyzed by FACS Calibur flow cytometer (BD Biosciences San Jose, CA) and analyzed with the WinMDI software.

5.21. Measurement of caspase activation

Caspase-3-like activity was measured by the cleavage of the fluorogenic tetrapeptide-amino-4-methylcoumarine conjugate (DEVD-AMC) as described previously (Virag et al., 1998), with modifications as follows. 24 hours after hydrogen peroxide exposure, floating and adherent cells were pooled and resuspended in lysis buffer (10 mM HEPES, 0.1% m/v CHAPS, 5 mM DTT, 2 mM EDTA, 10 μg/mL aprotinin, 20 μg/mL leupeptin, 10 μg/mL pepstatin A, and 1 mM PMSF, pH 7.25). Cell lysates and substrates (50 μM) were combined in triplicate in the caspase reaction buffer (100 mM HEPES, 10% sucrose, 5 mM DTT, 0.1% CHAPS, pH 7.25) and incubated for 1 hour at 37^{o}C. Fluorescence of released AMC has been measured by a Fluoreskan Ascent FL plate reader (Thermo Labsystem, Vantaa, Finland) at excitation wavelength of 380 nm and emission wavelength of 460 nm.

5.22. Detection of DNA fragmentation

Internucleosomal DNA fragmentation was quantitatively assayed by antibody-mediated capture and detection of cytoplasmic mononucleosome- and oligonucleosome-associated histone-DNA complexes (Cell Death Detection ELISA Plus, Roche Applied Science, Indianapolis, IN). Cells were grown in six well plates and exposed to hydrogen peroxide for 24 hours. After treatment, floating and adherent cells were pooled and resuspended in 200 μL of lysis buffer (supplied by the manufacturer) and incubated for 30 min at room temperature. After pelleting nuclei (200 rpm, 10 min), 20 μL of the supernatant (oligonucleosome-sized fragments derived form apoptotic cells) was used in the enzyme linked immunosorbent assay (ELISA) following the manufacturer's standard protocol. Finally, absorbance at 405 nm, upon incubation with a peroxidase substrate was determined with a Multiskan MS plate reader (Labsystem, Vantaa, Finland). Background values (incubation buffer alone) were substracted and OD values representing nucleosomal DNA fragments in treated samples were compared with those values obtained from untreated control cells and expressed as fold increase.

5.23. Giemsa staining

Cells were seeded on glass coverslips for overnight. Following 24 hours of hydrogen peroxide treatment cells were washed with PBS, fixed with 4% formalin then stained with

May-Grünwald-Giemsa for 10 min. After intensive washing with tap water, coverslips were viewed with a Zeiss Axiolab microscope (Carl Zeiss, Oberkochen, Germany). Pictures were taken with a Zeiss Axiocam digital camera.

5.24. Analyses of mitochondrial membrane potential

Cells were seeded on glass coverslips and cultured overnight before the experiment. Following 24 hours of hydrogen proxide exposure, coverslips were rinsed in phosphate-buffered saline then cells were loaded with 1 μM JC-1 mitochondrial membrane potential-sensitive fluorescent dye for 30 min. JC-1 is a cationic dye that indicates mitochondrial polarization by shifting its fluorescence emission from green to red. This potential-sensitive color shift is due to concentration-dependent formation of red fluorescent J-aggregates. After 30-min loading, digital images were acquired using a fluorescent microscope (Carl Zeiss, Oberkochen, Germany) equipped with a digital camera. The same microscopic field was imaged first with red, then with green filters.

5.25. Comet assay

DNA single strand breaks were assayed by single cell gel electrophoresis (comet assay) (Hegedűs et al., 2008). Broken DNA unwinds under alkalic conditions and forms comet-like structures after cell lysis and electrophoresis. Cells were treated with hydrogen-peroxide. Comet slides (Spektrum 3D, Debrecen, Hungary) were covered with 1% normal melting point agarose. Cells (10,000/slide) were embedded into low melting point agarose and were layered onto the agarose-covered slides. After the agarose has cooled down, slides were placed into lysis solution (2.5 M NaCl, 100 mM EDTA, 10 mM Tris, 10% DMSO, 1% Triton X-100 pH 10.0) for 1 hour at 4 °C. Slides were equilibrated in electrophoresis buffer (300 mM NaOH, 1 mM EDTA) for 30 min. Electrophoresis was performed in electrophoresis buffer (0.74 V/cm, 300 mA, 25 min). Slides were then equilibrated in 0.4 M Tris (pH 7.5) and were stained with ethidium bromide (10 μg/mL). Comets were analyzed by fluorescent microscopy (Zeiss Axiolab microscope (Carl Zeiss, Oberkochen, Germany)). A visual score system was set up for comet analysis. 0-10 = normal, minor DNA damage, most DNA in the head. 10-20 = weakly damaged, about half of DNA in the tail, head is still visible, 20- = highly damaged, no head and all DNA is in the tail. From each slide, at least 25 cells were scored.

5.26. Preparation of subcellular fractions of A459 cells

The isolation of nuclear and cytosolic fractions was adapted from published methods (Lontay at al., 2005) with minor modifications. 24 hours after hydrogen peroxide exposure, floating and adherent cells were pooled and washed twice with ice-cold PBS. Cells were diluted with four volumes of homogenization buffer (0.5 M sucrose, 20 mM HEPES, pH 7.5, 1 mM EDTA, 1 mM EGTA and protease inhibitors). The cell suspension was homogenized by 45 passages through a Dounce homogenizer then Nonidet P-40 was added to a final concentration of 0.5%. The lysate was vortexed gently for 10 sec (the extent of lysis was monitored by staining with trypan blue). Lysates were centrifuged at 8,000 rpm at 4°C for 15 sec. The pellet, containing the nuclei and cell debris, was resuspended in 3 volumes of buffer A (0.5 M sucrose, 10 mM HEPES, pH 7.9, 3.3 mM $MgCl_2$, 10 mM KCl, 0.5 mM DTT and protease inhibitors) and centrifuged at 2,000 rpm for 15 min at 4 °C. The supernatant was discarded and the pellet was resuspended in 2.5 volumes buffer B (buffer A except for 0.35 M sucrose). The suspension was centrifuged at 1,100 rpm for 15 min at 4°C. The pellet was resuspended in buffer B and sonicated on ice to disrupt the nuclear structures with 2×20 pulses with 15 sec intervals; the sonicated suspension was used as the nuclear fraction. The 8,000 rpm supernatant was used as postnuclear fraction. Protein concentrations were determinated using BCA method (Pierce Biotechnologie Inc., Rockford, IL). Fractions were subsequently analysed by Western blot. Dilutions of primary antibodies were as follows: histonH3 (Sigma-Aldrich Co., St. Loius MO) 1:2000, AIF (Santa Cruz Biotechnology, Santa Cruz, CA) 1:1000, ATP5B (Sigma-Aldrich Co., St. Loius MO) 1:500.

Statistical analysis

All experiments were preformed three times on different days. Student's *t*-test was applied for statistical analysis and for the determination of significance with $p < 0.05$ considered as significant. Mann and Whitney's *U*-test was applied for the statistical analysis of the comet assay experiments.

6. RESULTS

6.1. The effect of PARP-1 inhibitor PJ34 and a potent PARG inhibitor gallotannin (GT) on the TNFα/IL-1β induced chemokine and cytokine gene-expression in A549 human lung epithelial cells

6.1.1. Effects of GT and PJ-34 on the expression pattern of chemokines and cytokines in immunostimulated A549 Cells

We have used a nylon-based thematic low density array to investigate the effects of GT and PJ34 on the expression pattern of chemokines and inflammatory cytokines in A549 cells. Ten positions on the arrays were occupied by positive controls (housekeeping genes), whereas six positions contained no cDNA (blank) or plasmid DNA (negative control). The remaining positions of the membrane contained 96 cDNAs of chemokines and inflammatory cytokines (**Figure 12.**). Of these 96 genes, TNFα/IL-1β treatment significantly (minimum 2-fold induction) induced the expression of 12 genes and suppressed the expression of two cytokine receptor genes (**Table 4.**). Pretreatment of cells with GT significantly (by at least 50%) reduced these alterations with the exception of one chemokine (MIP-3α). PJ34 significantly enhanced fractalkine expression. To confirm our results, we also carried out RT-PCR reactions for seven genes; each reaction gave similar results which were in accordance with the array data (**Figure 13.**). In addition, the expression of IL-8, a key neutrophil-recruiting chemokine that was not represented on the array, was also investigated with RT-PCR and found to be inhibited by both GT and PJ34. GT (30 μM) alone did not induce any of the chemokines or cytokines tested (**Figure 13.**). At a lower concentration (30 μM), GT suppressed IL-8 expression.

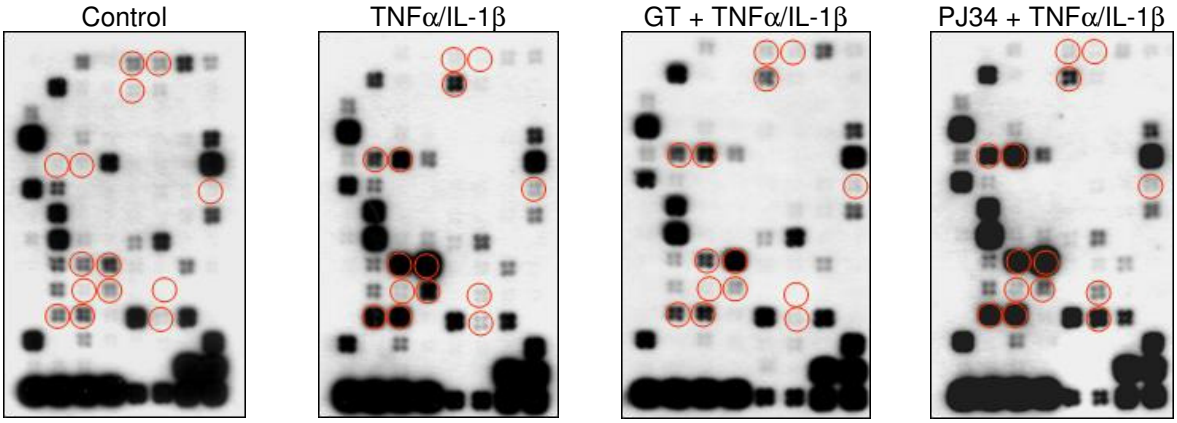

Figure 12. Chemokine and cytokine gene exression pattern analyses in immunostimulated A549 cells. *Nylon-based thematic macroarrays were used in order to investigate the effect of gallotannin and PJ34 on the TNFα/IL-1β induced chemokine and cytokine gene expression in A549 cells. Red cirles indicate genes exhibiting significant alterations from nontreated control. These genes are (from top to the bottom; from left to the right): CCR4, CCR5, CXCR4, IL-1α, IL-1β, IL-6, MCP-1, MIP-3α, MIP-1β, RANTES, MCP-2, ENA-78, GCP-2, Fractalkine*

	Gene Name	Gene Product Name	Common Name	TNFα/IL-1β		
					GT	PJ34
				Fold induction		
Chemokines						
CC	SCYA2	CCL2	MCP-1	9,6	2,5	9,7
	SCYA4	CCL4	MIP-1β	28,4	4,1	15,6
	SCYA5	CCL5	RANTES	60,0	21,8	64,7
	SCYA8	CCL8	MCP-2	32,2	0,8	36,7
	SCYA20	CCL20	MIP-3α	7,2	4,1	8,2
CXC	SCYB5	CXCL5	ENA-78	4,1	1,5	5,0
	SCYB6	CXCL6	GCP-2	3,0	1,2	3,7
CX3C	SCYD1	CX3CL1	Fractalkine	50,5	6,7	107,3
Inflammatory cytokines						
	IL-1A	IL-1α		138,7	43,4	152,7
	IL-1B	IL-1β		183,0	69,3	192,3
	IL-6	IL-6		19,6	3,5	23,1
Chemokine receptors						
	CCR4	CCR4		-9,3	-1,6	-1,55
	CCR5	CCR5		-13,5	-1,3	-1,9
	CXCR4	CXCR4		55,5	39,8	66,8

Table 4. Effect of gallotannin and PJ34 on TNFα/IL-1β-induced chemokine and cytokine expression

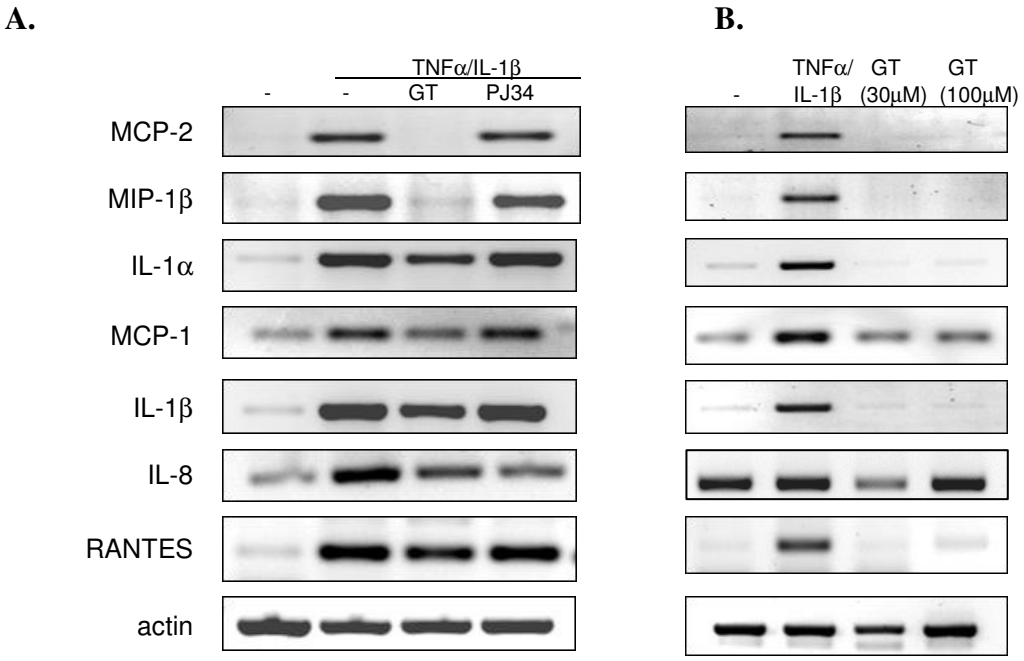

Figure 13. RT-PCR analysis of the expression of chemokines and cytokines in cytokine-stimulated A549 cells. *Cells were pretreated for 30 min with 30 μM GT or 10 μM PJ34 and were then stimulated with TNFα and IL-1β. After 4 h, RNA was isolated and was reverse-transcribed into cDNA. Specific transcripts were amplified with PCR* ***(A.)****. The effect of GT (30 and 100 μM) on the expression of the same set of chemokines/cytokines. Cytokine stimulation was used as positive control (****B.****).*

6.1.2. Effects of GT and PJ34 on NF-κB activation

Because NF-κB and AP-1 are known to regulate the expression of various inflammatory cytokines and chemokines, we have also investigated the effects of GT and PJ34 on the activation of these transcription factors. Treatment of A549 cells with TNFα/IL-1β induced NF-κB activation as demonstrated by EMSA analysis (**Figure 14.**). Pretreatment of the cells with PJ34 or GT markedly reduced the binding of NF-κB to its consensus oligonucleotide. TNFα/IL-1β-induced nuclear translocation of NF-κB was blocked by GT but was unaffected by PJ34, indicating that PARP inhibition by PJ34 may inhibit the DNA binding of the transcription factor (**Figure 15**).

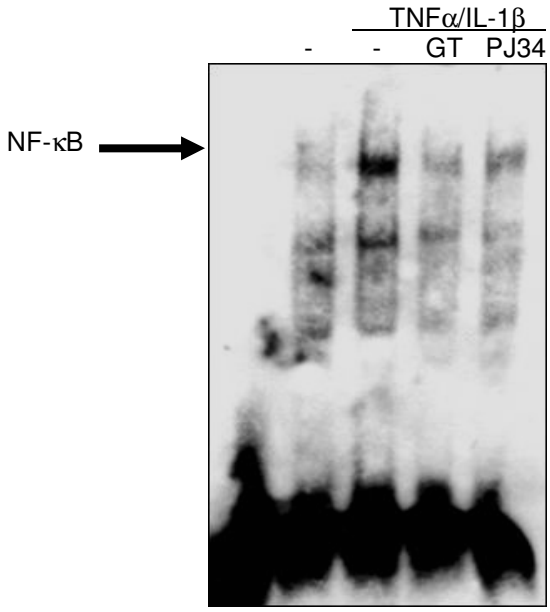

Figure 14. NF-κB activation in A549 cells. *Cells were pretreated for 30 min with 30 μM GT or 10 μM PJ34 and were then stimulated with TNFα and IL-1β. After 1 h, nuclear extracts were prepared and the binding of nuclear protein to NF-κB consensus oligonucleotide was studied with EMSA.*

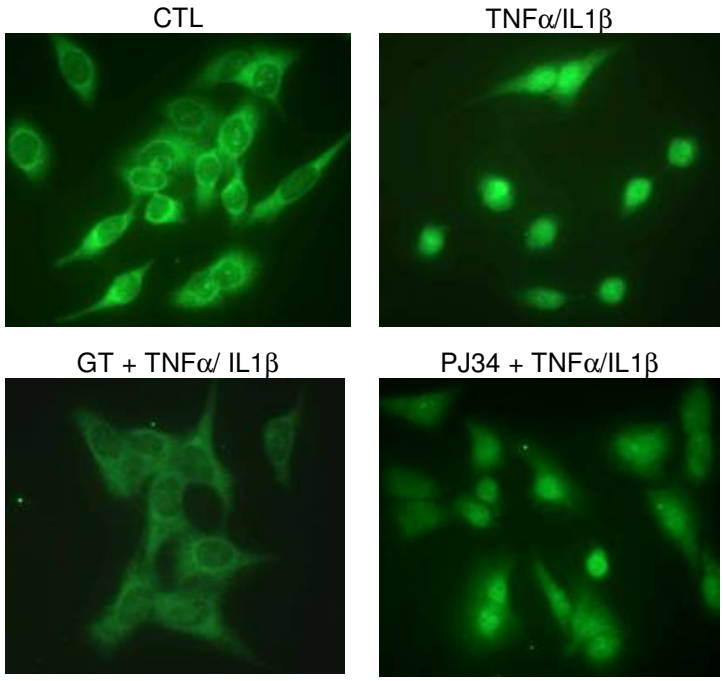

Figure 15. Nuclear translocation of NF-κB. *A549 cells were pretrated with GT and PJ34 for 30 min. following treatment with TNFα/IL-1β. Translocation of NF-κB was demonstrated with immunocytofluorescent staining 30 min after cytokine stimulation*

As for GT, we have also investigated IκB phosphorylation, an event laying upstream in the NF-κB pathway. GT abolished phosphorylation, suggesting that GT may inhibit the kinase cascade (IκB kinase or upstream kinases) (**Figure 16.**).

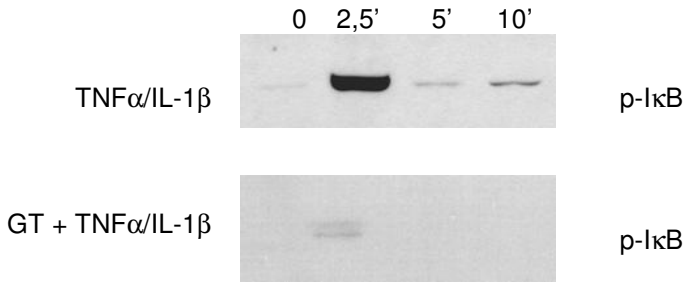

Figure 16. Time course of IκB phosphorylation. *Phosphorylation of IκB was detected on Western blots using phosphopeptide-specific antibody. Pretreatment cells with GT markedly abolished the IκB phosphorylation.*

6.1.3. Effects of GT and PJ34 on AP-1 activation

Regarding the AP-1 activation, we have observed a basal AP-1 activity as demonstrated by EMSA experiments using the TRE consensus element; TNFα/IL-1β treatment triggered further AP-1 activation (**Figure 17.**). GT pretreatment abolished both basal and TNFα/IL-1β-induced AP-1 activation. PJ-34 had no effect on AP-1 activation (**Figure 17.**).

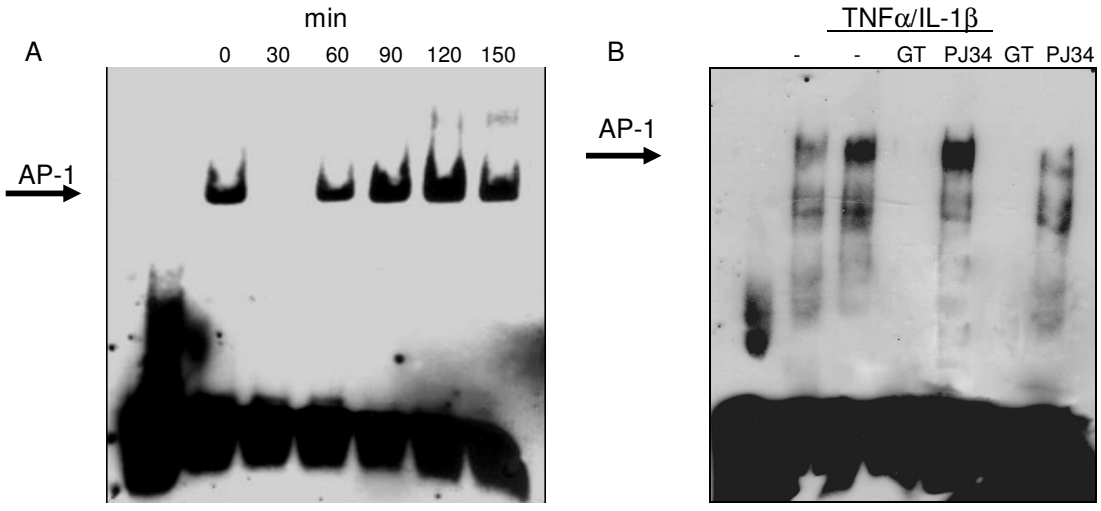

Figure 17. Time courses for the TNFα/IL-1β induceed AP-1 acivation. *A549 cells were treated with TNFα and IL-1β for the indicated time periods. After that nuclear extract were prepared and the binding of AP-1 transcription factor to its consensus oligonucleotide was studied with EMSA (**A.**). Cells were pretreated for 30 min with 30 μM GT or 10 μM PJ34 and were then stimulated with TNFα/IL-1β. After 2 h, AP-1 activation was detected with EMSA (**B**.).*

6.1.4. Activation of the JNK-c-Jun-AP-1 pathway in immunostimulated A549 cells

Mitogen-activated protein kinases (MAPK) c-Jun NH_2-terminal kinase (**JNK**), **p38MAPK**, and extracellular signal-regulated kinase (**ERK1/2**) play key roles in cytokine-induced signaling (Johnson and Lapadat, 2002). Because formation of the c-Jun/c-Fos heterodimer of AP-1 is induced by JNK-mediated phosphorylation of c-Jun (Kyriakis and Avruch, 2001), we investigated the time course phosphorylation both of them. We have also investigated the effects of GT and PJ34 on these upstream events of the AP-1 pathway. TNFα/IL-1β induced a rapid phosphorylation of JNK detectable as early as 2.5 min, peaking between 5 and 10 min and fading 40 min after the cytokine treatment (**Figure 18.**). It is surprising that GT stimulated basal JNK phosphorylation that was not further increased by the cytokines. PJ34 had no effect on JNK phosphorylation. Phosphorylation of c-Jun has shown a prolonged pattern with signals detectable even in unstimulated cells. Whereas PJ34 had no effect on c-Jun phosphorylation, GT treatment, even in the absence of cytokines, induced maximal c-Jun phosphorylation that was not further enhanced by TNFα/IL-1β. We used JNK antibody as a loading control (**Figure 18.**).

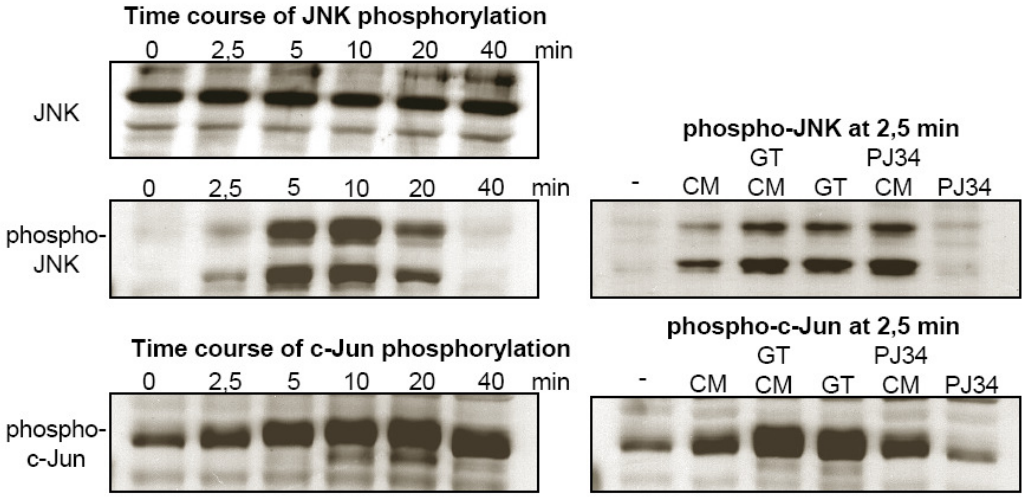

Figure 18. *Time courses for the cytokine induced phosphorylation of JNK and c-Jun were established in Western blot experiments using phosphopeptide specific antibodies. Effect of GT and PJ34 were studied at selected time points as indicated (CM, cytokine mixture).*

Since c-Jun can heterodimerize with Activating transcription factor-2 (ATF2) which is regulated mainly by p38MAPK we have also determined the effect of GT and PJ34 on the p38MAPK-ATF2 pathway. TNFα/IL-1β induced a rapid phosphorylation of

p38MAPK, which did not fade during the 40-min period tested (**Figure 19.**). PJ34 had no effect on p38MAPK phosphorylation (**Figure 19.**). Although GT alone caused the phosphorylation of p38MAPK, the TNFα/IL-1β-induced signal was not further increased by GT. Phosphorylation of ATF2 was similarly affected by the two drugs with no effect of PJ34 and inhibition of cytokine-induced ATF2 phosphorylation by GT (**Figure 19.**).

Although MAPK ERK1/2 is mainly involved in the regulation of cell proliferation (Johnson and Lapadat, 2002), it has also been implicated in transcriptional regulation of inflammatory mediators (Neff et al., 2003; Lecureur et al., 2005). One of the downstream events in the activation of the ERK1/2 (and p38) pathway is the phosphorylation of the transcription factor CREB (Yang et al., 2003). Phosphorylated CREB has been shown to be involved in the transcriptional regulation of inflammatory mediators. We found that ERK1/2 and CREB are regulated by GT in the same way as seen with p38MAPK and ATF2 (**Figure 19.**). Whereas PJ34 had no effect on the basal and cytokine-induced phosphorylation of ERK1/2 and CREB, GT induced the phosphorylation of these proteins but inhibited their further activation by cytokines (**Figure 19.**).

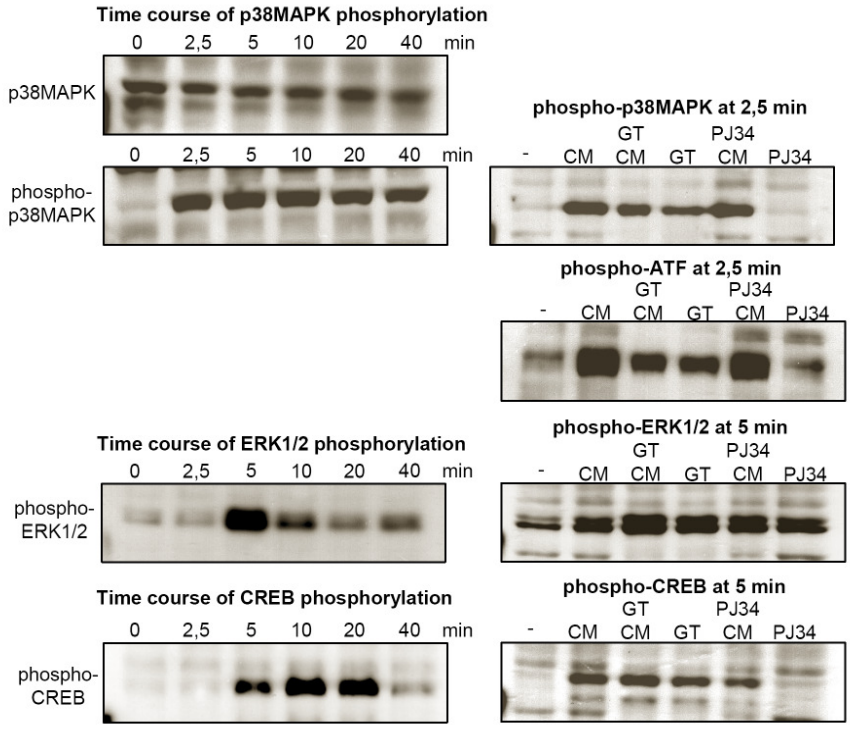

Figure 19. Phosphorylation of p38MAPK, ATF2, ERK1/2, and CREB in immunostimulated A549 cells. *Time courses for the cytokine induced phosphorylation of p38MAPK, ATF2, ERK1/2, and CREB were established in Western blot experiments using phosphopeptide specific antibodies. Effect of GT and PJ34 were studied at the selected time points as indicated (CM, cytokine mixture).*

6.1.5. Effects of GT on the activity of protein phosphateses 1 and 2A

Considering that GT increased the phosphorylation state of many proteins (JNK, c-Jun, p38MAPK, ATF2, ERK1/2, and CREB), we hypothesized that GT may interfere with protein phosphatases activity. We have determined the effect of GT on the activities of protein phosphatases 1 (PP1) and 2A (PP2A) catalytic subunits and found that GT inhibited both enzymes in a concentration-dependent manner (**Figure 20**). GT also inhibited the PP1 catalytic subunit associated with a regulatory subunit as assayed with the myosin phosphatase holoenzyme (data not shown), indicating that regulatory subunits do not mask the gallotannin-binding site on the catalytic subunit.

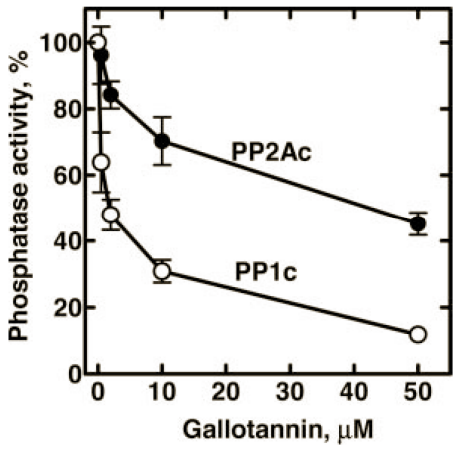

Figure 20. Effect of gallotannin on the activity of PP1c and PP2Ac. *Gallotannin was assayed on the phosphatase activity at concentrations of 0.5, 2, 10, and 50 μM. Gallotannin was preincubated with the catalytic subunits of PP1 or PP2A for 5 min. The reaction was initiated by the addition of ^{32}P-labeled 20-kDa gizzard myosin light chain and the $^{32}P_i$ released from the substrate was determined. Phosphatase activity of PP1c (○) or PP2Ac (●) in the absence of gallotannin was taken as 100%. Values represent means ± S.E.M. (n = 7-9).*

6.1.6. Effect of GT on poly(ADP-ribosyl)ation

Beside the phosphatase inhibitory effect of GT we sought to determine whether GT affects the poly(ADP-ribosyl)ation in immunostimulated A549 cells. We found that treatment of the cells with the cytokines for various time periods (5 min to 4 h) caused no elevation in cellular poly(ADP-ribose) content as determined by immunofluorescence (**Figure 21**) or Western blotting (**Figure 22**) using the anti-poly(ADP-ribose) monoclonal antibody. Hydrogen peroxide used as a positive control triggered poly(ADP-ribose) elevation in the nucleus as demonstrated by immunocytochemistry (**Figure 21**). On Western blot, the lysates of hydrogen peroxide-treated cells contained many positive bands with most immunopositivity found in the region above 116 kDa (the molecular mass of PARP-1) corresponding to automodified PARP-1 (**Figure 22**). Treatment of cells with GT in the absence or presence of the cytokines caused no elevation in the cellular poly(ADP-ribose) content.

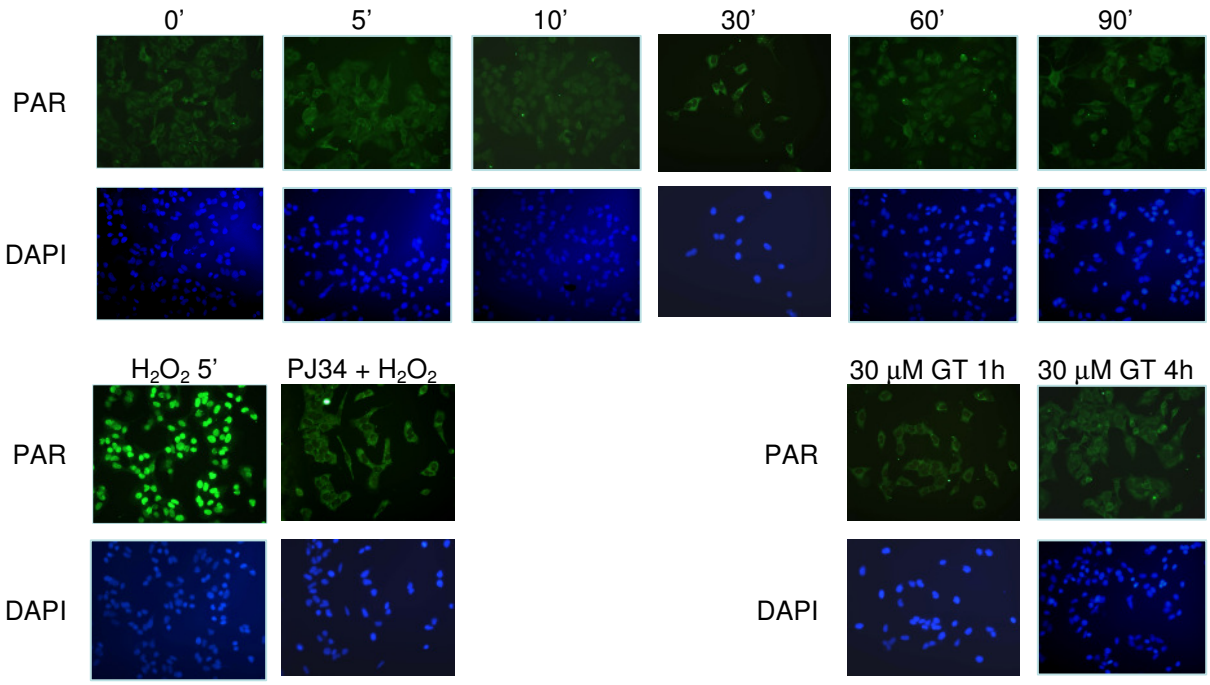

Figure 21. Lack of effect of 30 µM gallotannin on the poly(ADP-ribose) metabolism. *Cells were stimulated with TNFα and IL-1β or GT for various periods of times, as indicated. Poly(ADP-ribose) was detected with immunofluorescent staining using anti-poly(ADP-ribose) antibody. Hydrogen peroxide treatment (5 min) was used as a positive control. Nuclei were stained blue with DAPI. Identical exposure times were used for all of the photographs taken.*

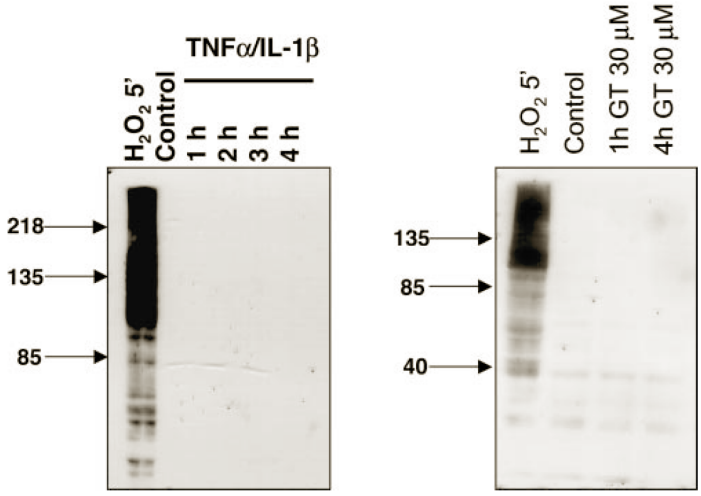

Figure 22. Lack of effect of 30 µM gallotannin on the poly(ADP-ribose) metabolism. *Cells were stimulated with TNFα and IL-1β or 30 µM GT or various periods of times, and poly(ADP-ribose) was detected with Western blotting using anti-poly(ADP-ribose) antibody. Hydrogen peroxide treatment (5 min) was used as a positive control.*

6.1.7. Antioxidant effects of GT

Another feature that could, at least in part, explain the effect of gallotannin on cytokine/chemokine expression is the well known antioxidant effect of tannins (Ho et al., 1999; Riedl and Hagerman, 2001). Considering that both NF-κB and AP-1 are redox-sensitive transcription factors (Schulze-Osthoff et al., 1995), modification of the cellular redox state by GT could be responsible for the described effects. We have studied the radical-scavenging effect of GT and PJ34 by ABTS decolorization assay. Using ascorbic acid as positive control, we have determined the ABTS-scavenging effect of GT and PJ-34 (**Figure 23A.**). In this assay, GT displayed an even more potent radical-scavenging effect compared with ascorbic acid. However, PJ34 did not scavenge the radical (**Figure 23A.**). We have also used the pathophysiologically relevant oxidant peroxynitrite. Peroxynitrite oxidizes DHR123 into fluorescent rhodamine. The addition of GT and ascorbic acid inhibited peroxynitrite-induced DHR123 oxidation, with GT being the more potent antioxidant. PJ-34 had no antioxidant effect (**Figure 23B.**).

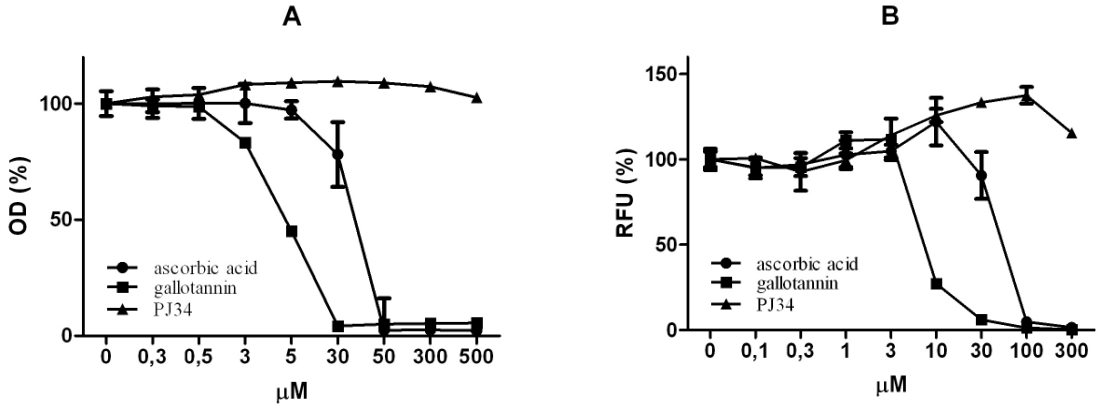

Figure 23. Antioxidant effects of gallotannin. *The general antioxidant effect of the indicated concentrations of gallotannin and PJ34 was determined in the ABTS-scavenging assay (A) The peroxynitrite-specific scavenging activity was determined in the dihydrorhodamine oxidation assay and results are given in relative fluorescent units (RFU) as a percentage of control. Ascorbic acid was used as a positive control in both assays. Mean ± S.D. of triplicate samples are shown (B).*

We can conclude that in epithelial cells gallotannin acts as an anti-inflammatory agent. This effect results from the inhibiton of the AP-1 pathway and, to a lesser extent, the NF-κB pathway. In A549 cells, poly(ADP-ribosyl)ation is not a crucial mechanism in the regulation of inflammatory gene expression and PARG is probably not the target of gallotannin in this system

6.2. The role of PARP-1 and PARG proteins in hydrogen peroxide induced cell death in A549 cells

6.2.1. Establishment and characterization of A549 cell lines with stably suppressed hPARG and hPARP-1

To investigate the contribution of PARG to oxidative stress-induced cell death in A549 cells, we have generated cell lines with suppressed expression of PARG. As reference, a PARP-1-knockdown cell line has also been established. Silencing PARG and PARP-1 was achieved through the use of lentiviral vector-mediated short hairpin RNA (shRNA) interference. Two individual clones from Mission shRNA target sets NM_003631 and NM_001618 (for PARG and PAPR1, respectively) were cotransfected with a lentivirus packaging plasmid into HEK 293T cells. The resulting lentiviral particles were used to infect A549 cells, followed by selection in the presence of puromycin. PARG and PARP-1 mRNA levels were monitored by reverse transcription-coupled PCR (**Figure 24 A.**) and real-time quantitative PCR (**Figure 24 B.**). Actin mRNA was used as an internal control. Knockdown of PARP-1 has also been confirmed at the protein level by Western blotting (**Figure 24 C.**). Our data demonstrate that the shPARG and shPARP-1 cell lines display efficient reduction of targeted mRNAs and (in the case of PARP-1) the corresponding protein. Of note, slightly decreased PARP-1 mRNA and protein levels could be observed in the shPARG cell lines. This is in line with previous data reporting the regulation of PARP-1 expression by poly(ADP-ribosyl)ation and may indicate that PARG also plays a role in the regulation of PARP-1 expression. Expression of PARG protein was not detected because of the lack of commercially available antibody that would be able to detect endogenous PARG. However, functional characterization of the shPARG cell line (**Figure 25.**), proves the efficient suppression of PARG protein.

A.

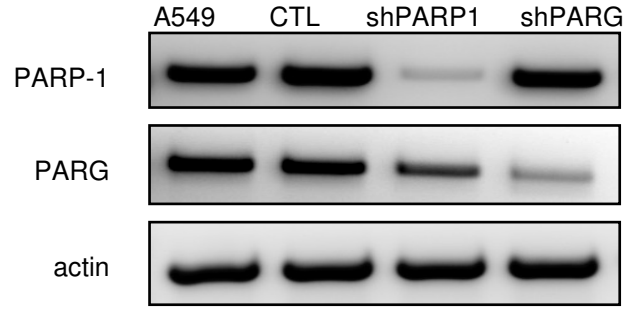

B.

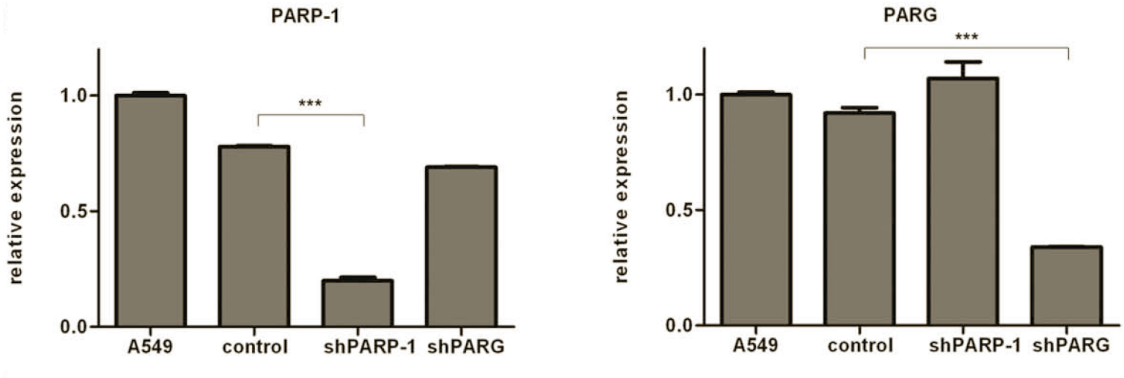

C.

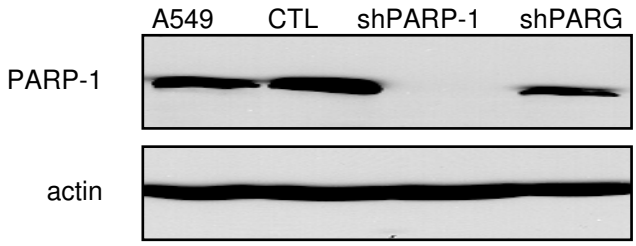

Figure 24. Knockdown of PARG and PARP-1 in A549 cells. Following transduction with control (CTL), PARP-1-specific and PARG-specific shRNA, knockdown efficiency on gene expression was determined by PCR (**A**) and real-time quantitative PCR (**B**). Actin was used as the invariant control. Significant drops in PARP-1 and PARG mRNA were observed. (**C**) Western blot analysis of whole-protein extracts from nontransduced A549 cells, cells infected with control viruses, shPARP-1 cells, and shPARG cells. Immunoblotting was performed with the anti-PARP-1 antibody and the anti-actin antibody as a loading control.

6.2.2. Functional characterization of the shPARG and shPARP-1 cell lines

To further characterize our cell lines and to learn how knockdown of PARG and PARP-1 affects poly(ADP-ribose) metabolism, the cell lines were subjected to functional characterization. In A549 cells, hydrogen peroxide treatment caused transient nuclear synthesis of poly(ADP-ribose), as assessed by immunocytochemical analysis using a polymer-specific antibody. The polymer level was restored in 15 min (**Figure 25 A., B**.). Cells infected with control lentiviruses showed the same response. In the shPARP-1 cell line, however, poly(ADP-ribose) synthesis was strongly suppressed, with only a few scattered cells displaying immunopositivity for poly(ADP-ribose). Poly(ADP-ribose) synthesis was apparently unchanged in shPARG cells; however, degradation of the polymer was significantly delayed, with no obvious sign of poly(ADP-ribose) degradation at 15 min (**Figure 25.**) and strong immunopositivity detected even 120 min after hydrogen peroxide treatment (not shown). Lack of poly(ADP-ribose) synthesis in shPARP-1 cells and blocked poly(ADP-ribose) degradation in shPARG cells has also been confirmed in Western blot experiments (**Figure 25 B.**). In the untreated control cells, no poly(ADP-ribose)-modified proteins could be detected. After hydrogen peroxide treatment, a smear between 115 and 160 kDa, indicating automodified PARP-1, became visible, but the signal disappeared during 15 min of recovery (**Figure 25 B**). In the shPARP-1 cells, only a very faint signal indicated a low degree of poly(ADP-ribose) synthesis. Hydrogen peroxide treatment in shPARG cells triggered a robust PARP activation response, cells contained many positive bands with most immunopositivity found in the region above 116 kDa corresponding to automodified PARP-1. Polymers showed a markedly prolonged half-life (**Figure 25 B**). These data clearly demonstrate that efficient suppression of the main poly(ADP-ribose) synthesizing and degrading enzymes has been achieved in A549 cells.

A.

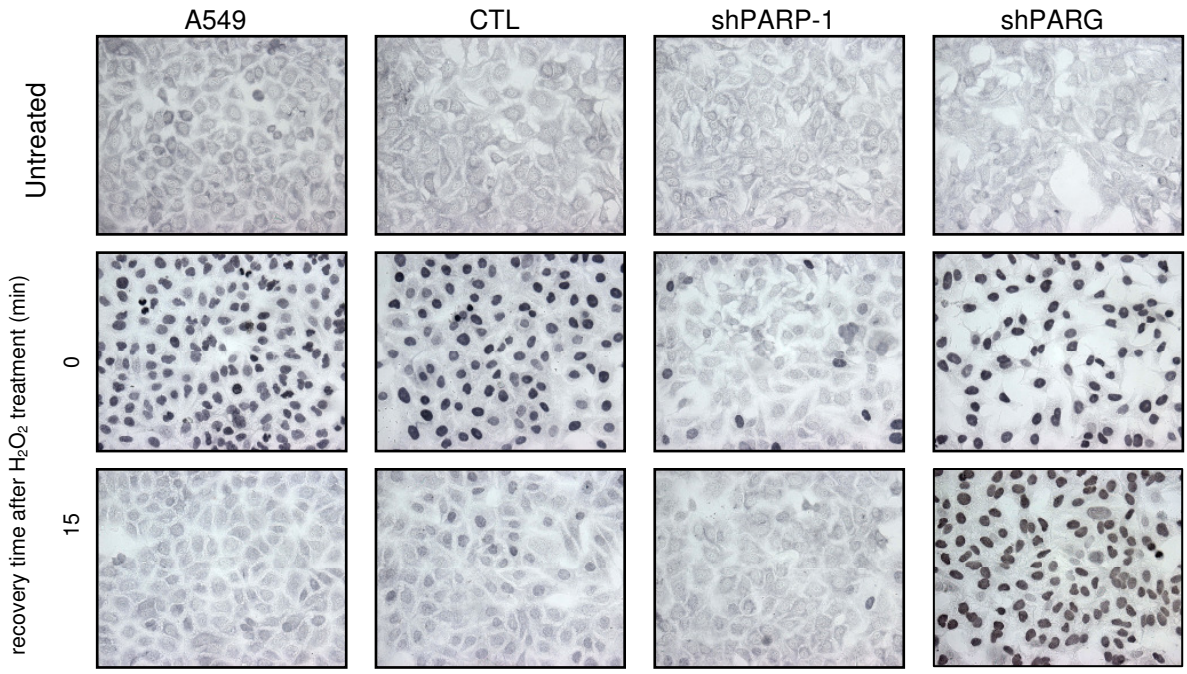

B.

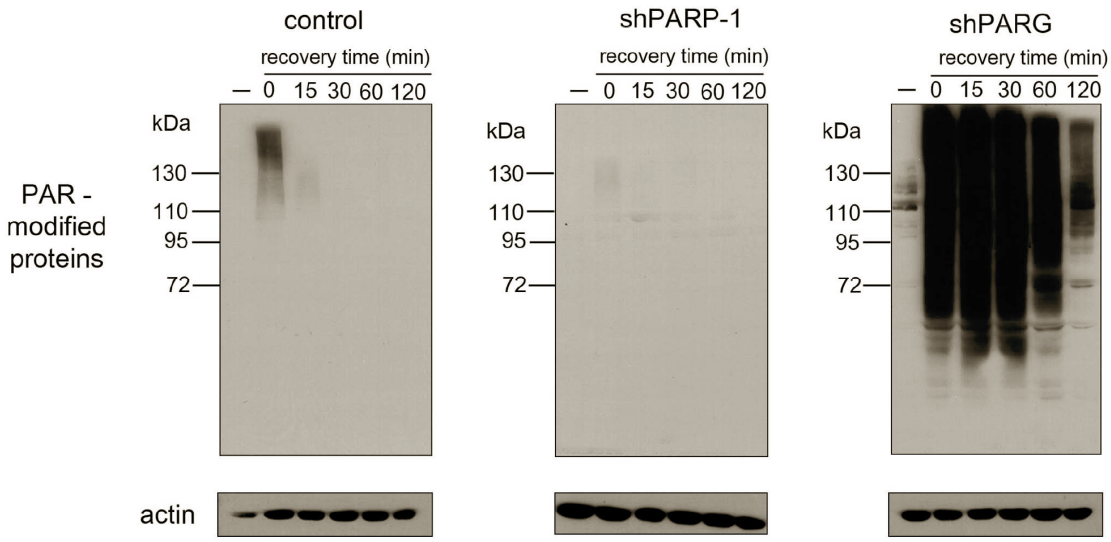

Figure 25. Functional characterization of shPARG and shPARP-1 cells. *Oxidative stress-induced poly(ADP-ribose) accumulation in A549, control, shPARP-1-, and shPARG cells was detected by immunocytochemistry (A) or immunoblotting (B). Following treatment with 400 μM hydrogen peroxide, poly(ADP-ribose) polymers were detected immediately (0 time) and after increasing recovery times. β-actin was used as the loading control (B). Lack of poly(ADP-ribose) polymer synthesis was observed in shPARP-1 cells, while delayed poly(ADP-ribose) polymer degradation was detected in shPARG cells.*

6.2.3. Measurement of PARP activity

Both basal and hydrogen peroxide-induced PARP activity was reduced in the shPARP-1 cell line (**Figure 26.**). Knockdown of PARG had no effect on basal PARP activity, whereas hydrogen peroxide-induced PARP activity was significantly reduced. These data indicate that by removing inhibitory poly(ADP-ribose) polymers from PARP-1, PARG permits constantly high PARP-1 activity in oxidatively stressed cells.

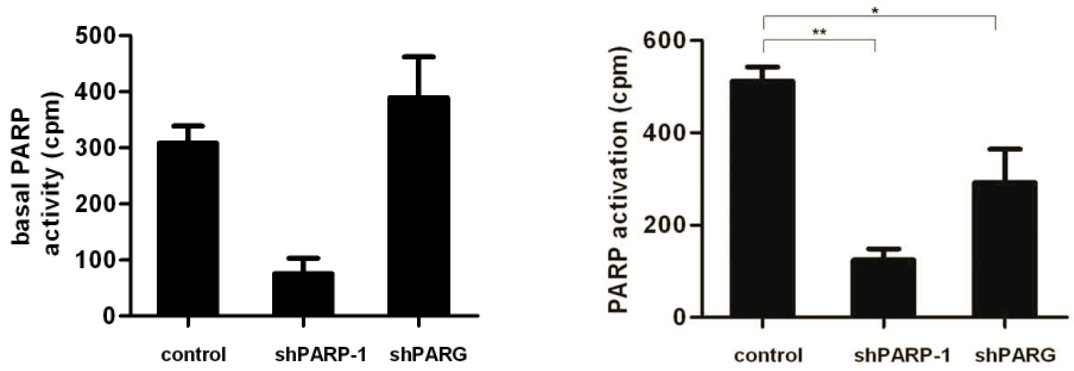

Figure 26. Measurement of PARP activity. *PARP activity was determined by ^{3}H-NAD incorporation in unstimulated and hydrogen peroxide-treated (400 μM) cells. shPARP-1 cells exhibited significantly lower basal PARP activity. Hydrogen peroxide induced PARP activation. PARP activation was significantly lower in shPARP-1 and, to a lesser extent, in shPARG cells (*P < 0.05; **P < 0.01).*

6.2.4. Role of PARG in oxidative stress-induced cell death

Similarly to most cell types, oxidative stress-induced cell death of A549 cells is mediated, at least in part, by poly(ADP-ribosyl)ation (Nanavaty et al., 2002). The role of PARG in the regulation of cell death is not known. Hydrogen peroxide caused a concentration-dependent decrease in the viability of control A549 cells. shPARG and shPARP-1 cells were significantly protected from toxicity of the oxidant, with PARG knockdown providing weaker protection (**Figure 27A.**). Similar patterns could be observed in the drop of cellular NAD^{+} and ATP levels (**Figure 27B., C.**), indicating that compromised cellular energetics could explain the PARP/PARG-dependent component of hydrogen peroxide-induced cytotoxicity. Indeed, tricarboxylicacid-cycle (TCA-cycle), substrates, methyl pyruvate and ketoglutarate, provided significant protection against hydrogen peroxide-induced cell death (**Figure 27D**.), indicating that slowdown of glycolysis contributes to loss of viability in this model. Inhibition of glycolysis may result in mitochondrial depolarization, an event mediated by PARP activation in cells exposed to DNA damage. In

our model, hydrogen peroxide triggered a concentration-dependent mitochondrial depolarization that was blocked in shPARP-1 and shPARG cells (**Figure 28.**).

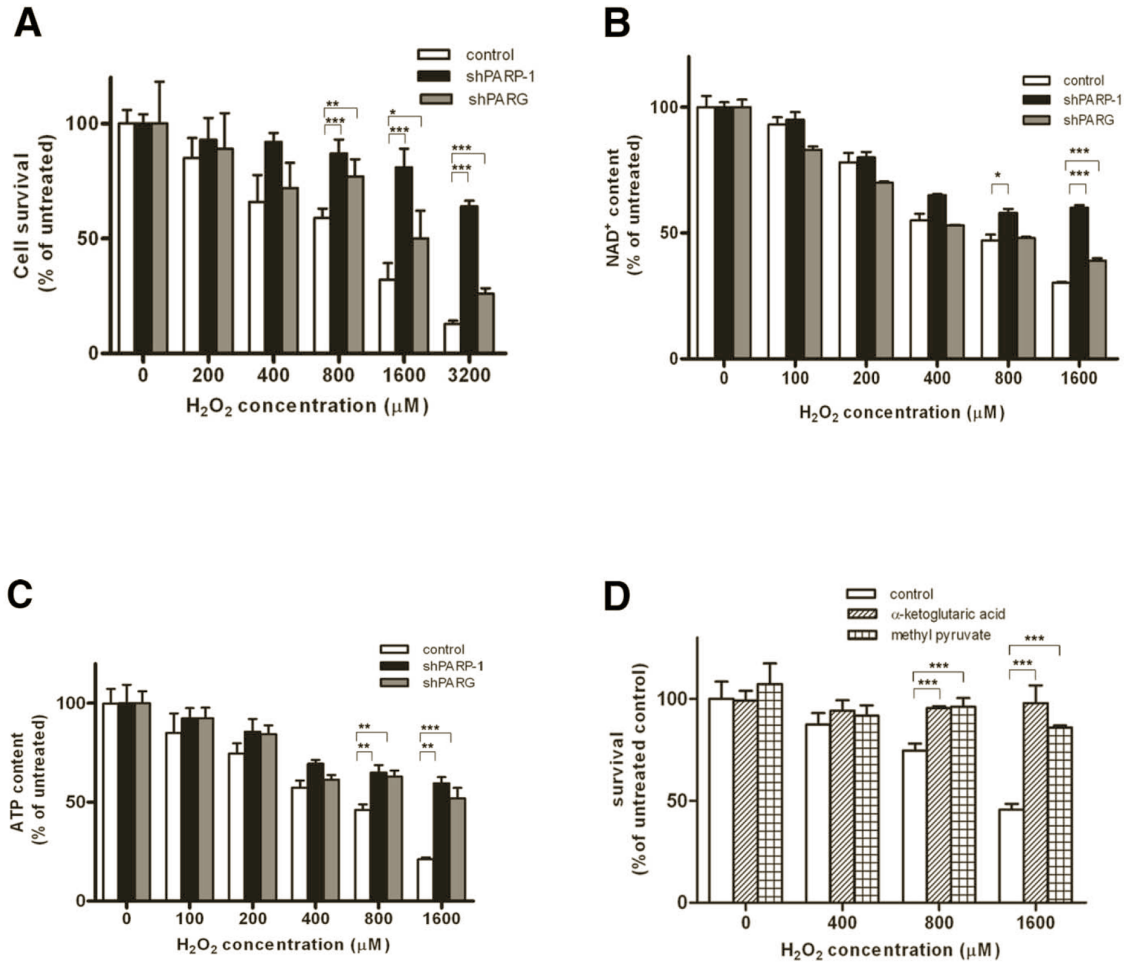

Figure 27. Hydrogen peroxide induced cell death: apoptotic and energetic parameters (A-C) *Concentration dependent cell death (**A**), NAD^+ consumption (**B**) and ATP consumption (**C**) induced by hydrogen peroxide in control, shPARP-1 and shPARG cells. Hidrogen peroxide caused a significant cell death (as determined by MTT reduction) and significant drop in cellular levels of NAD^+ and ATP at 24 hours in control cells. Cell death and loss of cellular NAD^+ and ATP could be significantly prevented by gene silencing of PARP-1 and PARG as compared to control (**D**.) Hydrogen peroxide-induced cytotoxicity was prevented by TCA-cycle substrates methyl pyruvate and a-ketoglutarate. Data represent mean ± standard error of the mean of four independent experiments (*P < 0.05; **P < 0.01; ***P < 0.001, respectively).*

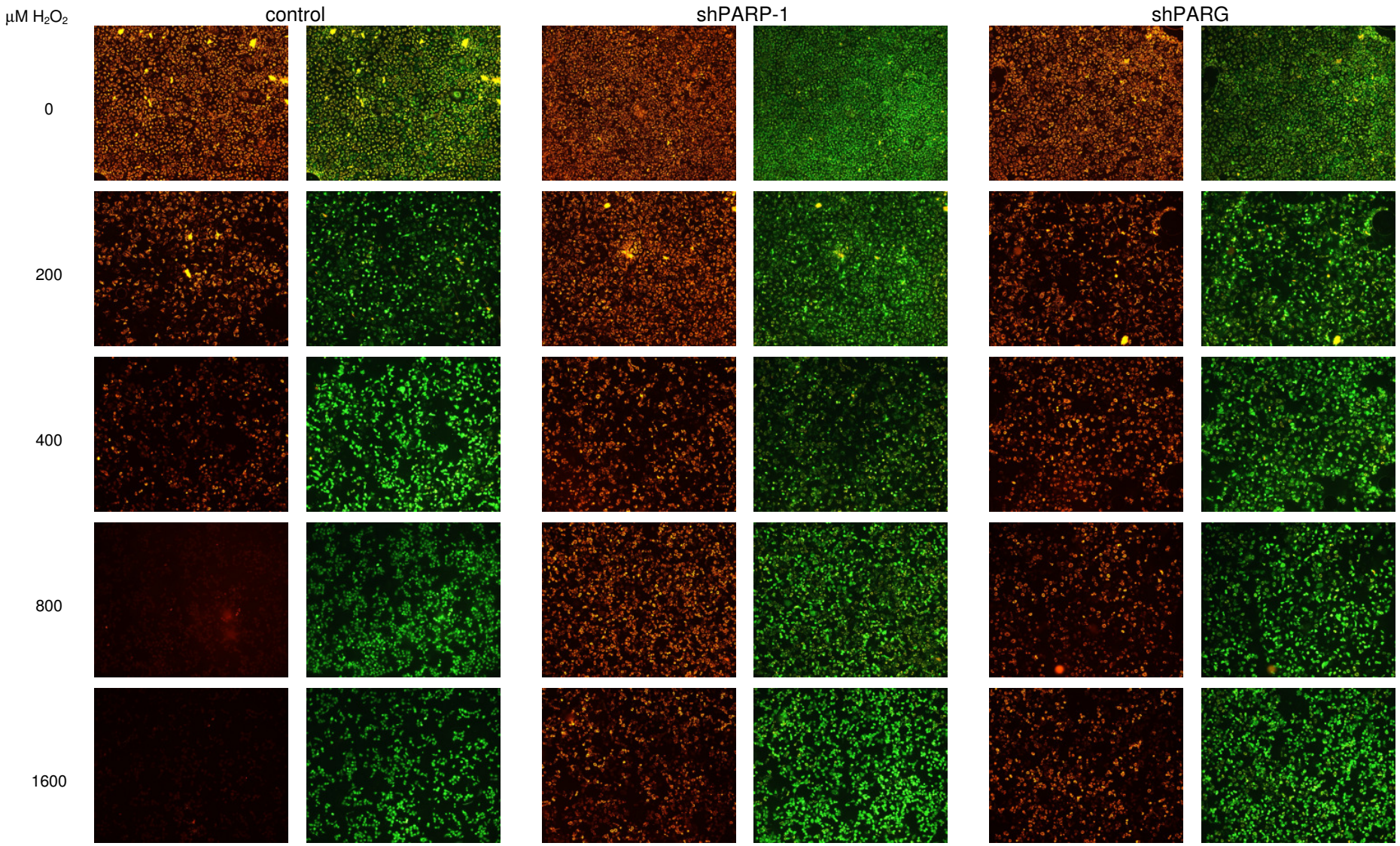
μM H_2O_2
control
shPARP-1
shPARG
0
200
400
800
1600

Figure 28. Effect of PARP-1 and PARG depletion on the mitochondrial membrane potential of A549 cells in oxidative stress. *Control, shPARP-1 and shPARG cells were treated for 24 hours with increasing concentration of hydrogen peroxide. After treatment, cells were stained with JC-1 and subsequently analysed by fluorescent microscope. Untreated cells showed strong J-aggregation (red). Control cells showed the progressive loss of red J-aggregate by the increasing concentration of hydrogen peroxide. shPARP-1 and shPARG cells exhibited lower decrease of mitochondial membrane potential.*

6.2.5. Concerted action of PARG and PARP-1 mediates apoptosis to necrosis switch in severe oxidative stress

To further characterize the mechanism of cell death in our model, we have determined plasma membrane permeability. Exposure of cells to high concentrations of hydrogen peroxide lead to increased plasma membrane permeability, as indicated by propidium iodide uptake (**Figure 29.**). Loss of plasma membrane integrity is mediated by the activation of PARP-1, as shPARP-1 cells were resistant to hydrogen peroxide-induced plasma membrane permeabilization. PARG may also contribute to the permeabilization of the plasma membrane, as shPARG cells were, although to a lesser extent, also protected from the loss of plasma membrane integrity (**Figure 29.**).

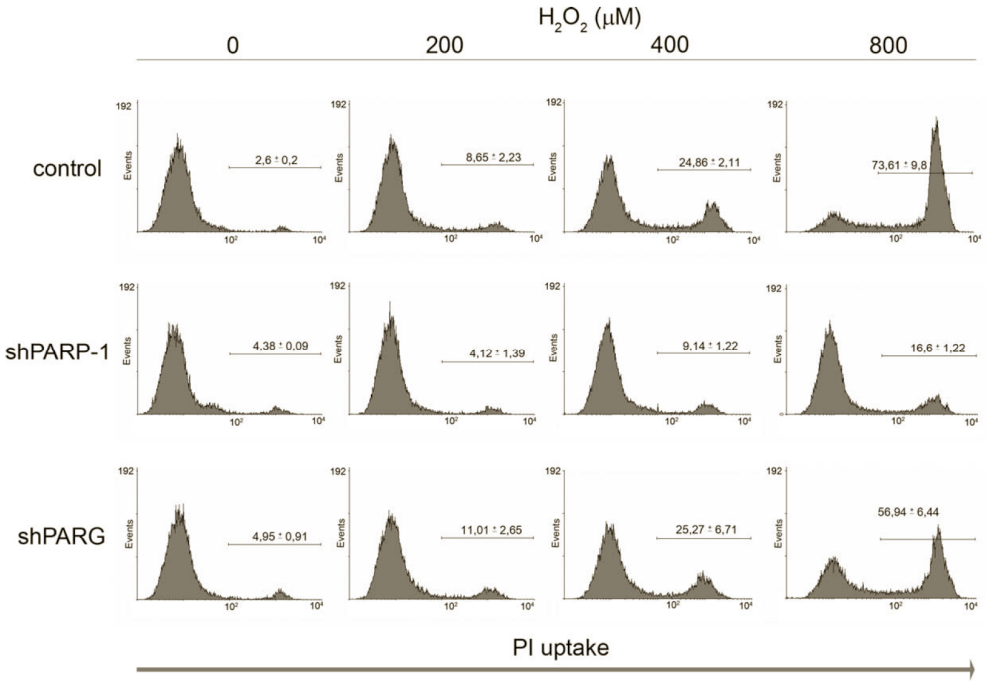

Figure 29. Fow cytometric analyses of PI uptake. *Permeabilization of the plasma membrane in oxidatively stressed cells requires the concerted action of PARP-1 and PARG. Cells were exposed to indicated concentrations of hydrogen peroxide. Plasma membrane injury was assessed after 12 hours by propidium iodide staining. Significant protection from oxidative stress was observed in shPARP-1 and shPARG ± cells as compared to control. Data represent means ± sd of triplicate samples.*

6.2.6. Measurement of caspase activation and DNA fragmentation

Hydrogen peroxide also induces caspase activation and DNA fragmentation, biochemical markers of apoptosis, (**Figure 30.**) in parallel to the appearance of necrotic parameters (loss of plasma membrane integrity, drop in ATP level). Apoptotic parameters such as caspase-3-like activity and internucleosomal DNA fragmentation declined at higher concentrations of the oxidant. In shPARP-1 cells and, to a lesser extent, in shPARG cells, these apoptotic parameters were significantly more preserved at higher concentrations of hydrogen peroxide (**Figure 30 A., B.**), indicating that a concerted action of PARP-1 and PARG is required for the apoptosis-to-necrosis switch in oxidatively stressed A549 cells. We also show that DNA fragmentation is caspase-dependent in our model because DNA fragmentation could be abolished by the pancaspase inhibitor zVAD-fmk (**Figure 30 C.**).

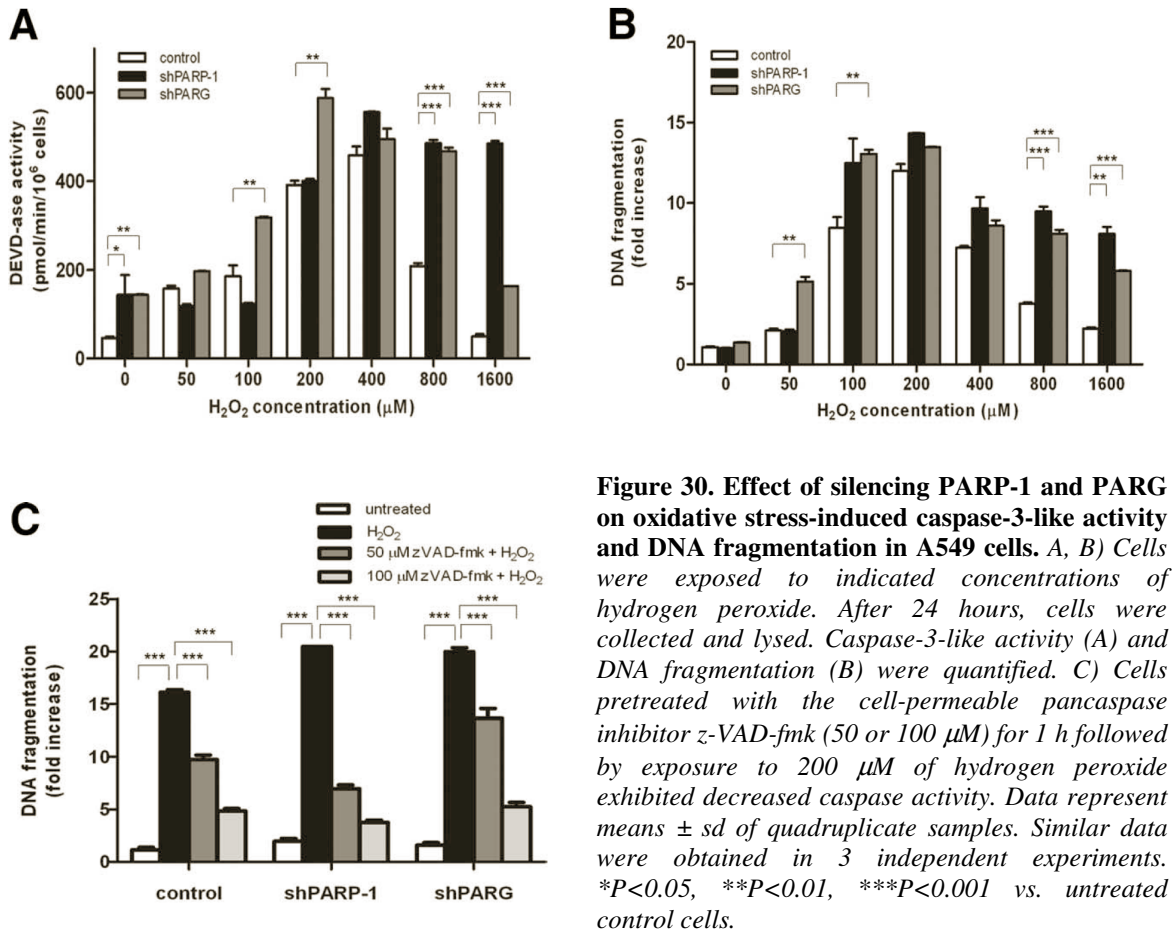

Figure 30. Effect of silencing PARP-1 and PARG on oxidative stress-induced caspase-3-like activity and DNA fragmentation in A549 cells. *A, B) Cells were exposed to indicated concentrations of hydrogen peroxide. After 24 hours, cells were collected and lysed. Caspase-3-like activity (A) and DNA fragmentation (B) were quantified. C) Cells pretreated with the cell-permeable pancaspase inhibitor z-VAD-fmk (50 or 100 μM) for 1 h followed by exposure to 200 μM of hydrogen peroxide exhibited decreased caspase activity. Data represent means ± sd of quadruplicate samples. Similar data were obtained in 3 independent experiments. *P<0.05, **P<0.01, ***P<0.001 vs. untreated control cells.*

6.2.7. Morfological analysis of cell death

Hydrogen peroxide-induced alterations in cell morphology as observed in May-Grünwald-Giemsa-stained cells also support apoptotic death (condensed chromatin) at low hydrogen peroxide concentrations (400 μM) and necrotic morphology at higher concentrations (800–1600 μM). In the shPARP-1 line and, to a lesser extent, in shPARG cells, necrosis was inhibited at 800–1600 μM of hydrogen peroxide, and most cells displayed apoptotic morphology **(Figure 31.)**. Moreover, at low concentrations (200 μM) of hydrogen peroxide, when no morphological alterations could be observed in control cells, shPARG cells have still shown signs of apoptosis **(Figure 31.)**.

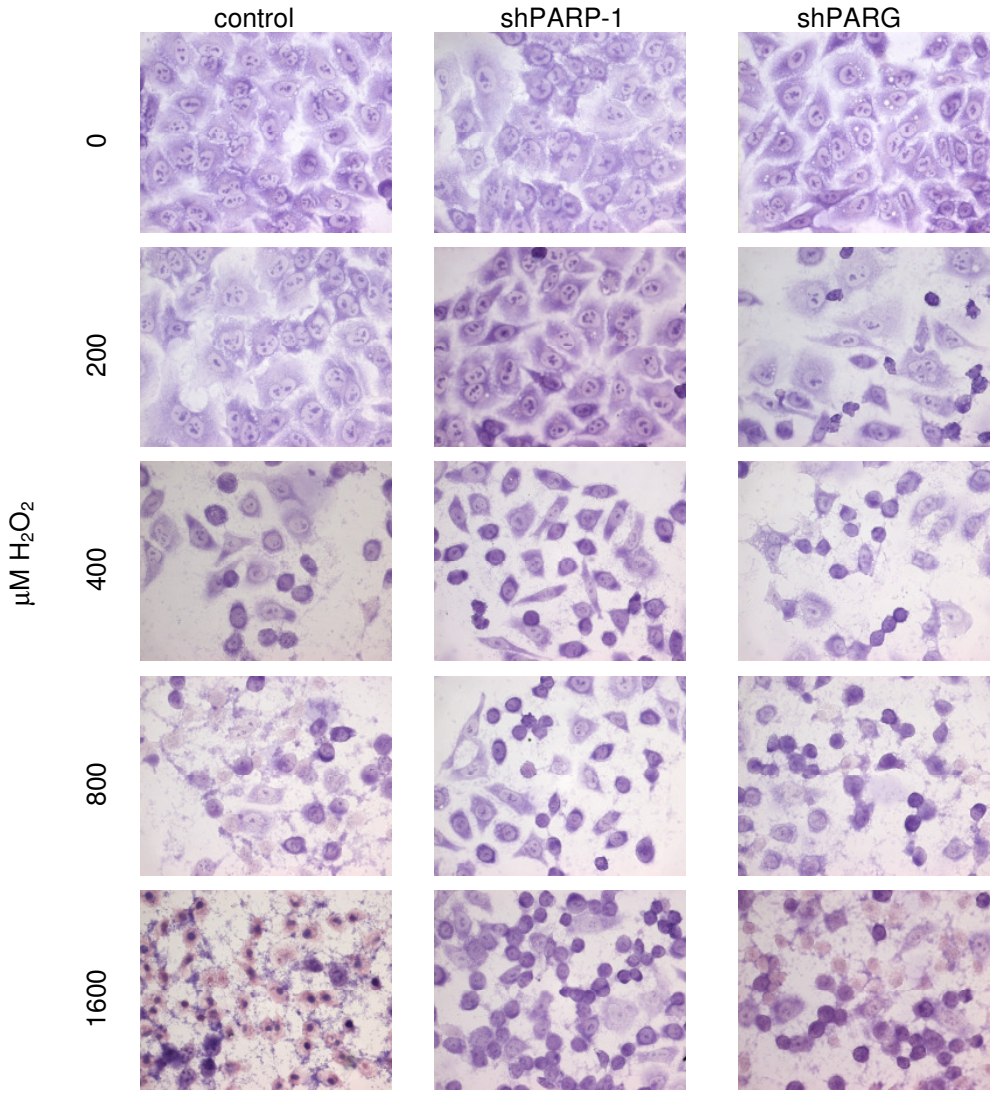

Figure 31. Morphological examination of apoptosis. *Following 24 hours of hydrogen peroxide treatment A549 control, shPARP-1 and shPARG cells were stained with May-Grünwald-Giemsa and subsequently analysed by light microscopy*

6.2.8. Analysis of AIF nuclear translocation

As AIF release has been proposed to propagate poly(ADP-ribose) mediated cell death, we sought to determine AIF relocation following hydrogen peroxide treatment (**Figure 32.**). In untreated cells, AIF exhibited a punctuated distribution in the cytoplasm, corresponding to the mitochondrial localization of the protein. Hydrogen peroxide failed to induce AIF translocation from the mitochondria to the nucleus, indicating that AIF is not likely to mediate cell death in our model (**Figure 32A.**). Human umbilical cord-derived mesenchymal cells (MSC UCs) were used as a positive control. Hydrogen peroxide induced nuclear translocation of AIF in MSC UCs (**Figure 32B.**). Lack of nuclear translocation of AIF in A549 cells could also be confirmed in subcellular fractionation experiments (**figure 32C.**). Cells were fractionated into nuclear and postnuclear fractions, and AIF was detected with Western blotting. ATP5B was used as mitochondrial marker, whereas PARP-1 served as a nuclear marker.

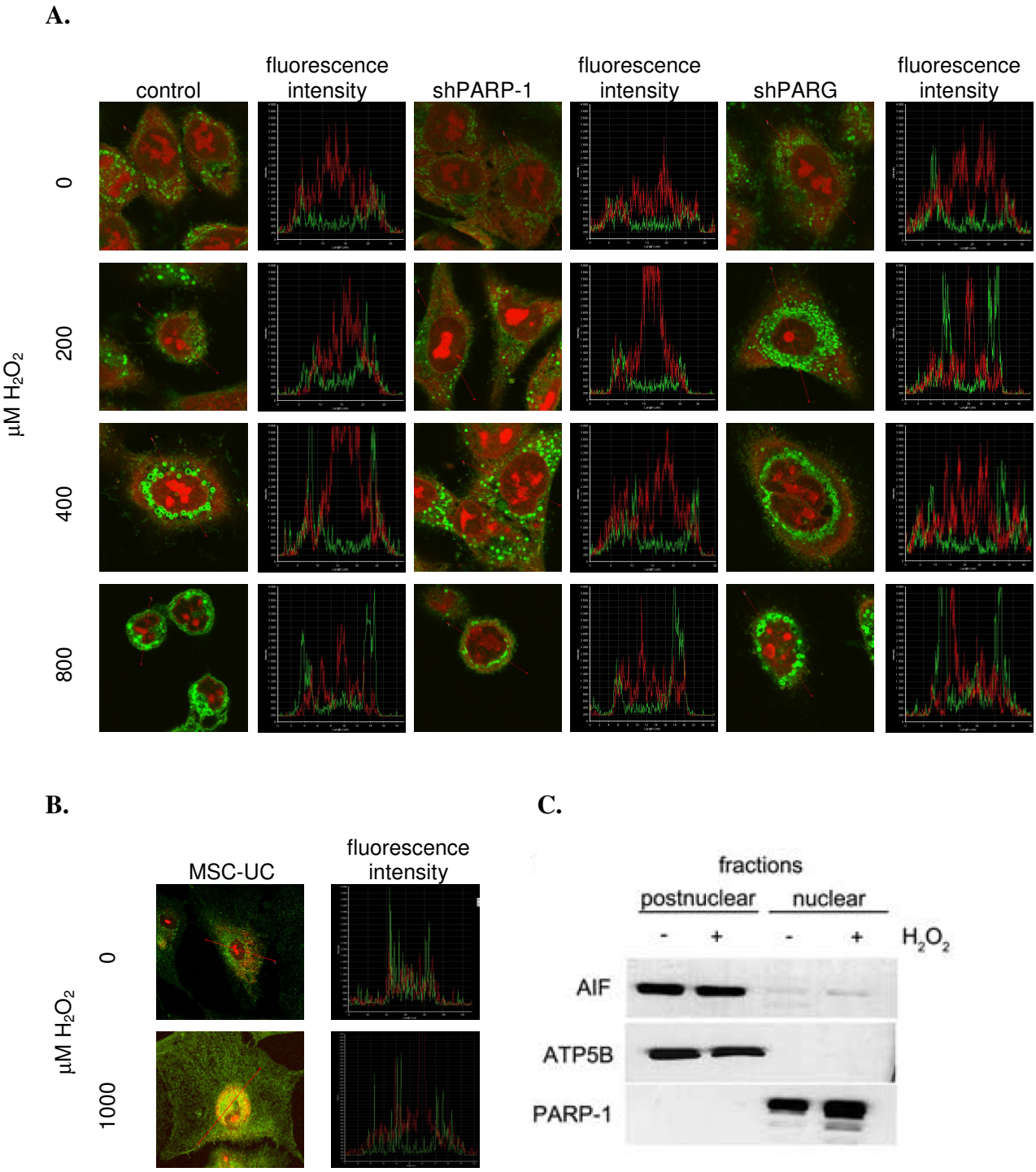

Figure 32. Lack of AIF translocation in A549 cells. *Cells exposed to indicated concentration of hydrogen peroxide for 24 hours were strained for AIF (green). Nuclei were counterstained with propidium iodide (red). AIF translocation was not observed in any of 3 cell lines. Z-stack fluorescent intensity plots prove lack of nuclear translocation of AIF. (**A**) Umbilical cord-derived human mesenchymal stem cells (UC MSCs) were used as a positive control. UC MSCs were treated with 1000 µM hydrogen peroxide for 16 hours and were stained similarly to A549 cells. UC MSCs showed clear signs of AIF translocation. (**B**) Lack of AIF translocation in A549 cells was also confirmed by subcellular fractionation into nuclear and postnuclear (including cytoplasmic and mitochondial) fractions. Proteins were separated by electrophoresis and stained for AIF, ATP5B (mitochondial marker) and PARP-1 (nuclear marker) (**C**).*

6.2.9. Concerted action of PARG and PARP-1 is required for the repair of oxidative stress-induced DNA breaks

One of the best-described biological functions of poly(ADP-ribosyl)ation is to assist DNA repair. Hydrogen peroxide (100, 200, and 400 μM) induced a concentration-dependent DNA breakage (**Figure 33A.**) as assessed by single-cell gel electrophoresis (comet assay). At 400 μM of hydrogen peroxide, massive DNA breakage was observed. Considering the severity of DNA damage, cells coped remarkably well with the repair of DNA breaks, as shown by images obtained during the recovery phase (**Figure 33 B.**). As an almost complete repair of damage could be observed at 45 min following hydrogen peroxide treatment, we compared the repair capacity of our cell lines at this time point. We observed an impaired DNA strand break repair in shPARP-1 cells and an almost complete blockage of repair in shPARG cells (**Figure 33C.**). Compromised DNA single-strand break repair may result in limited long-term clonogenic survival of shPARG and shPARP-1 cells. Indeed, we determined clonogenic survival following treatment with 200 μM hydrogen peroxide, and we found that both knockdown cells exhibited impaired clonogenicity (**Figure 33D.**).

A.

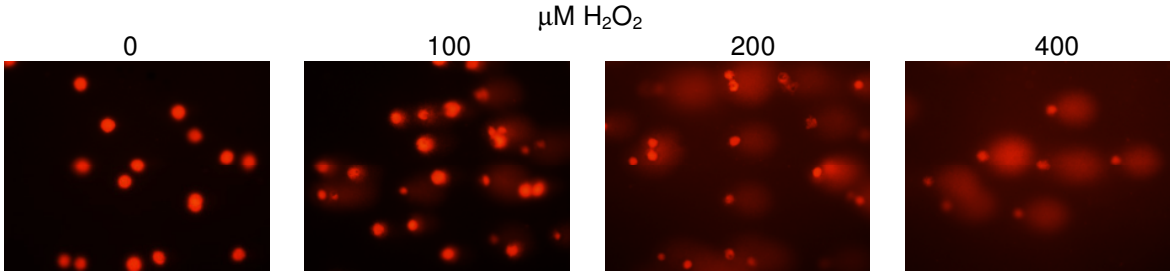

B.

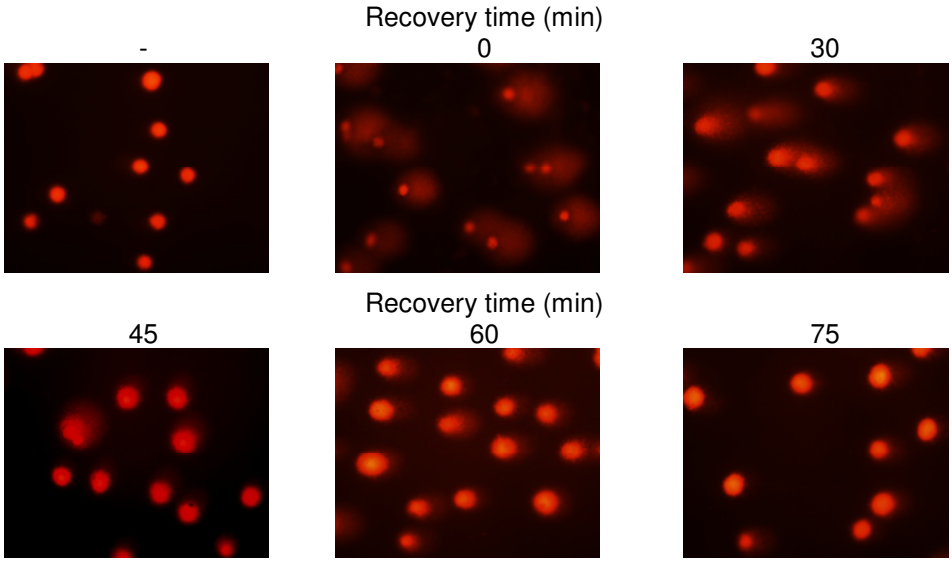

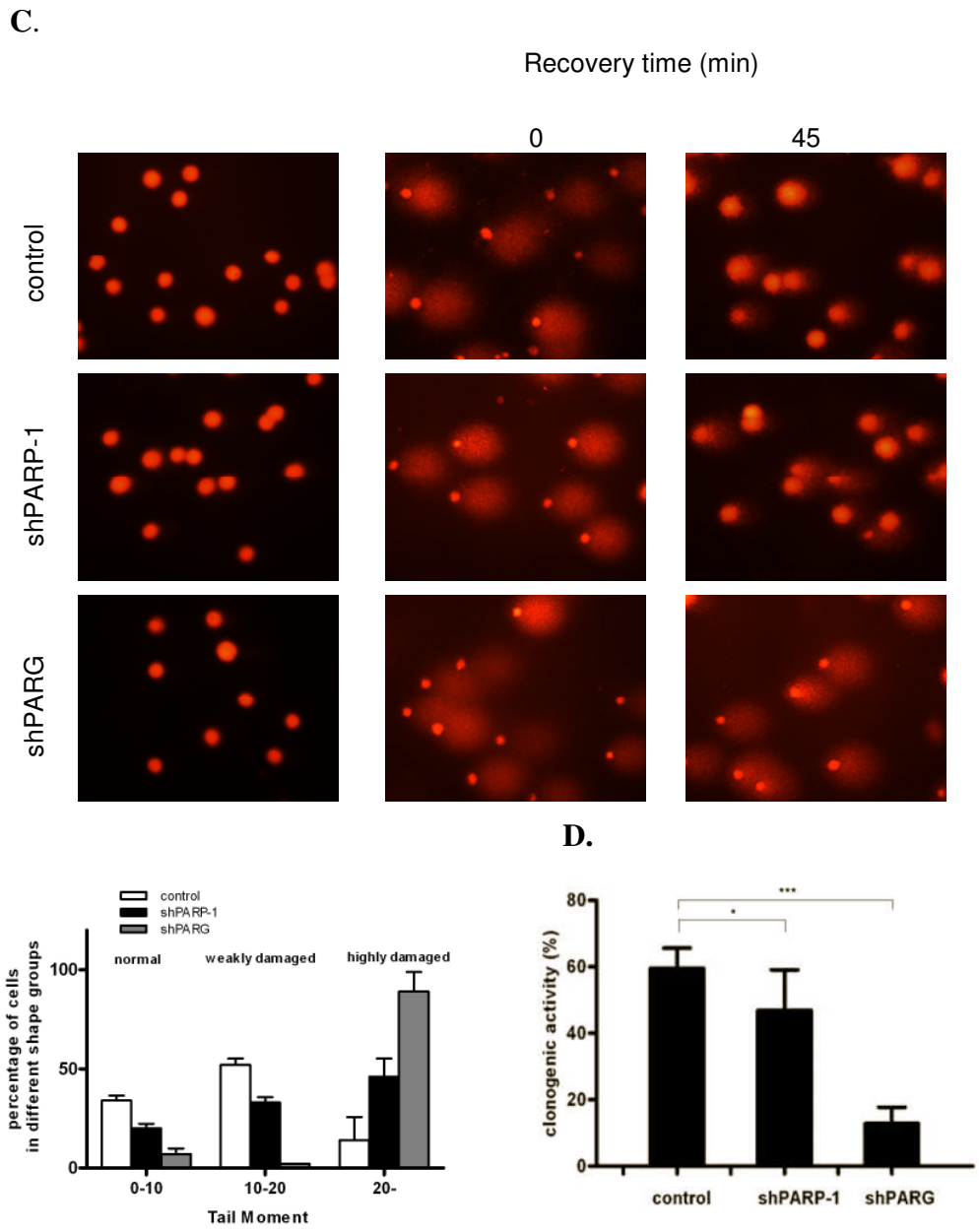

Figure 33. **Knockdown of PARG and PARP-1 delays single-stand break repair.** *DNA single-strand breakage was measured with the comet assay. Hydrogen peroxide induced a concentration dependent DNA breakage in A549 cells (**A**.). A549 cells were treated with 400 μM hydrogen peroxide for 15 min and then allowed to recover in culture medium for indicated time periods. Single cells were then exposed to an electric field in agarose gel and staind with ethidium bromide. Labeled DNA was visualised under fluorescent microscope (**B.**). Control, shPARP-1 and shPARG cells were exposed to 400 μM hydrogen for 15 min and then allowed to recover in culture medium for 45 minutes. Single cells then underwent electrophoresis and were processed as describped above. Distribution of olive tail moments is shown below (**C.**). Representative images are presented. Clonogenic activity of 200 μM hydrogen peroxide treated control, shPARP-1 and shPARG cells (**D**).*

7. DISCUSSION

7.1. Gallotannin inhibits the expression of inflammatory cytokines and chemokines in A549 cells

PARP-1 has been shown to regulate the expression of inflammatory mediators. We hypothesized that PARG inhibition by gallotannin may contribute to this anti-inflammatory effect. Beside the hypothetical PARG inhibitory effect of tannins they exert potent anti-inflammatory effects mainly by their anti-oxidant properties.

In A549 lung epithelial cells, our study revealed no major role of poly(ADP-ribosyl)ation as indicated by the lack of effect of PJ34 on the expression of most chemokines, with the exception of IL-8, CCR4, CCR5, and fractalkine. However, this finding does not exclude the possibility that PARP-1 regulates inflammatory gene expression via protein-protein interaction as previously demonstrated in experiments using PARP-1 knock-out cells (Ha et al., 2004; Carrillo et al., 2004). PJ34 has previously been shown to inhibit chemokine expression in macrophages (Hasko et al., 2002), a finding also confirmed by us (data not shown). This finding emphasizes the importance of cell type- and stimulus-dependent differences in the requirement of PARP activity for transcriptional regulation.

In contrast to PJ34, GT exerted a robust suppression of inflammatory gene expression. This effect is not caused by a general suppression of gene expression, because GT also prevented the cytokine-induced down-regulation of three chemokine receptors. In theory, the effects of GT could be attributed to hyper-poly(ADP-ribosyl)ation of PARP-1 or other poly(ADP-ribose) acceptors, including the transcription factors NF-κB and AP-1. Oliver et al. (1999) identified deficient NF-κB activation in PARP-$1^{-/-}$ mice, and it was later proposed that PARP-1 physically interacts with the NF-κB-p50. However, the DNA-binding and catalytic activity of PARP-1 was found not to be required for the NF-κB coactivator function (Hassa et al., 2001). In certain cellular systems, however, PARP inhibitors did inhibit NF-κB activation (Ha et al., 2002; Hasko et al., 2002).

Our data showing normal nuclear translocation but decreased DNA binding of NF-κB in PJ34-treated cells indicate that, in cytokine-stimulated A549 cells, DNA binding of NF-κB requires poly(ADP-ribosyl)ation. GT also blocked the NF-κB pathway. However, GT targeted an event upstream of IκB phosphorylation. Nonetheless, the inhibition of NF-κB activation by GT does not fully explain the marked effects of GT on cytokine/chemokine expression because PJ34, which has also inhibited NF-κB, failed to affect cytokine

expression. Therefore, we have considered the possibility that GT also interferes with the activation of AP-1, the other key transcription factor regulating inflammatory gene expression.

The redox-sensitive transcription factor AP-1 is composed of a mixture of heterodimeric protein complexes derived from the Fos and Jun families. AP-1 heterodimers bind to DNA on a serum-response element with the 5'-TGA(C/G)TCA-3' sequence. AP-1 is regulated at the level of both jun and fos gene transcription and by post-translational modifications of their gene products. MAPKs with special regard to JNK play a key role in AP-1 activation by phosphorylating c-Jun (Kyriakis and Avruch, 2001; Johnson and Lapadat, 2002). Zingarelli et al. (2004) reported increased basal JNK activity and c-Jun phosphorylation but decreased AP-1 DNA binding in PARP-1 knock-out cells. It is remarkable that, in A549 cells, we found similar effects with GT but PJ34 had no major effect on the AP-1 pathway.

Our current data suggest that AP-1, rather than NF-κB, plays a key role in the regulation of cytokine/chemokine gene expression in A549 cells. It is remarkable that suppression of AP-1 DNA binding by GT was paralleled by maximal activation (phosphorylation) of JNK and c-Jun, even in the absence of cytokines. To elucidate the mechanism by which GT "un-couples" phosphorylation of JNK and c-Jun from DNA binding of AP-1 requires further investigation. It is possible that GT triggers the JNK-c-Jun pathway by an unknown mechanism (e.g., by inhibiting protein phosphatases) and, independent of this, it also interferes with the DNA binding of AP-1.

Decreased AP-1 DNA binding in GT-treated cells may result from the inhibition of the p38-ATF2 pathway that is also important in the TNFα/IL-1β-induced inflammatory gene expression. The MAPK ERK1/2 can also regulate inflammatory gene transcription by indirectly activating CREB. The ERK-CREB pathway and the p38MAPK pathway were similarly affected by GT. GT inhibited cytokine-induced activation of both ERK1/2 and CREB, but GT alone caused a moderate phosphorylation of these proteins.

Gallotannin-induced phosphorylation of MAPKs and their targets may be due to interference of GT with protein phosphatases. Our data indicate that GT inhibits the catalytic subunits of protein phosphatases 1 and 2A. This inhibitory activity could also be observed on the phosphatase holoenzyme. PP1 and PP2A have been proposed to regulate the MAPK pathways in various systems (Garcia et al., 2002; Kim et al., 2003). Therefore, inhibition of PP1 and PP2A by GT may contribute to the increased phosphorylation level of MAPK in GT-treated cells. MAPK phosphatases also play a key role in

dephosphorylation of MAPK. Whether MAPK phosphatases are also inhibited by GT remains to be seen (**Figure 34.**).

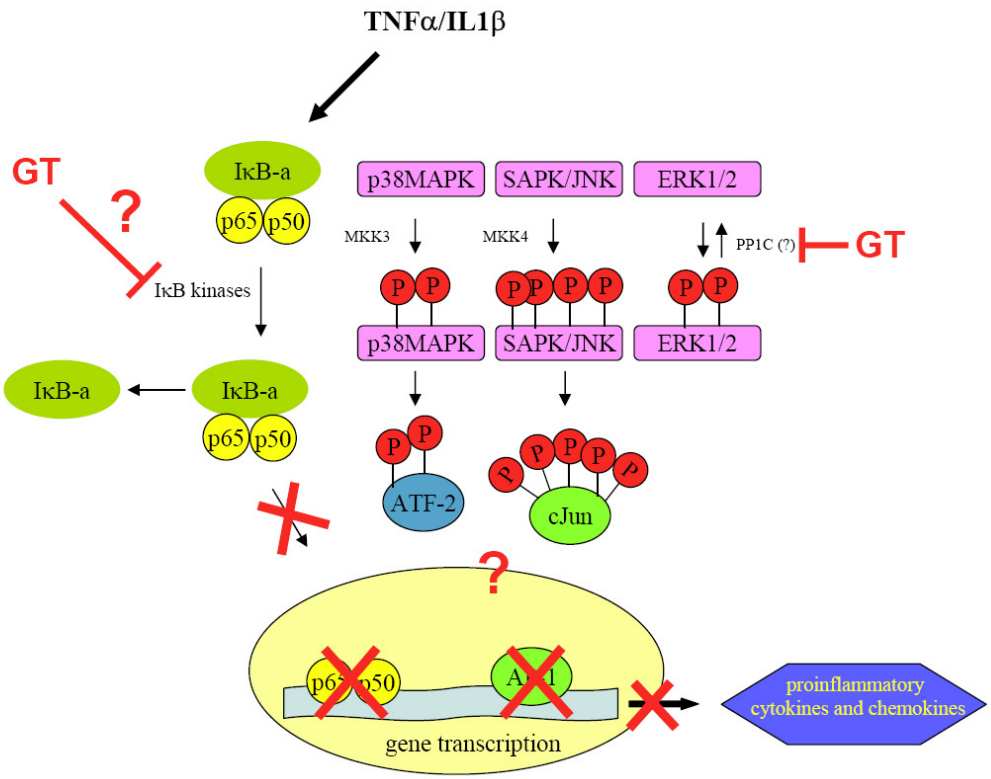

Figure 34. Mechanism for the anti-inflammatory effect of GT in immunostimulated A549 cells. NF-κB and AP-1 have crucial roles in the regulation of cytokine induced gene expression. GT inhibited the DNA binding of both key transcription factors. In case of NF-κB GT prevented its nuclear translocation by inhibiting the IκB protein phosphorylation. Although we could detect maximal phosphorylation of the AP-1 subunit c-Jun, its DNA binding was markedly reduced, even in the absence of cytokines. GT alone also induced the phosphorylation of MAPKs. This effect is likely to be the inhibition of protein phosphatases.

We also sought to determine whether the transcriptional regulatory effect of GT is related to PARG inhibition. Considering that a basal PARP activity is usually present in cultured cells (Bakondi et al., 2002), we expected GT to cause poly(ADP-ribose) accumulation. Our data showing the lack of poly(ADP-ribose) accumulation in GT-treated cells suggest that no major alterations of poly(ADP-ribose) metabolism occur in response to GT treatment. This is in line with previous reports from Falsig et al. (2004), demonstrating that GT inhibits PARG in a cell-free assay but has no effect on PARG activity in intact cells. Moreover, the cytokine exposure stimulated no poly(ADP-ribose) synthesis in either the

absence or presence of GT. In light of these data, it seems unlikely that PARG is the major target of GT in our system. Furthermore, a GT concentration of 50 μM or higher was previously shown to be required for poly(ADP-ribose) accumulation in cell lysates (Keil et al., 2004), whereas the marked transcriptional inhibitory effects in our current study required lower concentrations. Nonetheless, poly(ADP-ribose) accumulation on certain low abundance proteins may remain undetected in Western blots or immunocytofluorescent stainings and may be important for the regulation of transcription.

Considering that both NF-κB and AP-1 are regarded as redox-sensitive transcription factors, the antioxidant effect of GT may explain its effect on inflammatory gene expression. Our data showing potent antioxidant effects of GT at relatively low concentrations (30 μM) support this hypothesis. As opposed to macrophages, where GT seems to act as a proinflammatory stimulus (Rohrbach et al., 1989; Rapizzi et al., 2004), in epithelial cells, it acts as an anti-inflammatory agent. This effect results from the inhibition of the AP-1 pathway and, to a lesser extent, the NF-κB pathway. Unlike in macrophages, in A549 epithelial cells, poly(ADP-ribosyl)ation is not a crucial mechanism in the regulation of inflammatory gene expression and PARG is probably not the target of GT in this system.

7.2. Dual role of PARG in the regulation of cell death in oxidatively stressed A549 cells

In order to investigate the poly(ADP-ribose) metabolism in A549 cells we established A549 cell lines with stable suppressed PARG and PARP-1 proteins.

Once regarded as a DNA repair-assisting process, poly(ADP-ribosyl)ation has emerged in recent years as a pleiotropic mediator of a wide range of biological phenomena. Moreover, it has also been suggested that in cases of severe DNA damage, such as the ones observed in oxidative stress-related pathologies, accelerated poly(ADP-ribose) turnover may also mediate cellular suicide. A high number of studies based on the use of pharmacological inhibitors or knockout cells proved the role of PARP-1 in mediating genotoxicity-induced cell death (Virág and Szabo, 2002). Moreover, Virag et al. (1998) and others also demonstrated that PARP-1 acts as a molecular switch between apoptosis and necrosis (Ha and Snyder 1999; Moroni et al, Tentori et al., 2001). Recently the role of poly(ADP-ribosyl)ation has also been suggested in the regulation of a third form of cell death,

autophagy (Huang et al., 2008; Muñoz-Gámez et al., 2009). Of note, in line with the dual role of PARP-1 in cell death regulation activation of PARP-1 may also act as a protective mechanism in mild oxidative stress (Diaz-Hernandez et al., 2007), likely via assisting the repair of DNA breaks.

In contrast to the plethora of papers dealing with the role of PARP-1 in cell death, the role of PARG in the PARP-1-mediated suicidal pathway is largely unexplored. Studies based on the use of tannins as PARG inhibitors suggested that PARG is a mediator of cell death, whereas other studies reported opposite results (Falsig et al., 2004). However, the cellular effects of gallotannin in models of oxidative stress are difficult to interpret due to the potent antioxidant properties of tannins (Erdélyi et al., 2005). Moreover, embryonic lethality of PARG KO mice and neurotoxicity observed in PARG mutant Drosophila indicated that PARG activity may promote cell survival in genotoxic stress. More recently, poly(ADP-ribose) has been identified as a death-signaling molecule that, on release from the nucleus, may trigger AIF-mediated cell death. The role of PARG in the regulation of the mode of cell death has not yet been investigated.

Knocking down PARG did not cause toxicity in untreated cells. Hydrogen peroxide-induced poly(ADP-ribose) accumulation clearly demonstrated efficient knockdown of the protein. Our current work underscores the dual role of PARG in cell-death regulation. Knockdown of PARG provided protection from hydrogen peroxide-induced loss of viability; however, the degree of protection was less than that observed in shPARP-1 cells. Of note, similar but less pronounced protection could be observed in shPARP-1 and shPARG cells if other genotoxic stimuli (doxorubicine or MNNG) were used as cytotoxic agents (data not shown). Increased short-term viability of hydrogen peroxide treated shPARG cells, however, did not translate to increased long-term clonogenic survival. This is likely because of deficient repair of oxidative DNA breaks both in shPARP-1 and especially in shPARG cells. Concerted action of PARG and PARP-1 in DNA repair has been previously demonstrated (Fisher et al., 2007, Keil et al., 2006). Disruption of the poly(ADP-ribose) cycle on the side of either polymer synthesis or degradation leads to delayed DNA repair. Fisher et al. (2007) also reported decreased clonogenic survival in PARP-1- and PARG-knockdown cells; however, the effect of PARP-1 knockdown appeared to be more pronounced. Our data are in line with those of Fisher (2007), with the exception that PARG knockdown compromised DNA repair and clonogenic survival more than PARP-1 knockdown did, which might be due to different knockdown efficiency. Contribution of PARG to DNA repair may explain the increased sensitivity of shPARG

cells to mild genotoxic stimuli. What is the mechanism of oxidative stress-induced cytotoxicity in the absence of PARG?

Suppression of PARG expression decreased necrosis (as assessed by membrane permeability and ATP measurements) and led to increased apoptotic parameters, such as caspase-3 like activity and oligonucleosomal DNA fragmentation. These data indicate that PARG, similarly to PARP-1, mediates apoptosis-to-necrosis switch in severe oxidative stress. According to this scenario, PARG suppression leads to increased automodification of PARP-1, which is known to lead to PARP-1 autoinhibition (**Figure 35.**). In support of this, the major band of poly(ADP-ribose)-modified proteins in untreated shPARG cells corresponds to the size of PARP-1. Furthermore, PARG knockdown resulted in reduced PARP activation in hydrogen peroxide-treated cells, suggesting that auto-poly(ADP-ribosyl)ation indeed down-regulates PARP-1 activity.

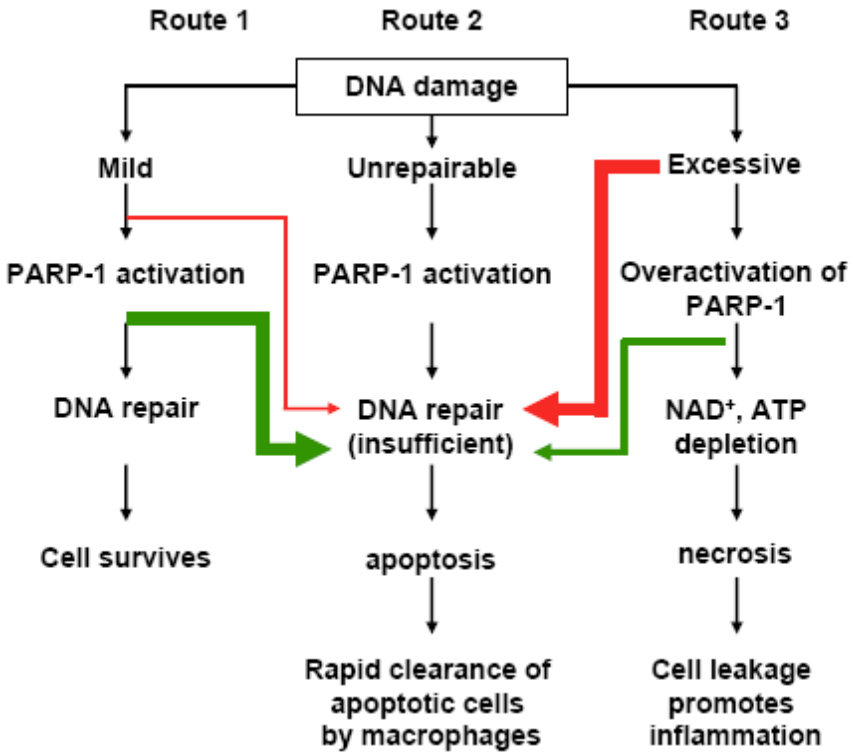

Figure 35. PARP-1 deficient cells are resistant to oxidative stress-induced necrotic cell death and undergo apoptosis (red arrow). PARG depletion contributes to the same effect, however in a lesser extent (green arrow). This is due the lack of PARP-1 overactivation (shPARP-1 cells) or auto-inhibition of PARP-1 (shPARG cells), which consequently leads to NAD^+ and ATP preservation. However, both cell lines exhibit sensitivity against mild

DNA damage. This could be in line with inefficient (shPARG) or delayed DNA repair (shPARP-1).

Depletion of PARP-1 protein prevent oxidative stress induced necrosis, similarly to PARG, mediates apoptosis-to-necrosis switch in severe oxidative stress.

Previously, it has been suggested that in neurons the lethal effects of PARP activation are mediated by AIF. If released from the nuclei, poly(ADP-ribose) may trigger AIF release from the mitochondria, which may propagate cell death. In our model, however, nuclear translocation of AIF could not be detected, and therefore AIF is not likely to mediate the cell-death response in oxidatively stressed A549 cells. Lack of AIF translocation has also been observed in a model of mild endogenous oxidative stress in neuronal cells (Diaz-Hernandez et al., 2007). Furthermore, heat shock protein 70 (Hsp70) has been shown to prevent nuclear relocation of AIF (Ravagnan et al.,2001). As lung tumors have been shown to express Hsp70 (Ciocca et al., 2005) and stressed A549 cells also up-regulate Hsp70 (Wong et al., 1998), therefore induction of Hsp70 may explain the absence of AIF translocation in our model. However, Hsp70 does not interfere with the release of AIF from the mitochondria; instead, it sequesters released AIF in the cytoplasm, thus blocking nuclear translocation. In our model, however, AIF did not appear to be released from the mitochondria, because a punctuate staining pattern was maintained. (AIF release would be indicated by a diffuse staining pattern.) Whether Hsp70 interferes with AIF signaling in oxidatively stressed A549 cells requires further investigation. Nonetheless, our data underscore the importance of cell type- and death-model-dependent differences in the dependence of cell death on AIF or other mediators. In light of the potential clinical applications of PARG inhibitors, these differences should be especially carefully evaluated by comparing responses of primary untransformed cells (e.g., neurons) with those of tumor cell lines.

As the AIF pathway does not play a role in mediating hydrogen peroxide-induced cell death of A549 cells, compromised cellular energetics may underlie the PARP-1/PARG-mediated cell death. This “classic” scenario of poly(ADP-ribosyl)ation-mediated cell death is based on PARP-1- mediated depletion of NAD^+, which slows glycolysis at the level of the NAD^+-dependent glyceraldehyde-3-phosphate dehydrogenase, leading to mitochondrial depolarization. NAD^+ depletion, mitochondrial depolarization, and the protective effect of TCA-cycle substrates support this scenario in our model.

Recent findings indicate that DNA-damaging signals, including doxorubicin and hydrogen peroxide, may also trigger autophagy (Huang et al., 2008; Muñoz-Gámez et al., 2009). As autophagy may inhibit other types of cell death, e.g., necrosis, it is plausible to hypothesize that autophagic process may be important in our model. Hydrogen peroxide-induced and PARP-1-mediated autophagy may down-regulate cell death seen at low concentrations of the oxidant. This effect may contribute to increased sensitivity of shPARP-1 and shPARG cells, as observed in clonogenic assays. Similarly to our model, PARP-1-mediated autophagy could also be inhibited by the TCA-cycle substrate methyl pyruvate (Muñoz-Gámez et al., 2009), indicating that suppressed cellular energetics may be a central regulator of the autophagic process. The exact role of autophagy in hydrogen peroxide-induced cytotoxicity in A549 cells and the interrelationship of PARP-1/PARG and the autophagic process require further investigation.

8. FUTURE PROSPECTS

Use of PARP inhibitors as adjuvant anticancer agents and to reduce tissue injury in oxidative stress-related pathologies has previously been proposed and is being tested in clinical trials.

Enhanced PAPR-1 expression and/or activity has been shown in several tumor cell lines including malignant lymphomas, hepatocellular carcinoma, colorectal carcinoma, non-Hodgkin's lymphoma, leukemic lymphocytes and colon adenomatous polyps. This may allow tumor cells to withstand genotoxic stress and increase their resistance to DNA-damagint agents. (Ratman and Low, 2007). Inhibition of PARP potentiates the activity of DNA-damaging agents such as alkylation, topoisomerase inhibitors, and radiation in *in vitro* and *in vivo* models. In addition, tumors with DNA repair defects, such as those arising from patients with BRCA mutation, may be more sensitive to PARP inhibiton.

Our data indicate that the effects of PARG inhibition are similar to the inhibition of PARP-1. Therefore, it appears to be plausible to test the effects of PARG inhibition in the same pathological conditions in which PARP inhibitors proved beneficial. Potent, selective, and cell-permeable PARG inhibitors are clearly needed to test whether PARG inhibition represents a valid approach in these disease models.

9. CONCLUSIONS

1. TNFα/IL1β induces chemokine and cytokine gene-expression through NF-κB and AP-1 activation in A549 cells which is strongly suppressed by GT and weakly inhibited by the PARP-1 specific inhibitor PJ34.

2. GT decreased NF-κB transactivation by inhibiting its nuclear translocation. This effect is due to the inhibition of IκB phosphorylation. PJ34 did not affect the nuclear translocation of the transcription factor, however it inhibited its DNA binding.

3. GT also inhibited the DNA binding of the transcription factor, AP-1 even in the absence of cytokines. However, GT did not inhibit the activation of the AP-1 subunits. Moreover, we observed an elevated phosphorylation of c-Jun.

4. GT alone induced phosphorylation of JNK, p38MAPK and ERK1/2 and their targets. This might be due to the inhibition of protein phosphatases.

5. Lack of poly(ADP-ribose) accumulation in GT-treated cells suggests that no major alteration of poly(ADP-ribose) metabolism occur in response to GT treatment. Moreover, the cytokine exposure stimulated no detectable poly(ADP-ribose) synthesis in either the absence or presence of GT.

6. Stable gene silencing of PARG provided protection from hydrogen peroxide-induced loss of viability; however, the degree of protection was less than that observed in shPARP-1 cells.

7. Increased short-term viability of hydrogen peroxide treated shPARG cells, however, did not translate to increased long-term clonogenic survival.

8. PARG deficiency led to enhanced sensitivity against mild DNA damage.

9. Hydrogen peroxide-induced apoptosis seemed to be caspase dependent and AIF independent in A549 cells.

10. Deficient repair of oxidative DNA breaks was observed both in shPARP-1 and especially in shPARG cells.

10. SUMMARY

Poly(ADP-ribosyl)ation, catalysed by poly(ADP-ribose) polymerases (PARP-s), is a reversible post-translational modification of glutamate and aspartate residues of nuclear proteins and represents an immediate eukaryotic cellular response to DNA damage as induced by ionizing radiation, alkylating agents and oxidants. The ADP-ribose polymer formed by sequential attachment of ADP-ribosyl moieties form NAD^+ can reach high complexity with chain lengths of up to 200 units and multiple branching points. The major enzyme catalyzing poly(ADP-ribose) catabolism is poly(ADP-ribose) glycohydrolase (PARG), splitting the polymer's unique ribose-ribose linkages generating free ADP-ribose units. Here we have investigated the possible role of poly(ADP-ribosyl)ation in cytokine-stimulated A549 cells. Cells were pretreated with a potent PARP-1 inhibitor PJ34 or the PARG inhibitor gallotannin (GT). Cytokines induced the expression of several chemokines and cytokines through NF-κB and AP-1 activation in A549 cells which was strongly suppressed by GT and weakly inhibited by PJ34. GT decreased NFκB transactivation by inhibiting its nuclear translocation. This effects was due to the inhibition of IκB phosphorylation. PJ34 did not affect the nuclear translocation of the transcription factor, however it inhibited its DNA binding. GT also inhibited the DNA binding of the transcription factor, AP-1 even in the absence of cytokines. However, GT did not inhibit the activation of the AP-1 subunits. Moreover, we observed an elevated phosphorylation of c-Jun. GT alone induced phosphorylation of JNK, p38MAPK and ERK and their targets. This might be due to the inhibition of protein phosphatases (PP1 and PP2A). The cytokine exposure stimulated no detectable poly(ADP-ribose) synthesis in either the absence or presence of GT. Lack of poly(ADP-ribose) accumulation in GT-treated cells suggests that no major alteration of poly(ADP-ribose) metabolism occur in A549 cells in response to GT treatment. Since GT didn't prove to be a suitable tool for the investigation of PARG, we established A549 cell lines with stable suppression of the PARG and PARP1 genes. These knockdown cells were protected from necrosis (propidium iodide uptake) induced by severe oxidative stress, however, they were more sensitive to apoptosis (as measured by caspase activation and DNA fragmentation) induced by mild oxidative stress. We identified inefficient DNA repair as the underlying mechanism of this latter effect. The similar responses of the PARG and PARP1 knockdown cells indicate that PARG knockdown may result in indirect inhibition of PARP-1 via inhibitory auto-poly(ADP-ribosyl)ation.

11. ÖSSZEFOGLALÁS

A poli-ADP-riboziláció, melyet poli(ADP-ribóz) polimerázok (PARP) katalizálnak, egy reverzibilis poszttranszlációs módosítás fehérjék glutamát és aszpartát oldalláncán. A jelenséget elsősorban DNS károsodást követően figyelhetjük meg, melyet okozhat ionizáló sugárzás, alkiláló és oxidatív ágens. A DNS törés hatására aktiválódott PARP-1 szubsztrátjából, a NAD^+-ból ADP-ribózt hasít ki, és ezekből az egységekből hosszú, elágazó láncot szintetizál. A folyamat reverzibilitásáért elsősorban a poli(ADP-ribóz) glikohidroláz (PARG) felel, mely ADP-ribóz egységekre bontja a láncot.

Kísérleteink első felében a poli-ADP-riboziláció esetleges szabályozó mechanizmusát vizsgáltuk citokinekkel stimulált A549 sejtekben. A sejteket specifikus PARP-1 gátlószerrel (PJ34) és egy PARG inhibitor vegyülettel (gallotannin, GT) kezeltük elő. A citokin kezelés hatására kemokinek és további citokin gének expressziója jelentős mértékben nőtt, melyet a GT fokozottabb, a PJ34 pedig kis mértékben gátolt. A citokinek génexpressziós hatásukat az NF-κB és az AP-1 transzkripciós faktorokon keresztül fejtették ki. Mind a GT, mind a PJ34 gátolta a NF-κB transzaktivációját; a GT gátolta az IκB foszforilálódását, és emiatt az NF-κB sejtmagba történő transzlokációját, míg a PJ34 gátolta az NF-κB DNS-hez való kötődését. A GT gátolta az AP-1 DNS-hez való kötődését is, ez a hatás a citokin kezelés hiányában is fennállt. Érdekes módon, a GT önmagában is kiváltotta az AP-1 egyik komponensének, a cJun-nak a foszforilálódását, sőt indukálta a JNK, p38MAPK és ERK1/2 valamint azok targetjeinek foszforilálódását. Feltételezzük, hogy a jelenség hátterében foszfatáz enzimek (PP1 és PP2A) gátlása áll. Megállapítottuk továbbá, hogy a citokin kezelés nem okozott jelentős poli-ADP-ribóz szintézist, a polimerek akkumulációját pedig nem tudtuk megfigyelni GT jelenlétében.

A PARG további vizsgálata céljából stabil géncsendesítést valósítottunk meg A549 sejtekben. Mind a PARG, mind a PARP-1 gén csendesítése rezisztenciát okozott nagy dózisú hidrogén peroxid kezeléssel kiváltott citotoxicitással szemben. Ez a védelem azonban csak rövidtávon érvényesült. Megfigyeltük, hogy alacsonyabb, apoptózist indukáló hidrogén peroxid kezeléssel szemben mind a PARG, mind a PARP-1 csendesített sejtek érzékenyebbek, ennek hátterében pedig azok elégtelen DNS hibajavítását igazoltuk. Az apoptózis az általunk vizsgált rendszerben kaszpáz-függő de az apoptózis indukáló faktortól függetlennek találtuk. A PARP-1 és a PARG csendesített sejtvonalak hasonló viselkedése arra utal, hogy a PARG gátlása fokozza a PARP-1 gátló hatású auto-poli-ADP-ribozilációját.

12. REFERENCES

Affar EB, Germain M, Winstall E, Vodenicharov M, Shah RG, Salvesen GS, Poirier GG. **Caspase-3-mediated processing of poly(ADP-ribose) glycohydrolase during apoptosis.** *J Biol Chem.* (2001) 276(4):2935-42

Albert JM, Cao C, Kim KW, Willey CD, Geng L, Xiao D, Wang H, Sandler A, Johnson DH, Colevas AD, Low J, Rothenberg ML, Lu B. **Inhibition of poly(ADP-ribose) polymerase enhances cell death and improves tumor growth delay in irradiated lung cancer models.** *Clin Cancer Res.* (2007) 13(10):3033-42

Althaus FR, Richter C. **ADP-ribosylation of proteins. Enzymology and biological significance.** *Mol Biol Biochem Biophys*. (1987) 37:1-237

Amé JC, Apiou F, Jacobson EL, Jacobson MK. **Assignment of the poly(ADP-ribose) glycohydrolase gene (PARG) to human chromosome 10q11.23 and mouse chromosome 14B by in situ hybridization** *Cytogenet Cell Genet.* (1999) 85(3-4):269-70

Amé JC, Spenlehauer C, de Murcia G. **The PARP superfamily.** *Bioessays.* (2004) 26(8):882-93

Andreone TL, O'Connor M, Denenberg A, Hake PW, Zingarelli B**. Poly(ADP-ribose) polymerase-1 regulates activation of activator protein-1 in murine fibroblasts.** *J Immunol.* (2003) 170(4):2113-20

Bai P, Bakondi E, Szabó E, Gergely P, Szabó C, Virág L. **Partial protection by poly(ADP-ribose) polymerase inhibitors from nitroxyl-induced cytotoxity in thymocytes.** *Free Radic Biol Med.* (2001) 31(12):1616-23

Bakondi E, Bai P, Erdélyi K, Szabó C, Gergely P, Virág L. **Cytoprotective effect of gallotannin in oxidatively stressed HaCaT keratinocytes: the role of poly(ADP-ribose) metabolism.** *Exp Dermatol.* (2004) 13(3):170-8

Bakondi E, Bai P, Szabó E E, Hunyadi J, Gergely P, Szabó C, Virág L. **Detection of poly(ADP-ribose) polymerase activation in oxidatively stressed cells and tissues using biotinylated NAD substrate.** *J Histochem Cytochem.* (2002) 50(1):91-8

Berger NA. **Poly(ADP-ribose) in the cellular response to DNA damage**. *Radiat Res.* (1985) 101(1):4-15

Bhatia M, Kirkland JB, Meckling-Gill KA. **Modulation of poly(ADP-ribose) polymerase during neutrophilic and monocytic differentiation of promyelocytic (NB4) and myelocytic (HL-60) leukaemia cells.** *Biochem J.* (1995) 308 (Pt 1):131-7

Blenn C, Althaus FR, Malanga M**. Poly(ADP-ribose) glycohydrolase silencing protects against H2O2-induced cell death.** *Biochem J.* (2006) 396(3):419-29

Boulares AH, Zoltoski AJ, Sherif ZA, Jolly P, Massaro D, Smulson ME. **Gene knockout or pharmacological inhibition of poly(ADP-ribose) polymerase-1 prevents lung**

inflammation in a murine model of asthma. *Am J Respir Cell Mol Biol.* (2003) 28(3):322-9

Bonicalzi ME, Haince JF, Droit A, Poirier GG. **Regulation of poly(ADP-ribose) metabolism by poly(ADP-ribose) glycohydrolase: where and when?** *Cell Mol Life Sci.* (2005) 62(7-8):739-50

Bürkle A, Chen G, Kupper J H, Grube K, Zeller W J. **Increased poly(ADP-ribosyl)ation in intact cells by cisplatin treatment.** *Carcinogenesis* (1993) 14**:** 559–561

Burzio LO, Riquelme PT, Koide SS. **ADP ribosylation of rat liver nucleosomal core histones.** *J Biol Chem* (1979) 254(8):3029-37

Butler AJ, Ordahl CP**. Poly(ADP-ribose) polymerase binds with transcription enhancer factor 1 to MCAT1 elements to regulate muscle-specific transcription**. *Mol Cell Biol.*(1999) 19(1):296-306

Carpenter LR, Moy JN, Roebuck KA. **Respiratory syncytial virus and TNF alpha induction of chemokine gene expression involves differential activation of Rel A and NF-kappa B1.** *BMC Infect Dis.* (2002) 2:5

Carrillo A, Monreal Y, Ramírez P, Marin L, Parrilla P, Oliver FJ, Yélamos J. **Transcription regulation of TNF-alpha-early response genes by poly(ADP-ribose) polymerase-1 in murine heart endothelial cells.** *Nucleic Acids Res.* (2004) 32(2):757-66

Cervellera MN, Sala A. **Poly(ADP-ribose) polymerase is a B-MYB coactivator**. *J Biol Chem*. (2000) 275(14):10692-6

Chambon P, Weill JD, Mandel P. **Nicotinamide mononucleotide activation of new DNA-dependent polyadenylic acid synthesizing nuclear enzyme.** *Biochem Biophys Res Commun.* (1963) 11:39-43

Chang WJ, Alvarez-Gonzalez R. **The sequence-specific DNA binding of NF-kappa B is reversibly regulated by the automodification reaction of poly (ADP-ribose) polymerase 1.** *J Biol Chem.* (2001) 276(50):47664-70

Chiarugi A. **Poly(ADP-ribose) polymerase: killer or conspirator? The 'suicide hypothesis' revisited.** *Trends Pharmacol Sci*. (2002) 23(3):122-9

Christopherson K, Hromas R. **Chemokine regulation of normal and pathologic immune responses.** *Stem Cells.* (2001) 19(5):388-96

Ciocca DR, Calderwood SK. **Heat shock proteins in cancer: diagnostic, prognostic, predictive, and treatment implications.** *Cell Stress Chaperones.* (2005) 10(2):86-103

Cortes U, Tong WM, Coyle DL, Meyer-Ficca ML, Meyer RG, Petrilli V, Herceg Z, Jacobson EL, Jacobson MK, Wang ZQ. **Depletion of the 110-kilodalton isoform of poly(ADP-ribose) glycohydrolase increases sensitivity to genotoxic and endotoxic stress in mice.** *Mol Cell Biol*. (2004) 24(16):7163-78

D'Amours D, Desnoyers S, D'Silva I, Poirier GG. **Poly(ADP-ribosyl)ation reactions in the regulation of nuclear functions**. *Biochem J*. (1999) 342 (Pt 2):249-68

Dantzer F, Amé JC, Schreiber V, Nakamura J, Ménissier-de Murcia J, de Murcia G. **Poly(ADP-ribose) polymerase-1 activation during DNA damage and repair.** *Methods Enzymol.* (2006) 409:493-510

Diaz-Hernandez JI, Moncada S, Bolaños JP, Almeida A**. Poly(ADP-ribose) polymerase-1 protects neurons against apoptosis induced by oxidative stress.** *Cell Death Differ.* (2007) 14(6):1211-21

Diefenbach J, Bürkle A. **Introduction to poly(ADP-ribose) metabolism.** *Cell Mol Life Sci.* (2005) 62(7-8):721-30

Eki T, Hurwitz J. **Influence of poly(ADP-ribose) polymerase on the enzymatic synthesis of SV40 DNA**. *J Biol Chem.* (1991) 266(5):3087-100

Falsig J, Christiansen SH, Feuerhahn S, Bürkle A, Oei SL, Keil C, Leist M. **Poly(ADP-ribose) glycohydrolase as a target for neuroprotective intervention: assessment of currently available pharmacological tools.** *Eur J Pharmacol.* (2004) 497(1):7-16

Farmer H, McCabe N, Lord CJ, Tutt AN, Johnson DA, Richardson TB, Santarosa M, Dillon KJ, Hickson I, Knights C, Martin NM, Jackson SP, Smith GC, Ashworth A. **Targeting the DNA repair defect in BRCA mutant cells as a therapeutic strategy.** *Nature.* (2005) 434(7035):917-21

Feldman KS, Sahasrabudhe K, Lawlor MD, Wilson SL, Lang CH, Scheuchenzuber WJ. **In vitro and In vivo inhibition of LPS-stimulated tumor necrosis factor-alpha secretion by the gallotannin beta-D-pentagalloylglucose.** *Bioorg Med Chem Lett.* (2001) 11(14):1813-5

Fisher AE, Hochegger H, Takeda S, Caldecott KW. **Poly(ADP-ribose) polymerase 1 accelerates single-strand break repair in concert with poly(ADP-ribose) glycohydrolase.** *Mol Cell Biol.* (2007) 27(15):5597-605

Gao H, Coyle DL, Meyer-Ficca ML, Meyer RG, Jacobson EL, Wang ZQ, Jacobson MK. **Altered poly(ADP-ribose) metabolism impairs cellular responses to genotoxic stress in a hypomorphic mutant of poly(ADP-ribose) glycohydrolase.** *Exp Cell Res.* (2007) 313(5):984-96

Garcia L, Garcia F, Llorens F, Unzeta M, Itarte E, Gómez N. **PP1/PP2A phosphatases inhibitors okadaic acid and calyculin A block ERK5 activation by growth factors and oxidative stress.** *FEBS Lett.* (2002) 523(1-3):90-4

Genovese T, Di Paola R, Catalano P, Li JH, Xu W, Massuda E, Caputi AP, Zhang J, Cuzzocrea S. **Treatment with a novel poly(ADP-ribose) glycohydrolase inhibitor reduces development of septic shock-like syndrome induced by zymosan in mice**. *Crit Care Med.* (2004) 32(6):1365-74

Gergely P, Erdodi F, Bot G. **Heparin inhibits the activity of protein phosphatase-1**. *FEBS Lett* (1984) 169:45-48

Gilmore TD. **The Rel/NF-kappaB signal transduction pathway: introduction.** *Oncogene.* (1999) 18(49):6842-4

Ha HC, Snyder SH. **Poly(ADP-ribose) polymerase is a mediator of necrotic cell death by ATP depletion.** *Proc Natl Acad Sci U S A.* (1999) 96(24):13978-82

Ha HC, Hester LD, Snyder SH. **Poly(ADP-ribose) polymerase-1 dependence of stress-induced transcription factors and associated gene expression in glia.** *Proc Natl Acad Sci U S A.* (2002) 99(5):3270-5

Ha HC. **Defective transcription factor activation for proinflammatory gene expression in poly(ADP-ribose) polymerase 1-deficient glia.** *Proc Natl Acad Sci U S A.* (2004) 101(14):5087-92

Hagerman AE, Riedl KM, Rice RE. **Tannins as biological antioxidants.** *Basic Life Sci.* (1999) 66:495-505

Hanai S, Kanai M, Ohashi S, Okamoto K, Yamada M, Takahashi H, Miwa M. **Loss of poly(ADP-ribose) glycohydrolase causes progressive neurodegeneration in Drosophila melanogaster** *Proc Natl Acad Sci U S A*. (2004) 101(1):82-6

Haskó G, Mabley JG, Németh ZH, Pacher P, Deitch EA, Szabó C. **Poly(ADP-ribose) polymerase is a regulator of chemokine production: relevance for the pathogenesis of shock and inflammation.** *Mol Med.* (2002) 8(5):283-9

Hassa PO, Buerki C, Lombardi C, Imhof R, Hottiger MO. **Transcriptional coactivation of nuclear factor-kappaB-dependent gene expression by p300 is regulated by poly(ADP)-ribose polymerase-1.** *J Biol Chem.* (2003) 278(46):45145-53

Hassa PO, Covic M, Hasan S, Imhof R, Hottiger MO. **The enzymatic and DNA binding activity of PARP-1 are not required for NF-kappa B coactivator function** *J Biol Chem.* (2001) 276(49):45588-97

Hassa PO, Hottiger MO. **The diverse biological roles of mammalian PARPS, a small but powerful family of poly-ADP-ribose polymerases.** *Front Biosci.* (2008) 13:3046-82

Hassa PO, Hottiger MO. **The functional role of poly(ADP-ribose)polymerase 1 as novel coactivator of NF-kappaB in inflammatory disorders.** *Cell Mol Life Sci.* (2002) 59(9):1534-53

Hatakeyama K, Nemoto Y, Ueda K, Hayaishi O. **Purification and characterization of poly(ADP-ribose) glycohydrolase. Different modes of action on large and small poly(ADP-ribose).** *J Biol Chem*. (1986) 261(32):14902-11

Hayashi K, Tanaka M, Shimada T, Miwa M, Sugimura T. **Size and shape of poly(ADP-ribose): examination by gel filtration, gel electrophoresis and electron microscopy.** *Biochem Biophys Res Commun.* (1983) 112(1):102-7

Hegedus C, Lakatos P, Oláh G, Tóth BI, Gergely S, Szabó E, Bíró T, Szabó C, Virág L. **Protein kinase C protects from DNA damage-induced necrotic cell death by inhibiting poly(ADP-ribose) polymerase-1.** *FEBS Lett.* (2008) 582(12):1672-8

Ho KY, Huang JS, Tsai CC, Lin TC, Hsu YF, Lin CC. **Antioxidant activity of tannin components from Vaccinium vitis-idaea L.** *J Pharm Pharmacol*. (1999) 51(9):1075-8

Homburg S, Visochek L, Moran N, Dantzer F, Priel E, Asculai E, Schwartz D, Rotter V, Dekel N, Cohen-Armon M. **A fast signal-induced activation of Poly(ADP-ribose) polymerase: a novel downstream target of phospholipase c.** *J Cell Biol.* (2000) 150(2):293-307

Huang Q, Wu YT, Tan HL, Ong CN, Shen HM. **A novel function of poly(ADP-ribose) polymerase-1 in modulation of autophagy and necrosis under oxidative stress.** *Cell Death Differ.* (2009) 16(2):264-77

Jagtap P, Szabó C. **Poly(ADP-ribose) polymerase and the therapeutic effects of its inhibitors.** *Nat Rev Drug Discov.* (2005) 4(5):421-40

Jo CH, Kim OS, Park EY, Kim BJ, Lee JH, Kang SB, Lee JH, Han HS, Rhee SH, Yoon KS. **Fetal mesenchymal stem cells derived from human umbilical cord sustain primitive characteristics during extensive expansion.** *Cell Tissue Res.* (2008) 334(3):423-33

Johnson GL, Lapadat R. **Mitogen-activated protein kinase pathways mediated by ERK, JNK, and p38 protein kinases.** *Science.* (2002) 298(5600):1911-2

Kannan P, Yu Y, Wankhade S, Tainsky MA. **PolyADP-ribose polymerase is a coactivator for AP-2-mediated transcriptional activation.** *Nucleic Acids Res.* (1999) 27(3):866-74

Kaufmann SH, Desnoyers S, Ottaviano Y, Davidson NE, Poirier GG. **Specific proteolytic cleavage of poly(ADP-ribose) polymerase: an early marker of chemotherapy-induced apoptosis.** *Cancer Res.* (1993) 53(17):3976-85

Keil C, Gröbe T, Oei SL. **MNNG-induced cell death is controlled by interactions between PARP-1, poly(ADP-ribose) glycohydrolase, and XRCC1.** *J Biol Chem.* (2006) 281(45): 34394-405

Keil C, Petermann E, Oei SL. **Tannins elevate the level of poly(ADP-ribose) in HeLa cell extracts.** *Arch Biochem Biophys.* (2004) 425(1):115-21

Kim HS, Song MC, Kwak IH, Park TJ, Lim IK. **Constitutive induction of p-Erk1/2 accompanied by reduced activities of protein phosphatases 1 and 2A and MKP3 due to reactive oxygen species during cellular senescence.** *J Biol Chem.* (2003) 278(39):37497-510

Koh DW, Lawler AM, Poitras MF, Sasaki M, Wattler S, Nehls MC, Stöger T, Poirier GG, Dawson VL, Dawson TM. **Failure to degrade poly(ADP-ribose) causes increased**

sensitivity to cytotoxicity and early embryonic lethality. *Proc Natl Acad Sci USA.* (2004) 101(51):17699-704

Kooy NW, Royall JA, Ischiropoulos H, Beckman JS. **Peroxynitrite-mediated oxidation of dihydrorhodamine 123.** *Free Radic Biol Med.* (1994) 16(2):149-56

Kraus WL, Lis JT**. PARP goes transcription.** *Cell.* (2003) 113(6):677-83

Kyriakis JM, Avruch J. **Mammalian mitogen-activated protein kinase signal transduction pathways activated by stress and inflammation**. *Physiol Rev.* (2001) 81(2):807-69

Kyriakis JM. **Activation of the AP-1 transcription factor by inflammatory cytokines of the TNF family.** *Gene Expr.* (1999) 7(4-6):217-31

Laing KJ, Secombes CJ. **Chemokines.** *Dev Comp Immunol.* (2004) 28(5):443-60

Langelier MF, Servent KM, Rogers EE, Pascal JM. **A third zinc-binding domain of human poly(ADP-ribose) polymerase-1 coordinates DNA-dependent enzyme activation.** *J Biol Chem.* (2008) 283(7):4105-14

Lecureur V, Ferrec EL, N'diaye M, Vee ML, Gardyn C, Gilot D, Fardel O. **ERK-dependent induction of TNFalpha expression by the environmental contaminant benzo(a)pyrene in primary human macrophages.** *FEBS Lett.* (2005) 579(9):1904-10

Lee SJ, Lee IS, Mar W. **Inhibition of inducible nitric oxide synthase and cyclooxygenase-2 activity by 1,2,3,4,6-penta-O-galloyl-beta-D-glucose in murine macrophage cells.** *Arch Pharm Res.* (2003) 26(10):832-9

Lontay B, Kiss A, Gergely P, Hartshorne DJ, Erdodi F. **Okadaic acid induces phosphorylation and translocation of myosin phosphatase target subunit 1 influencing myosin phosphorylation, stress fiber assembly and cell migration in HepG2 cells.** *Cell Signal.* (2005) 17(10):1265-75

Masson M, Niedergang C, Schreiber V, Muller S, Menissier-de Murcia J, de Murcia G. **XRCC1 is specifically associated with poly(ADP-ribose) polymerase and negatively regulates its activity following DNA damage.** *Mol Cell Biol.* (1998) 18(6):3563-71

Mendoza-Alvarez H, Alvarez-Gonzalez R. **Poly(ADP-ribose) polymerase is a catalytic dimer and the automodification reaction is intermolecular.** *J Biol Chem.* (1993) 268(30):22575-80

Mendoza-Alvarez H, Alvarez-Gonzalez R. **Regulation of p53 sequence-specific DNA-binding by covalent poly(ADP-ribosyl)ation.** *J Biol Chem.* (2001) 276(39):36425-30

Meyer RG, Meyer-Ficca ML, Whatcott CJ, Jacobson EL, Jacobson MK. **Two small enzyme isoforms mediate mammalian mitochondrial poly(ADP-ribose) glycohydrolase (PARG) activity.** *Exp Cell Res.* (2007) 313(13):2920-36

Meyer-Ficca ML, Meyer RG, Coyle DL, Jacobson EL, Jacobson MK. **Human poly(ADP-ribose) glycohydrolase is expressed in alternative splice variants yielding isoforms that localize to different cell compartments.** *Exp Cell Res.* (2004) 297(2):521-32

Miramar MD, Costantini P, Ravagnan L, Saraiva LM, Haouzi D, Brothers G, Penninger JM, Peleato ML, Kroemer G, Susin SA. **NADH oxidase activity of mitochondrial apoptosis-inducing factor.** *J Biol Chem.* (2001) 276(19):16391-8

Moroni F, Meli E, Peruginelli F, Chiarugi A, Cozzi A, Picca R, Romagnoli P, Pellicciari R, Pellegrini-Giampietro DE**. Poly(ADP-ribose) polymerase inhibitors attenuate necrotic but not apoptotic neuronal death in experimental models of cerebral ischemia.** *Cell Death Differ. (*2001) 8(9):921-32

Muñoz-Gámez JA, Rodríguez-Vargas JM, Quiles-Pérez R, Aguilar-Quesada R, Martín-Oliva D, de Murcia G, Menissier de Murcia J,Almendros A, Ruiz de Almodóvar M, Oliver FJ. **PARP-1 is involved in autophagy induced by DNA damage.** *Autophagy*. (2009) 5(1):61-74

Nanavaty UB, Pawliczak R, Doniger J, Gladwin MT, Cowan MJ, Logun C, Shelhamer JH. **Oxidant-induced cell death in respiratory epithelial cells is due to DNA damage and loss of ATP.** *Exp Lung Res.* (2002) 28(8):591-607

Neff L, Zeisel M, Druet V, Takeda K, Klein JP, Sibilia J, Wachsmann D. **ERK 1/2- and JNKs-dependent synthesis of interleukins 6 and 8 by fibroblast-like synoviocytes stimulated with protein I/II, a modulin from oral streptococci, requires focal adhesion kinase.** *J Biol Chem*. (2003) 278(30):27721-8

Nie J, Sakamoto S, Song D, Qu Z, Ota K, Taniguchi T. **Interaction of Oct-1 and automodification domain of poly(ADP-ribose) synthetase.** *FEBS Lett.* (1998) 424(1-2):27-32

Oei SL, Griesenbeck J, Schweiger M, Babich V, Kropotov A, Tomilin N. **Interaction of the transcription factor YY1 with human poly(ADP-ribosyl) transferase.** *Biochem Biophys Res Commun*. (1997) 240(1):108-11

Ogata N, Ueda K, Hayaishi O. **ADP-ribosylation of histone H2B. Identification of glutamic acid residue 2 as the modification site.** *J Biol Chem.* (1980) 255(16):7610-5

Ohashi Y, Ueda K, Kawaichi M, Hayaishi O. **Activation of DNA ligase by poly(ADP-ribose) in chromatin.** *Proc Natl Acad Sci U S A.* (1983) 80(12):3604-7

Oka J, Ueda K, Hayaishi O, Komura H, Nakanishi K. **ADP-ribosyl protein lyase. Purification, properties, and identification of the product.** *J Biol Chem.* (1984) 259(2):986-95

Oka S, Kato J, Moss J. **Identification and characterization of a mammalian 39-kDa poly(ADP-ribose) glycohydrolase.** *J Biol Chem.* (2006) 281(2):705-13

Okano S, Lan L, Caldecott KW, Mori T, Yasui A. **Spatial and temporal cellular responses to single-strand breaks in human cells.** *Mol Cell Biol.* (2003) 23(11):3974-81

Oliver FJ, Ménissier-de Murcia J, Nacci C, Decker P, Andriantsitohaina R, Muller S, de la Rubia G, Stoclet JC, de Murcia G. **Resistance to endotoxic shock as a consequence of defective NF-kappaB activation in poly (ADP-ribose) polymerase-1 deficient mice.** *EMBO J.* (1999) 18(16):4446-54

Otto H, Reche PA, Bazan F, Dittmar K, Haag F, Koch-Nolte F. **In silico characterization of the family of PARP-like poly(ADP-ribosyl)transferases (pARTs).** *BMC Genomics.* (2005) 6:139

Pechkovsky DV, Goldmann T, Ludwig C, Prasse A, Vollmer E, Müller-Quernheim J, Zissel G. **CCR2 and CXCR3 agonistic chemokines are differently expressed and regulated in human alveolar epithelial cells type II.** *Respir Res.* (2005) 6:75.

Rapizzi E, Fossati S, Moroni F, Chiarugi A**. Inhibition of poly(ADP-ribose) glycohydrolase by gallotannin selectively up-regulates expression of proinflammatory genes.** *Mol Pharmacol.* (2004) 66(4):890-8

Ratnam K, Low JA: **Current Development of Clinical Inhibitors ofPoly(ADP-Ribose) Polymerase in Oncology**. *Clin Cancer Res* (2007) 13(5):1383-8

Ravagnan L, Gurbuxani S, Susin SA, Maisse C, Daugas E, Zamzami N, Mak T, Jäättelä M, Penninger JM, Garrido C, Kroemer G. **Heat-shock protein 70 antagonizes apoptosis-inducing factor.** *Nat Cell Biol.* (2001) 3(9):839-43

Re R, Pellegrini N, Proteggente A, Pannala A, Yang M, Rice-Evans C. **Antioxidant activity applying an improved ABTS radical cation decolorisation assay.** *Free Radic Biol Med.* (1999) 26(9-10):1231-7

Riedl KM, Hagerman AE. **Tannin-protein complexes as radical scavengers and radical sinks.** *J Agric Food Chem.* (2001) 49(10):4917-23

Rohrbach MS, Kreofsky T, Rolstad RA, Russell JA. **Tannin-mediated secretion of a neutrophil chemotactic factor from alveolar macrophages. Potential contribution to the acute pulmonary inflammatory reaction associated with byssinosis.** *Am Rev Respir Dis.* (1989) 139(1):39-45

Rouleau M, Aubin RA, Poirier GG. **Poly(ADP-ribosyl)ated chromatin domains: access granted** *J Cell Sci.* (2004) 117(Pt 6):815-25

Ruscetti T, Lehnert BE, Halbrook J, Le Trong H, Hoekstra MF, Chen DJ, Peterson SR. **Stimulation of the DNA-dependent protein kinase by poly(ADP-ribose) polymerase.** *J Biol Chem.* (1998) 273(23):14461-7

Santilli G, Cervellera MN, Johnson TK, Lewis RE, Iacobelli S, Sala A. **PARP co-activates B-MYB through enhanced phosphorylation at cyclin/cdk2 sites.** *Oncogene.* (2001) 20(57):8167-74

Schulze-Osthoff K, Los M, Baeuerle PA. **Redox signalling by transcription factors NF-kappa B and AP-1 in lymphocytes**. *Biochem Pharmacol.* (1995) 50(6):735-41

Scovassi AI, Mariani C, Negroni M, Negri C, Bertazzoni U. **ADP-ribosylation of nonhistone proteins in HeLa cells: modification of DNA topoisomerase II.** *: Exp Cell Res.* (1993) 206(1):177-81

Shall S**,** de Murcia G**. Poly(ADP-ribose) polymerase-1: what have we learned from the deficient mouse model?** *Mutat Res.* (2000) 460(1):1-15

Schreiber V, Dantzer F, Ame JC, de Murcia G. **Poly(ADP-ribose): novel functions for an old molecule** *Nature Reviews Molecular Cell Biology* (2006) 7**,** 517-528

Shrivastav M, De Haro LP, Nickoloff JA. **Regulation of DNA double-strand break repair pathway choice.** *Cell Res.* (2008) 18(1):134-47

Singh NP, McCoy MT, Tice RR, Schneider EL. **A simple technique for quantitation of low levels of DNA damage in individual cells** *Exp. Cell Res.* (1988) 175:184–191.

Slama JT, Aboul-Ela N, Goli DM, Cheesman BV, Simmons AM, Jacobson MK. **Specific inhibition of poly(ADP-ribose) glycohydrolase by adenosine diphosphate (hydroxymethyl)pyrrolidinediol***. J Med Chem.* (1995) 38(2):389-93

Soldani C, Scovassi AI. **Poly(ADP-ribose) polymerase-1 cleavage during apoptosis: an update.** *Apoptosis.* (2002) 7(4):321-8

Susin SA, Lorenzo HK, Zamzami N, Marzo I, Snow BE, Brothers GM, Mangion J, Jacotot E, Costantini P, Loeffler M, Larochette N, Goodlett DR, Aebersold R, Siderovski DP, Penninger JM, Kroemer G. **Molecular characterization of mitochondrial apoptosis-inducing factor.** *Nature.* (1999) 397(6718):441-6

Suzuki H, Quesada P, Farina B, Leone E. **In vitro poly(ADP-ribosyl)ation of seminal ribonuclease.** *J Biol Chem.* (1986) 261(13):6048-55

Suzuki Y, Masini E, Mazzocca C, Cuzzocrea S, Ciampa A, Suzuki H, Bani D. **Inhibition of poly(ADP-ribose) polymerase prevents allergen-induced asthma-like reaction in sensitized Guinea pigs***. J Pharmacol Exp Ther.* (2004) 311(3):1241-8

Szabó C. **Role of poly(ADP-ribose)synthetase in inflammation**. *Eur J Pharmacol.* (1998) 350(1):1-19

Tanuma S, Sakagami H, Endo H. **Inhibitory effect of tannin on poly(ADP-ribose) glycohydrolase from human placenta.** *Biochem Int.* (1989) 18(4):701-8

Tanuma S, Tsai YJ, Sakagami H, Konno K, Endo H. **Lignin inhibits (ADP-ribose)n glycohydrolase activity.** *Biochem Int.* (1989) 19(6):1395-402

Tanuma S, Yagi T, Johnson GS. **Endogenous ADP ribosylation of high mobility group proteins 1 and 2 and histone H1 following DNA damage in intact cells.** *Arch Biochem Biophys.* (1985) 237(1):38-42

Tentori L, Balduzzi A, Portarena I, Levati L, Vernole P, Gold B, Bonmassar E, Graziani G. **Poly (ADP-ribose) polymerase inhibitor increases apoptosis and reduces necrosis induced by a DNA minor groove binding methyl sulfonate ester.** *Cell Death Differ.* (2001) 8(8):817-28

Thompson LH, West MG. **XRCC1 keeps DNA from getting stranded.** *Mutat Res.* (2000) 459(1):1-18

Tóth A, Kiss E, Gergely P, Walsh MP, Hartshorne DJ, Erdödi F. **Phosphorylation of MYPT1 by protein kinase C attenuates interaction with PP1 catalytic subunit and the 20 kDa light chain of myosin.** *FEBS Lett.* (2000) 484(2):113-7

Trucco C, Oliver FJ, de Murcia G, Ménissier-de Murcia J. **DNA repair defect in poly(ADP-ribose) polymerase-deficient cell lines.** *Nucleic Acids Res.* (1998) 26(11):2644-9

Tsai YJ, Abe H, Maruta H, Hatano T, Nishina H, Sakagami H, Okuda T, Tanuma S. **Effects of chemically defined tannins on poly (ADP-ribose) glycohydrolase activity.** *Biochem Int.* (1991) 24(5):889-97

Uchiumi F, Sato T, Tanuma S. **Identification and characterization of a tannic acid-responsive negative regulatory element in the mouse mammary tumor virus promoter** *J Biol Chem.* (1998) 273(20):12499-508

Uchiumi F, Maruta H, Inoue J, Yamamoto T, Tanuma S. **Inhibitory effect of tannic acid on human immunodeficiency virus promoter activity induced by 12-O-tetra decanoylphorbol-13-acetate in Jurkat T-cells.** *Biochem Biophys Res Commun.* (1996) 220(2):411-7

Van Molle W, Vanden Berghe J, Brouckaert P, Libert C. **Tumor necrosis factor-induced lethal hepatitis: pharmacological intervention with verapamil, tannic acid, picotamide and K76COOH.** *FEBS Lett.* (2000) 467(2-3):201-5.

Virág L, Scott GS, Cuzzocrea S, Marmer D, Salzman AL, Szabó C. **Peroxynitrite-induced thymocyte apoptosis: the role of caspases and poly (ADP-ribose) synthetase (PARS) activation.** *Immunology.* (1998) (3):345-55

Virag L, Marmer DJ, Szabo C. **Crucial role of apopain in the peroxynitrite-induced apoptotic DNA fragmentation.** *Free Radic. Biol. Med.* (1998) 25**:**1075–1082

Virág L, Szabó C. **The therapeutic potential of poly(ADP-ribose) polymerase inhibitors.** *Pharmacol Rev.* 2002 Sep;54(3):375-429.

Virág L, Bai P, Bak I, Pacher P, Mabley JG, Liaudet L, Bakondi E, Gergely P, Kollai M, Szabó C**. Effects of poly(ADP-ribose) polymerase inhibition on inflammatory cell migration in a murine model of asthma**. *Med Sci Monit.* (2004) 10(3):77-83

Wisdom R. **AP-1: one switch for many signals.** *Exp Cell Res.* 1999 Nov 25;253(1):180-5.

Wong HR, Menendez IY, Ryan MA, Denenberg AG, Wispé JR. **Increased expression of heat shock protein-70 protects A549 cells against hyperoxia.** *Am J Physiol.* (1998) 275:836-41

Yang SH, Sharrocks AD, Whitmarsh AJ. **Transcriptional regulation by the MAP kinase signaling cascades.** *Gene.* (2003) 320:3-21

Ye H, Cande C, Stephanou NC, Jiang S, Gurbuxani S, Larochette N, Daugas E, Garrido C, Kroemer G, Wu H. **DNA binding is required for the apoptogenic action of apoptosis inducing factor**. *Nat Struct Biol*. (2002) 9(9):680-4

Ying W, Sevigny M B, Chen Y, Swanson R A. **Poly (ADP-ribose) glycohydrolase mediates oxidative and excitotoxic neuronal death.** *Proc Natl Acad Sci USA* (2001) 98 (21): 12227–13298

Ying W, Swanson RA. **The poly(ADP-ribose) glycohydrolase inhibitor gallotannin blocks oxidative astrocyte death.** *Neuroreport.* (2000) 11(7):1385-8

Ying W, Alano CC, Garnier P, Swanson RA**. NAD+ as a metabolic link between DNA damage and cell death.** *J Neurosci Res.* (2005) 79(1-2):216-23

Yoshihara K, Itaya A, Tanaka Y, Ohashi Y, Ito K, Teraoka H, Tsukada K, Matsukage A, Kamiya T. **Inhibition of DNA polymerase alpha, DNA polymerase beta, terminal deoxynucleotidyl transferase, and DNA ligase II by poly(ADP-ribosyl)ation reaction in vitro.** *Biochem Biophys Res Commun.* (1985) 128(1):61-7

Yu SW, Wang H, Poitras MF, Coombs C, Bowers WJ, Federoff HJ, Poirier GG, Dawson TM, Dawson VL. **Mediation of poly(ADP-ribose) polymerase-1-dependent cell death by apoptosis-inducing factor.** *Science.* (2002) 297(5579):259-63

Zingarelli B, O'Connor M, Hake PW**. Inhibitors of poly (ADP-ribose) polymerase modulate signal transduction pathways in colitis***.] Eur J Pharmacol.* (2003) 469(1-3):183-94

Zingarelli B, Salzman AL and Szabo C **Genetic disruption of poly (ADP-ribose) synthetase inhibits the expression of P-selectin and intercellular adhesion molecule-1 in myocardial ischemia/reperfusion injury.** *Circ Res* (1998) 83: 85-94

Zingarelli B, Hake PW, O'Connor M, Denenberg A, Wong HR, Kong S, Aronow BJ. **Differential regulation of activator protein-1 and heat shock factor-1 in myocardial ischemia and reperfusion injury: role of poly(ADP-ribose) polymerase-1.** *Am J Physiol Heart Circ Physiol.* (2004) 286(4):1408-15

Zong WX, Ditsworth D, Bauer DE, Wang ZQ, Thompson CB. **Alkylating DNA damage stimulates a regulated form of necrotic cell death.** *Genes Dev*. (2004) 18(11):1272-82.

13. ACKNOWLEDGMENT

I wish to thank my supervisor László Virág for helping and guiding my work.

I would like to thank Prof. Pál Gergely, head of Department of Medical Chemistry for giving all the support for my work.

Many thanks to all the people in the Department of Medical Chemistry, highlighted our group: Edina Bakondi, Péter Bai, Annamária Kakuk, Csaba Hegedűs, Attila Brunyánszki, István Kovács, Katalin Kovács, Petra Lakatos, Magdolna Szántó for their scientific and personal support. I greatly appreciate the excellent technical assistance of Ms. Erzsébet Herbály, Ms. Julianna Hunyadi and Andrea Docsa.

I would like to thank Krisztián Csomós for his help with the lentiviral system and Gábor Mocsár for his help with the confocal microscopic analyses. I am very grateful for Andrea Kiss who measured the protein phosphatase activities and for Peter Bai who helped me by the flow cytometric analyses. I am much obliged to Annamária Kakuk and Istán Kovács who prepared the mesenchimal stem cells.

I would like thank to my family and friends for encouraging and supporting me.

14. PUBLICATIONS

This thesis is built on the following publications:

Erdélyi K, Bakondi E, Gergely P, Szabó C, Virág L: Pathophysiologic role of oxidative stess-induced poly(ADP-ribose) polymerase-1 activation: focus on the cell death and transcriptional regulation. *Cell. Mol. Life Sci*. **62**(7-8):751-9. Review.
IF: 4,812

Erdélyi K, Kiss A, Bakondi E, Bai P, Szabó C, Gergely P, Erdődi F, Virag L: Gallotannin inhibits the expression of chemokines and inflammatory cytokines in A549 cells. *Mol Pharmacol.* **68**(3):895-904. (2005)
IF: 5,080

Erdélyi, K., Bai, P., Kovács, I., Szabó, É., Mocsár, G., Kakuk, A., Szabó, Cs., Gergely, P., Virág, L.: Dual role of poly(ADP-ribose) glycohydrolase in the regulation of cell death in oxidatively stressed A549 cells *FASEB J.* **23**(10):3553-63. (2009)
IF: 7.049